**Scuola Internazionale Superiore di Studi Avanzati - Trieste**

**SISSA**
**40!**

# *In vivo* and *in vitro* characterization of an infectious synthetic prion amyloid

Candidate:

Edoardo Bistaffa

Supervisor:

Prof. Giuseppe Legname

Co-supervisor:

Dr. Fabio Moda

A thesis submitted for the degree of

*Doctor of Philosophy*

in Functional and Structural Genomics

November 2018

**SISSA - Via Bonomea 265 - 34136 TRIESTE - ITALY**

# Scuola Internazionale Superiore Studi Avanzati (SISSA)



# *In vivo* and *in vitro* characterization of an infectious synthetic prion amyloid

Candidate:

Edoardo Bistaffa

Supervisor:

Prof. Giuseppe Legname

Co-supervisor:

Dr. Fabio Moda

A thesis submitted for the degree of

*Doctor of Philosophy*

in Functional and Structural Genomics

November 2018

# Abstract

Prion pathologies are a group of fatal neurodegenerative disorders that afflict mammalian species. In these diseases the cellular prion protein (PrP$^C$) misfolds into a disease related form, known as prion (PrP$^{Sc}$). This misfolded protein is able to recruit and convert the physiological PrP$^C$ into pathogenic PrP$^{Sc}$ that accumulates and leads to neuronal death. Synthetic infectious prions generated from recombinant source of PrP (recPrP) were created in the past few years with the aim of assessing if these preparations could mimic the behaviors of natural prions. Particularly, synthetic prions offer a great tool for studying both the basis of prion replication and the mechanism behind the evolution of prion strains. Indeed, recent evidence suggests that, despite the absence of nucleic acids, prions can adapt their conformation in response to changes in the context of replication. In this thesis, we have analyzed the stability of a synthetic prion isolate previously generated and named amyloid #4. In particular, amyloid #4 was either injected in wild-type mice or amplified by means of an innovative technique named Protein Misfolding Cyclic Amplfication (PMCA) which is able to mimic *in vitro* the process of prion conversion which occurs *in vivo*. Injection of raw amyloid failed to induce any disease while the injection of the PMCA amplified material induced severe prion pathology characterized by the presence of an uncommon PrP$^{Sc}$. When further passaged in wild-type animals such PrP$^{Sc}$ was able to differentiate in two different isolates able to sustain different types of prion disease. These two isolates were finally assessed in PMCA and we observed the generation of an alternative conformation whose biophysical properties were different from those of both inocula, suggesting that the *in vitro* context of replication selectively amplified a third PrP$^{Sc}$ isolate. Taken together these results indicate that our synthetic prion undergoes to

process of evolution (selection/adaptation) dictated by the environment of its replication (bioassays VS PMCA).

Synthetic prions can be used for studying prion adaptation and selection. Since all the proposed pharmacological treatments failed to cure these pathologies, understanding these behaviors of prions is of fundamental importance to design effective therapies for these devastating disorders.

# List of publications

Moda F, Le TN, Aulić S, **Bistaffa E**, Campagnani I, Virgilio T, Indaco A, Palamara L, Andréoletti O, Tagliavini F, Legname G. *Synthetic prions with novel strain-specified properties.* PLoS Pathog. 2015 Dec 31;11(12):e1005354. doi: 10.1371/journal.ppat.1005354. eCollection 2015 Dec. PubMed PMID: 26720726; PubMed Central PMCID: PMC4699842.

Author contribution: contributed to performing the experiments, analyzing the data and writing the paper.

**Bistaffa E**, Moda F., Virgilio T, Campagnani I, De Luca CMG, Rossi M, Salzano G, Giaccone G, Tagliavini F and Legname G. *Synthetic prion selection and adaptation.* Mol Neurobiol. 2018 Aug 3. doi: 10.1007/s12035-018-1279-2.

Author contribution: Performed the experiments, analyzed the data and wrote the paper.

**Other publications not cited here**

Legname G, Virgilio T, **Bistaffa E**, De Luca CMG, Catania M, Zago P, Isopi E, Campagnani I, Tagliavini F, Giaccone G, Moda F. *Effects of peptidyl-prolyl isomerase 1 depletion in animal models of prion diseases.* Prion. 2018 Mar 4;12(2):127-137. doi: 10.1080/19336896.2018.1464367. Epub 2018 May 18. PubMed PMID: 29676205.

Author contribution: contributed to performing the experiments.

Vanni S, Moda F, Zattoni M, **Bistaffa E**, De Cecco E, Rossi M, Giaccone G, Tagliavini F, Haïk S, Deslys JP, Zanusso G, Ironside JW, Ferrer I, Kovacs GG, Legname G. *Differential overexpression of SERPINA3 in human prion diseases.* Sci Rep. 2017 Nov 15;7(1):15637. doi: 10.1038/s41598-017-15778-8. PubMed PMID: 29142239; PubMed Central PMCID: PMC5688139.

Author contribution: contributed to performing the experiments, analyzing the data and writing the paper.

Aulić S, Masperone L, Narkiewicz J, Isopi E, **Bistaffa E**, Ambrosetti E, Pastore B, De Cecco E, Scaini D, Zago P, Moda F, Tagliavini F, Legname G. *α-Synuclein Amyloids Hijack Prion Protein to Gain Cell Entry, Facilitate Cell-to-Cell Spreading and Block Prion Replication.* Sci Rep. 2017 Aug 30;7(1):10050. doi: 10.1038/s41598-017-10236-x. PubMed PMID: 28855681; PubMed Central PMCID: PMC5577263.

Author contribution: contributed to performing the experiments, analyzing the data and writing the paper.

Redaelli V, **Bistaffa E**, Zanusso G, Salzano G, Sacchetto L, Rossi M, De Luca CM, Di Bari M, Portaleone SM, Agrimi U, Legname G, Roiter I, Forloni G, Tagliavini F, Moda F. *Detection of prion seeding activity in the olfactory mucosa of patients with Fatal Familial Insomnia.* Sci Rep. 2017 Apr 7;7:46269. doi: 10.1038/srep46269. PubMed PMID: 28387370; PubMed Central PMCID: PMC5384244.

Author contribution: contributed to performing the experiments, analyzing the data and writing the paper.


**Book chapters**

**Bistaffa E**, Rossi M, De Luca CMG, Moda F. *Biosafety of Prions.* Prog Mol Biol Transl Sci. 2017;150:455-485. doi: 10.1016/bs.pmbts.2017.06.017. Epub 2017 Aug 2. Review. PubMed PMID: 28838674.

Author contribution: contributed to writing the chapter.

Moda F, **Bistaffa E**, Narkiewicz J, Salzano G, Legname G. (2017) *Synthetic Mammalian Prions.* In: Liberski P. (eds) Prion Diseases. Neuromethods, vol 129. Humana Press, New York, NY

Author contribution: contributed to writing the chapter.


**Other publications**

Di Fede G, Catania M, Maderna E, Ghidoni R, Benussi L, Tonoli E, Giaccone G, Moda F, Paterlini A, Campagnani I, Sorrentino S, Colombo L, Kubis A, **Bistaffa E**, Ghetti B, Tagliavini F. *Molecular subtypes of Alzheimer's disease.* Sci Rep. 2018 Feb 19;8(1):3269. doi: 10.1038/s41598-018-21641-1. PubMed PMID: 29459625; PubMed Central PMCID: PMC5818536.

Author contribution: contributed to performing the experiments.

Farinazzo A, Angiari S, Turano E, **Bistaffa E**, Dusi S, Ruggieri S, Bonafede R, Mariotti R, Constantin G, Bonetti B. *Nanovesicles from adipose-derived mesenchymal stem cells inhibit T lymphocyte trafficking and ameliorate chronic experimental autoimmune encephalomyelitis.* Sci Rep. 2018 May 10;8(1):7473. doi: 10.1038/s41598-018-25676-2. PubMed PMID: 29748664; PubMed Central PMCID: PMC5945853.

Author contribution: contributed to performing the experiments.

# List of abbreviations

**A**

*ASA*   Amyloid Seeding Assay

*AFM*   Atomic Force Microscopy

**B**

*BSE*   Bovine Spongiform Encephalopathy

*BH*   Brain Homogenate

*BSA*   Bovine Serum Albumin

**C**

*CWD*   Chronic Wasting Disease

*CPD*   Camel Prion Disease

*CJD*   Creutzfeldt-Jakob Disease

*CNS*   Central Nervous System

*CD*   Circular Dichroism

*CSF*   Cerebrospinal fluid

**D**

*DY*   Drowsy hamster prion strain

*DXMS*   Hydrogen/Deuterium exchange mass spectrometry

**E**

*EUE*   Exotic Ungulate Encephalopathy

*EEG*   Electroencephalography

*EM*   Electron Microscopy

*ER*   Endoplasmic reticulum

**F**

*FSE*   Feline Spongiform Encephalopathy

*FI*   Fatal Insomnia

*FTIR*   Fourier Transform Infrared Spectroscopy

**G**

*GSS*            Gerstmann–Sträussler–Scheinker syndrome

*GdnHCL*        Guanidine Hydrochloride

*GPI*            Glycophosphatidylinositol

*GFAP*           Glial Fibrillary Acidic Protein

**H**

*HY*             Hyper hamster prion strain

*H&E*            Hematoxylin-eosin

**I**

*iCJD*           Iatrogenic Creutzfeldt-Jakob Disease

**L**

*LPR*            Laminin Precursor Receptor

*LOTSS*          Low Toxicity Synthetic Strain

**M**

*mo-vCJD*        Mouse adapted variant Creutzfeldt-Jakob Disease

**N**

*NCAM*           Neural Cell Adhesion Molecule

*NMDAr*          N-methyl-D-Aspartate receptor

**P**

*PrP$^C$*        Cellular prion protein

*PrP$^{Sc}$*     Scrapie prion protein

*PK*             Proteinase K

*PMCA*           Protein Misfolding Cyclic Amplification

*PTA*            Phosphotungstic acid

*POPG*           1-Palmitoyl-2-oleoylphophati-dylglycerol

*PNGase F*       Peptide-N-glycosidase F

*[poly(rA)]*     polyriboadenylic acid

*PRNP*           Prion protein gene

**R**

*recPrP*  Recombinant prion protein

*RT-QuIC*  Real-Time Quaking Induced Conversion

*RML*  Rocky Mountain Laboratories mouse prion strain

*recMoPrP*  recombinant Mouse PrP

**S**

*SSLOW*  Synthetic Strain Leading to OverWeight

*sCJD*  sporadic Creutzfeldt-Jakob Disease

**T**

*ThT*  Thioflavin-T

*ThS*  Thioflavin-S

*TSEs*  Transmissible Spongiform Encephalopathies

*TME*  Transmissible Mink Encephalopathy

**V**

*vCJD*  Variant Creutzfeldt-Jakob Disease

*VPSPr*  Variably Protease-sensitive Prionophaty

# Table of contents

## CHAPTER III

## CHAPTER IV

# Introduction

## 1.1 Prion disorders in animals and humans

Prion diseases, or Transmissible Spongiform Encephalopathies (TSEs), are a large group of neurodegenerative diseases that afflict mammalian species. They can be (i) sporadic, (ii) genetic or (iii) acquired by infection. Animal TSEs include scrapie in sheep, goats and mufflons [1], Transmissible Mink Encephalopathy in ranch-reared mink (TME) [2], Chronic Wasting Disease in deer (CWD) [3], Bovine Spongiform Encephalopathy in cows (BSE) [4], Feline Spongiform Encephalopathy in domestic cats (FSE) [5], Exotic Ungulate Encephalopathy in exotic zoo ruminants (EUE) [6] and Camel Prion Disease in camels (CPD) [7]. Sporadic human prion disorders comprise: sporadic Creutzfeldt-Jakob disease (sCJD), Variably Protease-Sensitive Prionophaty (VPSPr) [8] and sporadic Fatal Insomnia (sFI). Genetic human prion disorders include Gerstmann-Sträussler-Scheinker (GSS) syndrome [9, 10] Fatal Familial Insomnia (FFI) [10] and familial CJD (fCJD) that are associated to genetic mutations (point mutations, insertional mutations, etc.) in the prion protein gene (*PRNP*) [11, 12]. Acquired forms of prion diseases comprise: kuru [13], iatrogenic CJD (iCJD) attributed to infection with prion contaminated surgical instruments or infected human derivatives and variant CJD (vCJD) that is related to consumption of BSE-contaminated cattle products (See section "Natural prion transmission"). Sporadic CJD is the most represented type of these diseases (85-90% of all CJD cases) with an incidence of 1-1.5 cases per 1 million population per year [14]. All these pathologies are

caused by the conformational conversion of the prion protein (PrP$^C$) into a pathological form, known as scrapie PrP (PrP$^{Sc}$), that acquire infectious properties. Table 1 summarized these mammalian prion pathologies.

| Disease | Host |
|---|---|
| Scrapie | Sheep, goats and mufflons |
| Chronic Wasting Disease (CWD) | Deer, mule, elk |
| Transmissible Mink Encephalopathy (TME) | Mink |
| Bovine Spongiform Encephalopathy (BSE) | Cattle |
| Feline Spongiform Encephalopathy (FSE) | Feline (Cats, Cheetah) |
| Exotic Ungulate Encephalopathy (EUE) | Exotic zoo ruminants (*Bovidae* family) |
| Camel Prion Disease (CPD) | Camel |
| sporadic CJD (sCJD) and sporadic Familial Insomnia (sFI) | Humans |
| Variably Protease Sensitive Prionopahty (VPSPr) | Humans |
| Familial CJD (E200K, V210I) | Humans |
| Fatal Familial Insomnia (FFI) | Humans |
| Gerstmann-Sträussler-Scheinker syndrome (GSS) | Humans |
| Iatrogenic CJD (iCJD) | Humans |
| Variant CJD (vCJD) | Humans |

**Table 1. Prion diseases in animals and humans.**

## 1.2 Historical background on prion diseases: from prion discovery to the "protein only hypothesis"

The first report of what now we know to be a prion disease dates back to 1732 in Lincolnshire after an outbreak of scrapie in British farms [15]. However, the real origin of scrapie still remains an open question. For almost one century the causes of this animal disease lacked any explanation. In the late 1800s, Besnoit reported a hypothetical viral nature of the infectious agent behind these diseases. An important step in the story of prion discovery was taken in 1936 when two French veterinarians, Jean Cullie and Paul-

Louis Chelle, tried to develop a vaccine against a common sheep virus (made of formalin fixed brain tissue from scrapie infected animals), and transmitted the scrapie disease to treated sheep. After this first accidental transmission, William Gordon (Moredun Institute in Edinburgh) tried to repeat the experiment by challenging 697 animals of which over 200 developed scrapie pathology after 2 years [16]. After these pioneering experiments, the scrapie was then transmitted from sheep to mice by Roger J. Morris and Daniel Carleton Gajdusek [17] and from goats to mice by Richard Chandler [18] thus creating a multitude of prion strains adapted to common laboratory animal models (prevalently mice and hamsters) and permitted extensive studies on prion transmission that would have been almost impossible to test in sheep. After the discovery of the transmissibility of scrapie many hypotheses on the nature of the infectious agent able to induce this disease were proposed: (i) a self-replicating membrane [19, 20], (ii) a subvirus [20], (iii) a viroid and a spiroplasma or a retrovirus-like element [21] but none of these was unequivocally demonstrated. Another step towards the prion discovery were moved in 1957 when a young virologist and pediatrician, Daniel Carleton Gajdusek, moved to Papua New Guinea to investigate the cause of an unknown encephalitis-like pathology that afflicted the indigenous population [22]. Today we know that such pathology is a prion disorder, named kuru, horizontally transmitted in this population by cannibalistic rituals. The crucial event that provided the first correlation between scrapie and kuru came from an intuition of William Hadlow, a veterinarian and neuropathologist. He was invited to a conference where he saw microphotographs of brain tissue from kuru subjects and recognized strong similarities with the neuropathological alterations observed in scrapie pathology. Immediately, Hadlow sent a letter to Gajdusek proposing that the kuru and scrapie pathologies may be caused by the same infectious agent. After that episode, Gajdusek started experiments to test the transmissibility of kuru to primates. Under the supervision

of Dr. Clarence Joseph Gibbs, Gajdusek performed the first transmission of kuru to chimpanzees providing direct evidence of the infectious nature of this pathology [13]. However, because the long incubation period of the disease, the infectious agent was initially thought to be a slow virus [23]. Working on this unknown pathology, Tikvah Alper and colleagues in 1967 observed that the infectious agent associated to scrapie appeared uncommonly resistant to UV treatment and ionizing radiation [24]. In the same study, the authors reported the minimum molecular weight necessary for the infectivity being at around $2x10^{5}$ Da thus ruling out the hypothesis of viral or bacterial nature of this infectious agent. These findings supported the "virino" theory of Alan G. Dikinson and George Outram [25] suggesting that the agent of infection could be a small nucleic acid tightly packaged and protected from conventional denaturing agents by a protein-coat that preserves the integrity of the genetic material. In 1967 a mathematician, John S. Griffith, on the basis of experimental observations proposed for the first time an innovative model ascribing the pathological agent of prion disorder to a protein able to self-replicate in the body of the host [26]. This is the so called "protein only hypothesis" supported by Stanley B. Prusiner that provided a significant amount of experimental evidence showing that the infectious agent causing prion diseases was a protein [27]. The term "prions" was coined by Prusiner to indicate this novel proteinaceous infectious agent. He went on to win the Nobel prize in 1997 for his discovery of prions, a new biological principle of infection. Prusiner's group, in 1982, purified for the first time the protease-resistant prion protein from infectious material [28] and described the dose dependent correlation between the amount of purified material and the infectivity of this agent. Particularly, his group discovered that the infectivity level of this protein could be reduced using (i) agent that altered or destroyed all the protein structure or (ii) antibodies against PrP [29]. These data further supported the protein only hypothesis and unequivocally linked this infectious

protein to prion diseases. In 1985, Bruce Chesebro and colleagues identified the gene that encoding for prion protein (*PRNP*) [30]. Structural studies on the physiological cellular prion protein (PrP$^C$) and the pathological related scrapie prion protein (PrP$^{Sc}$) demonstrate that these two proteins have the same chemical properties [31] and suggest that the origin of the infectivity seems to be dictated by a conformational rearrangement of PrP$^C$ induced by PrP$^{Sc}$ trough a conversion mechanism. Another important study that reinforces the "protein only hypothesis" was the discovery of the direct association between mutation on the *PRNP* gene and familial forms of prion disease. The first genetic prion disease described in humans was the Gerstmann-Sträussler-Scheinker (GSS) syndrome characterized by a point mutation (P102L) in the *PRNP* gene [32]. Further studies revealed several mutations (point mutations or insertions) of the *PRNP* gene that are associated with different familial forms of prion disorders [33]. Finally, in 1993, Charles Weissmann developed a transgenic mouse model devoid of PrP and demonstrated that these mice were resistant to prion infection [34]. This observation provided an important step forward indicating that PrP$^C$ is necessary to sustain prion pathologies.

## 1.3 PrP$^C$

### 1.3.1 Structure of PrP$^C$

PrP$^C$ is a glycophosphatidylinositol-anchored glycoprotein encoded by the *PRNP* gene located on chromosome 20 in humans and chromosome 2 in mice [35]. The *PRNP* gene, depending on the species considered, contains either 2 or 3 exons with the entire coding region being contained in the last exon thus excluding possible alternative splicing [36]. The PrP$^C$ is composed by two major domains: (1) the N-terminal unstructured domain and the (2) C-terminal structured domain. The N-terminal unstructured domain possesses

distinctive sequences identified as octarepeats with a consensus sequence of PHGGGWGQ that contains histidine residues able to bind monovalent and divalent cations (e.g. $Cu^+$ and $Cu^{2+}$). The octarepeat region of PrP binds $Cu^{2+}$ with different modls of ion coordination [37]. The C-terminal structured domain is composed of two short antiparallel β-sheet strands (β1 and β2) and three α-helices (α1, α2 and α3) which provide a compact conformation conserved in all mammalian species (Fig. 1.1).
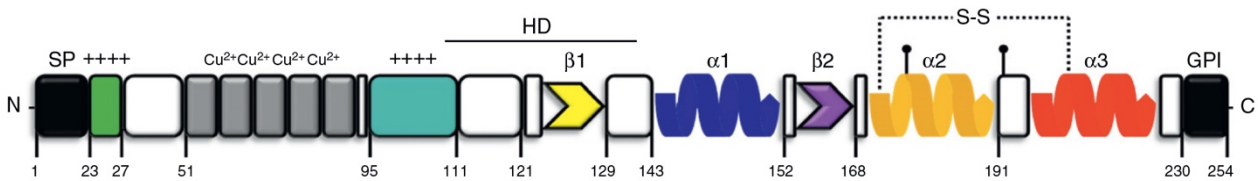


**Fig. 1.1 Schematic representation of PrP$^C$ structure.** The protein structure is constituted by two different domains, the structured C-terminus domain and the unstructured N-terminus domain. The C-terminus is composed by three α helices indicated as α1, α2 and α3 and two β sheet strands named β1 and β2. Two glycosylation sites at Asn181 and Asn197 and a disulfide bond are present in the C-terminus domain. (From Biasini *et al.*, Trends Neurosci 2012)

Recently, a third beta sheet strand (named β0) (Fig 1.2) has been described [38].
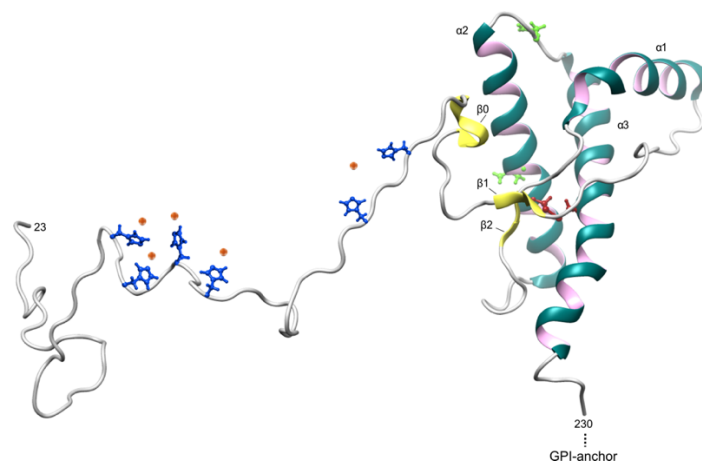


**Fig. 1.2 Structure of the cellular prion protein (PrP$^C$).** Tridimensional structure of PrP$^C$ showed the compact conformation of C-terminus domain. The third β sheet strand recently identified is indicated as β0 (yellow strand). The N-terminal domain is unstructured and possess octapeptide repeats that contain hystidine residues (in blue) able to bind divalent cations (orange dots). (from Legname, PLoS Path 2017)

PrP$^C$ is synthesized in the rough endoplasmic reticulum (ER) [35, 39] where it undergoes three main modifications: (1) addition of a GPI anchor, (2) formation of a disulfide bond between Cys179 and Cys214 [35, 40] and (3) N-linked glycosylation at Asn181 and Asn197 [41, 42]. Subsequently, the protein is directed to the Golgi network and the oligosaccharide chains are modified to produce complex-type chains with sialic acids [43]. Mature PrP$^C$ is composed of 208 amino acids and comprises three major forms differing in their glycosylation degree (referred as glycoform ratio): a di-glycosylated one (containing two glycan chains), a mono-glycosylated one (containing one glycan chain) and an un-glycosylated form (lacking glycan chains) that confers to the protein different molecular weights [41, 43-45] (Fig. 1.3). Proteolytic processing was also described as post-translation modification of PrP$^C$. Particularly, one of the sites is located in the central region of the protein and produces the N-terminal N1 soluble fragment and the GPI-anchored C-terminal C1 fragment [46] but PrP$^C$ may also be present as soluble full-length.
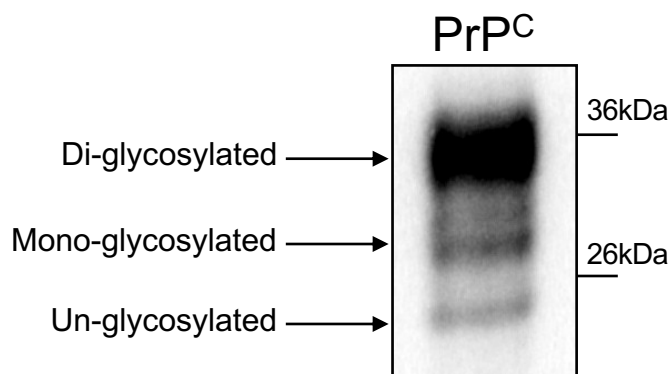


**Fig. 1.3 Typical western blot pattern of PrP$^C$.** After electrophoretic fractionation and immunoblot, three bands of PrP$^C$ protein can be appreciated. The di-glycosylated form prevails on the mono- and un-glycosylated ones.

*1.3.2 Functions of PrP$^C$*

The biological functions of PrP$^C$ are not completely understood, yet it appears that PrP$^C$ is involved in different cell functions. Moreover, PrP$^C$ is involved with the synaptic activity

[47], neurite elongation and synapse development [48, 49], metal metabolism [37, 50, 51], anti-apoptotic processes [52] and cell protection from oxidative stress [53, 54]. PrP[C] is also involved in cognitive and behavioral function such as long-term memory formation particularly for language development [55, 56] and the regulation of the circadian clock [57]. It is highly expressed in neurons and astrocytes and is concentrated in the synapses [58]. Moreover, one of the most fascinating aspects of PrP[C] functions is the involvement in cell signaling. The mechanism of signal transduction cannot be mediated directly by PrP[C] because it is a GPI anchored protein that can not interact with proteins of the cytosolic compartment but can instead interact with other transmembrane proteins and participate in signal transduction. The first evidence of these interactions was reported by Mouillet-Richard and colleagues that described the caveolin-1-dependent coupling of PrP[C] to the proto-oncogene tyrosine-protein kinase Fyn (Fyn) that plays a role in the maturation of neuroectodermal progenitor mouse cell line (C11 cells) [59]. After this first report other membrane proteins were described as PrP[C] interactors, including (i) a protein involved in the neurogenesis, the neural cell adhesion molecule (NCAM) [60] (ii) laminin precursor receptor (LPR) [61] (iii) the N-methyl-D-aspartate (NMDA) receptor [62-64] (iv) the $\alpha7$ nicotinic acetylcholine receptor [65] and (v) the metabotropic glutammate receptor mGluR1 [66].

## 1.4 PrP[Sc]

### 1.4.1 PrP[C] can convert to PrP[Sc] and acquire new biochemical features

The PrP[Sc] prions are the infectious agent behind the animal and human prion disorders. This protein arises from the conformational conversion of PrP[C], but contrarily to this latter, PrP[Sc] is rich in β-sheet structures, it is insoluble in mild detergents, partially resistant to

denaturation with chaotropic agents and is partially resistant to proteolytic digestion with proteinase K (PK). This specific resistance against PK digestion is commonly used for discriminating the PrP$^{Sc}$ from PrP$^{C}$. After PK treatment, PrP$^{C}$ is completely digested and the signal is undetectable at western blot (Fig. 1.4A). By contrast, PK treatment removes the N-terminal portion of the PrP$^{Sc}$ while leaving the C-terminal fragment of the protein which is enriched in β-sheet structures. This form of PrP$^{Sc}$, named PrP 27–30, has lower molecular weight than the un-glycosylated one and maintains the three glycosylated bands (i.e. with two, one or without glycosylation) (Fig.1.4B). The ratio between these three isoforms enables the classification of different PrP$^{Sc}$ conformation.
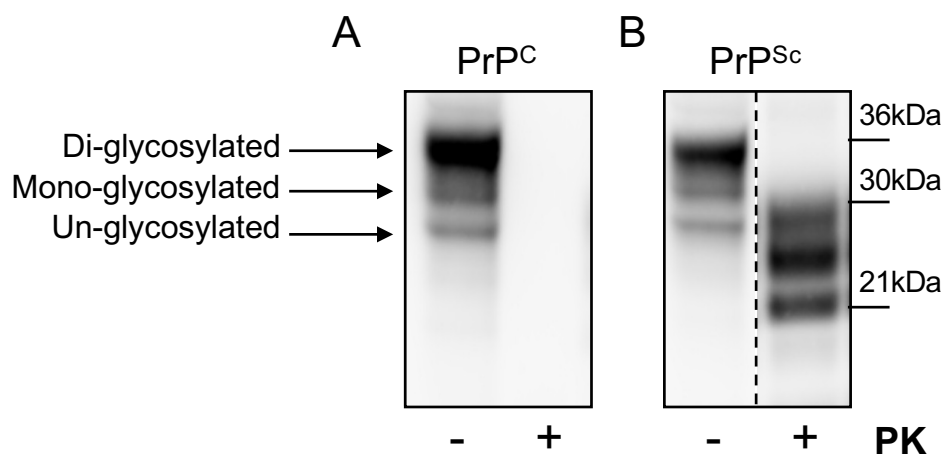


**Fig 1.4. Western blot analysis of PrP$^{C}$ and PrP$^{Sc}$.** PK digestion completely remove the signal of PrP$^{C}$ ((A), (-) line without PK and (+) line with PK) while the PrP$^{Sc}$ was partially digested and the C-terminal fragment can be detectable and maintained the three band of the different isoforms of the protein (B).

Misfolded PrP$^{Sc}$ is infectious [28] and has a strong tendency to polymerize and form amyloid aggregates which accumulate in the brain [67]. The discovery of these structures had been originally described by Mertz and colleagues [68] that identified "rod-shaped" particles in fraction enriched for scrapie infectivity. Notably, large PrP amyloid fibrils are not required for infectivity as demonstrated by Caughey and colleagues in 2005 [69] that

described nonfibrillar particles with masses equivalent to 14-28 PrP molecules as the most efficient initiators of prion diseases. The accumulation of PrP$^{Sc}$ amyloids in focal deposits, named "amyloid plaques", can be detected on brain sections with specific amyloid dyes like Congo-red or thioflavin-S.

*1.4.2 Structure of PrP$^{Sc}$*

While PrP$^{C}$ structure is well reported, high-resolution structural determination of PrP$^{Sc}$ is hard to solve due to its intrinsically insolubility and high propensity to aggregate. Defining the structure of the infectious conformers is essential for understanding the basis of prion replication and design structural-based therapeutic approaches. X-ray fiber diffraction [70, 71], Cryo-electron microscopy [72] and indirect structural studies proposed the structure of PrP monomer within PrP$^{Sc}$ particles as four-rung β-solenoid that provides molecular framework for the autocatalytic mechanism for propagation that gives rise to the alternative conformation of PrP$^{Sc}$ (Fig. 1.5). Recent evidence suggests these different conformations provide to PrP$^{Sc}$ different pathological characteristics [73, 74]. A β-solenoid structure is defined as a protein domain composed by regular secondary β-strands elements and can be classified by structural characteristics of (i) handedness, (ii) twist, (iii) oligomerization state, (iv) coil shape and (v) number of chains that wind around a common axis [75].
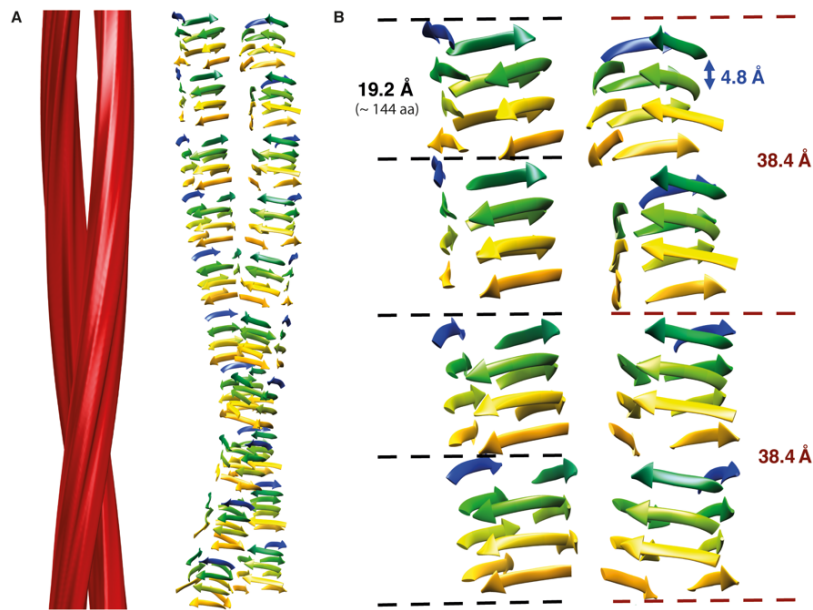
**Fig 1.5. View of the possible ß-sheet stacking in a four-rung ß-solenoid structure of GPI-anchorless PrP 27–30.** Characteristic distances of the four-rung ß-solenoid architecture are indicated. (from Vázquez-Fernández E *et al.,* PloS Path 2016)

One of the most important advantages of cryo-EM technique is the preservation of the native structure of the specimens analyzed and gives more realistic measurements than other techniques. The proposed structure [72] is based on the study of prion amyloids purified from transgenic mice expressing GPI-anchorless PrP 27–30 (tg44). Cryo-EM analysis determined the average fibril segments constituted by repeating unit of 19.1 Å. This measurement is in agreement with ß-solenoid architecture that is expected to have a height of 19.2 Å (4 spaces of 4.8 Å between individual β-strands). After 3D reconstructions of these fibrils, the data collected revealed two distinct protofilaments, and, together with a molecular volume of 18,990 Å$^3$, predicted the average height of each PrP 27–30 molecule as ~17.7 Å. This single particle analysis proposes an assembly unit along the fibril axis of 20 and 40 Å might be composed by two PrP$^{Sc}$ monomers configured in head-to-head arrangement. (Fig. 1.6). Another possible organization of these units is the head-to-tail that

gives rise to polar fibrils structure but the ~40 Å signal obtained [72] would favor the head-to-head model. (Fig. 1.6)
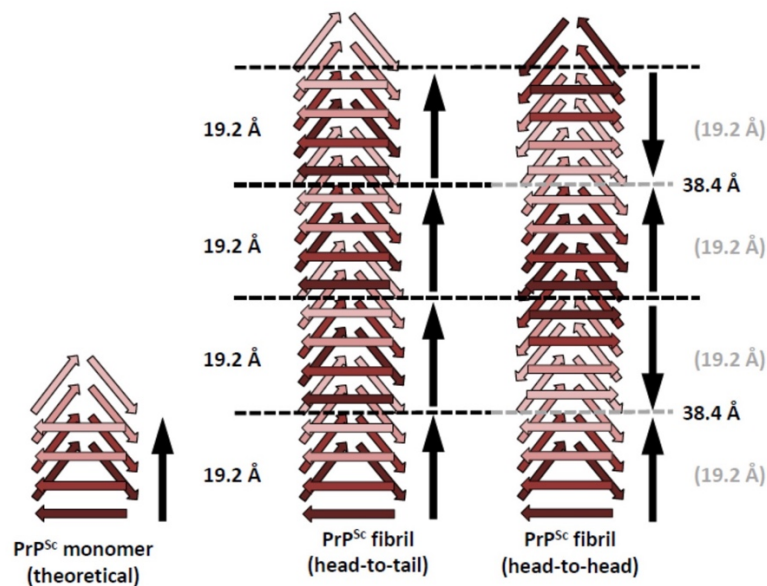


**Fig 1.6. Schematic representation of head-to-tail or head-to-head possible architecture of PrP$^{Sc}$ amyloid fibrils.** (from Wille H *et al.*, Pathogens 2018)

All these observations were in agreement with previous X-ray fiber diffraction results and provided clear evidence that the structure of the core of PrP$^{Sc}$ contains a four-rung β-solenoid fold [76]. The high compact nature of β-solenoid core is also congruent with the PK resistance of C-terminal core of PrP (PrP27-30) while the unstructured N-terminal residues were easily digested. On the other hand, it has been observed also the presence of smaller PK-resistant fragments besides PrP27-30 [77, 78] in "atypical" PrP$^{Sc}$ conformations. Particularly, many of these conformations are cleaved by PK at a position around 150-153 Amino Acids (AA) of PrP [79] that suggest the presence of an important loop that expose residues for PK cleavages also in the C-terminal domain of the PrP [79-81].

*1.4.3 Propagation mechanism of PrP$^{Sc}$*

The key pathogenic feature of PrP$^{Sc}$ consists in the ability to transmit its misfolding to the normal PrP$^{C}$ through a mechanism still poorly understood. Two different models have been proposed: (i) the template assisted model and (ii) the nucleation-polymerization model.

The template assisted model (or refolding model) assume that the conversion of PrP$^{C}$ and PrP$^{Sc}$ is prevented by a high-energy barrier. The interaction with exogenously introduced PrP$^{Sc}$ and PrP$^{C}$ induce the conformational conversion in a further PrP$^{Sc}$. This model implies the formation of heterodimeric PrP$^{C}$-PrP$^{Sc}$ unit that would initiate the conformational change of PrP$^{C}$ and became an homodimeric PrP$^{Sc}$-PrP$^{Sc}$. This latter might interact with other homodimer and eventually form larger aggregates. The rate-limiting state in this model is represented by the dimerization between PrP$^{C}$ and PrP$^{Sc}$ monomers.

The nucleation-polymerization model (or seeding model) proposes that PrP$^{C}$ and PrP$^{Sc}$ are in a reversible thermodynamic equilibrium. PrP$^{Sc}$ represent a minor and transient isoform and might be stabilized only when forming highly ordered structures, referred as nuclei or seeds. In such seeds, PrP$^{Sc}$ becomes stabilized and further PrP$^{Sc}$ can be recruited and eventually aggregate to amyloid structures. Fragmentation of PrP$^{Sc}$ aggregates increases the number of the nuclei that can recruit further PrP$^{Sc}$ molecules and results in the replication of the agent. The rate-limiting step of this model is the formation of the stable PrP$^{Sc}$ nucleus. This step reflects the lag phase of spontaneous conversion and it is accelerated by adding preformed PrP$^{Sc}$ seeds.

A schematic representation of these models is reported in Fig. 1.7.
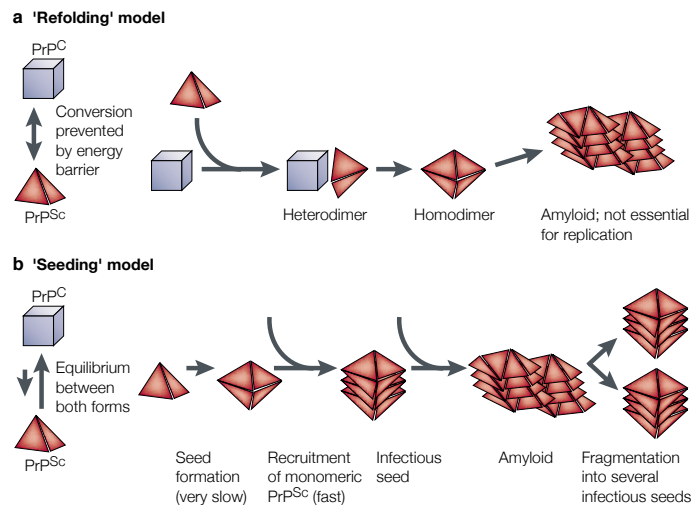
**Fig. 1.7 Schematic representation of the models for prion propagation.** The template assisted model (or refolding model) (A) and the nucleation-polymerization model (or seeding model) (B). (from Aguzzi *et. al.*, Nat Rev Mol Cell Biol. 2001)

These two models are not mutually exclusive and might represent different stages of PrP$^{Sc}$ propagation. In fact, the initial seed could be produced by nucleation-polymerization process while the template assisted model might be involved in the elongation of the fibrils. In both models, the $\Delta$G energy of the oligomeric or amyloid structures of PrP$^{Sc}$ is lower than the energy of the native folding of the PrP$^{C}$, and this shift thermodynamically favor this conversion in an exponential way (Fig. 1.8).
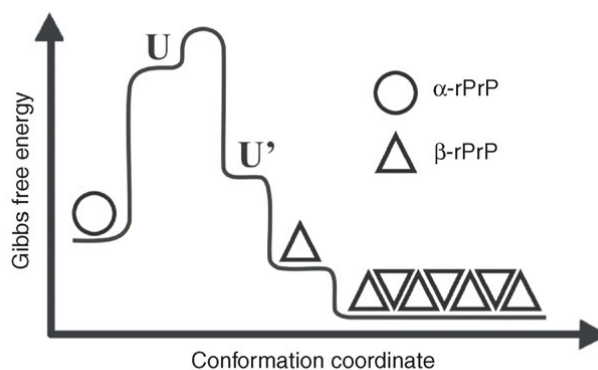


**Fig. 1.8 Free energy profile for the conversion of PrP$^{C}$ (referred as α-rPrP, circle) into PrP$^{Sc}$ (referred as β-rPrP, triangle).** This diagram highlights the slightly higher free-energy of PrP$^{C}$ with respect to misfolded PrP$^{Sc}$ while PrP$^{Sc}$ amyloids (triangles) displayed lower free-energy of both isoforms. The U and U' represent the unfolded state of the protein. (modified from Silva *et al.*, Cell 2008)

Recent findings about the PrP$^{Sc}$ structure enable the formulation of structural-based hypothesis on how PrP$^{Sc}$ prions propagate [82]. The β-solenoid structure has native templating capabilities through the upper- and lowermost rungs that contain "unpaired" β-strands that can transmit their hydrogen-bonding pattern into any amyloidogenic protein by direct contact [83]. The proteins that contain β-solenoid have evolved to be capped by loops or α-helices that protect the external edge of the protein from uncontrolled β-sheet propagation. Supporting this observation, the elimination of this edge capping by protein engineering produces unstable peptides that undergo to edge-to-edge-driven oligomerization [84]. Accordingly, the proposed β-solenoid structure of PrP$^{Sc}$ can template an incoming unfolded PrP protein into an additional β-solenoid structure and produce a fresh "sticky" surface that sustain the templating propagation mechanism [85] (Fig. 1.9).
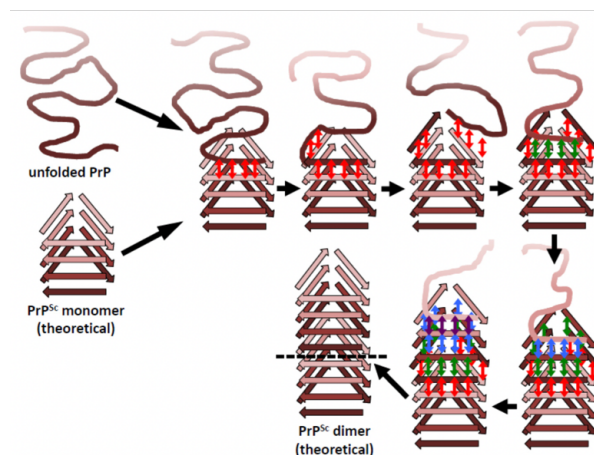


**Fig 1.9. Possible mechanism of PrP$^{Sc}$ templating mechanism.** In this schematic representation were reported the head-to-tail mechanism of PrP$^{Sc}$ templating. The unfolded PrP protein interacts with the uncapped β-solenoid edge of the PrP$^{Sc}$ dimer and adopts β-strand conformation by forming backbone hydrogen-bonds (indicated with red arrows). Once all the rungs have been templated (green, blue), the new molecule of PrP$^{Sc}$ provide "fresh" templating surface for other PrP proteins. (from Wille H *at al.* Pathogens 2018)

In this model, it's important to take into account that the large carbohydrate chains attached to PrP peptide probably impose constraints to this templating process. However, two possible mechanisms were proposed for this interaction: the head-to-head or head-to-

tail interaction. At the moment, considering structural data collected from cryo-EM experiments [82] the head-to-head model appears to slightly favor the head-to-tail mechanism but the evidence is not strong enough to resolve this point [85]. By these mechanisms, PrP$^{Sc}$ is able to accumulate in brain tissues of infected hosts and, with other neuropathological changes, represent the characteristic hallmark of prion pathologies.

## 1.5 Common pathological features of prion diseases

The common neuropathological characteristics of prion diseases comprise: (i) spongiform changes of the gray matter, (ii) reactive astrocytosis and microglial proliferation, (iii) neuronal loss and (iv) accumulation of PrP$^{Sc}$ [86].

### 1.5.1. Spongiform changes

Spongiform degeneration of the brain tissue is the pathognomonic lesion of prion disorders. It is characterized by numerous rounded vacuoles in the gray matter with a diameter from 2 to 20 μm. Microvacuolar spongiform change made of small vacuoles or confluent large coalescent vacuoles can be formed. These degenerations give the typical spongiform-like appearance of the brain tissue (Fig. 1.10).
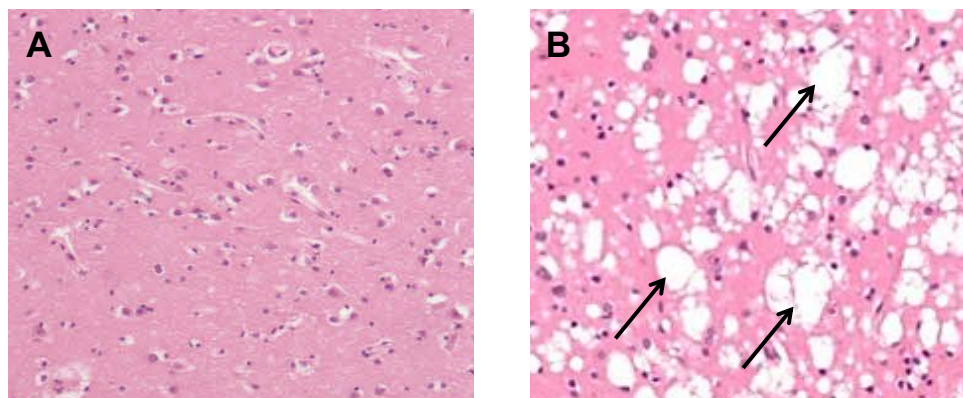


**Fig 1.10. Hematoxylin and eosin stained sections of brain tissue.** Normal brain tissue (A) and prion affected brain tissue (B). Arrows indicates the vacuoles typical of spongiform alteration.

## 1.5.2. PrP$^{Sc}$ accumulation and detection

The deposition of the disease-associated protein PrP$^{Sc}$ is the main neuropathological hallmark of these diseases. PrP$^{Sc}$ deposition can be (i) synaptic, (ii) perivacuolar, (iii) perineuronal and (iv) in plaque (Fig. 1.11) but these patterns may overlap in the same affected brain [87]. Focal PrP$^{Sc}$ accumulation can be divided in: plaque-like deposits (that are negative for specific amyloid staining) and amyloid plaques (that are detected by thioflavin-S or Congo Red). The distribution of PrP deposits and the spongiform degeneration do not always correlate [88].

| Synaptic | Perivacuolar | Perineuronal | Plaques |
|----------|--------------|--------------|---------|
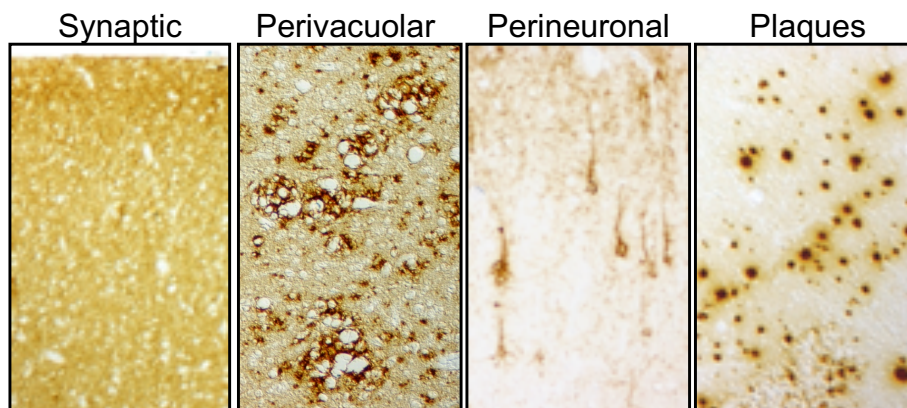


**Fig 1.11. PrP$^{Sc}$ deposition patterns.** Different PrP$^{Sc}$ distribution patterns can be appreciated by immunohistochemical staining (after PK-treatment) of human brain tissues with anti-PrP antibody. (from Budka *et al*., Neurodegeneration: The Molecular Pathology of Dementia and Movement Disorders (eds D. W. Dickson and R. O. Weller) 2011)

PrP$^{Sc}$ is able to accumulate in specific brain structures leading to typical patterns of deposition. This characteristic appears closely related to the conformation of PrP$^{Sc}$ and produce specific signatures of accumulation of PrP$^{Sc}$ in affected brains [89]. An example of this tropism for brain structures can be appreciated in human prion pathologies where distinct conformation of PrP$^{Sc}$ accumulate in different brain regions (Fig. 1.12).

PrP<sup>Sc</sup> conformation 1    PrP<sup>Sc</sup> conformation 2
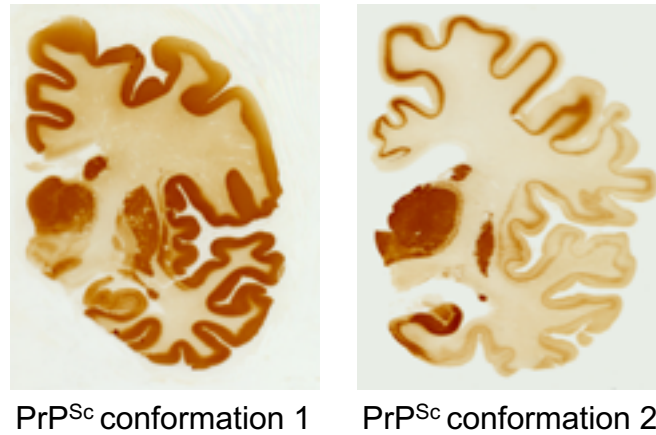
**Fig 1.12. Accumulation of different PrP$^{Sc}$ conformations in human brains.** Immunohistochemical staining of PK-resistant PrP in human brains of patients affected by prion pathology showed different accumulation of pathogenic PrP$^{Sc}$ among brain regions.

PrP$^{Sc}$ can be detected post-mortem by (i) immunohistochemical examination of brain tissues and (ii) biochemical assays using brain homogenates. Histologically, PrP$^{Sc}$ can be detected on fixed-brain slices after treatment with PK enzyme and immunodetection with anti-PrP antibodies. Since PrP$^{C}$ and PrP$^{Sc}$ share the same amino acidic sequence, PK treatment is necessary for removing all the PrP$^{C}$ from the tissue and permitting the detection of the PK-resistant isoform of PrP. Biochemically, PrP$^{Sc}$ can be easily detectable in brain tissues by means of Western blotting after enzymatic digestion with PK. This assay, supported by neuropathological examination, is routinely used as diagnostic tool for prion diseases.

*1.5.3. Gliosis*

Prion diseases are characterized by the presence of prominent gliosis involving the proliferation of microglia and neuroinflammation of microglia and astrocytes. Increased glial fibrillary acidic protein (GFAP) is a common marker for astrogliosis in prion diseases [90] that is closely associated with the accumulation of PrP$^{Sc}$. The role of reactive

astrocytes that can be deleterious for neuronal survival in prion disease is unclear and may stimulate neurodegeneration in this pathological context. Microglial activation appears at early stages of prion diseases, before both spongiform changes and neuronal loss [91] and might contribute to neurodegeneration. Moreover, the evidence that the distribution of microglial proliferation correlates with spongiform changes and astrogliosis suggests a close association between microglial activation and neurodegeneration induced by prions [92].

## 1.6 PrP$^{Sc}$ tissues distribution in human and animals

The distribution of PrP$^{Sc}$ in peripheral tissues of human and animal TSEs is extremely variable and depends on the type of prion disease but generally its accumulation lower than that of brain tissue.

### 1.6.1 Animal TSEs PrP$^{Sc}$ distribution

- BSE: PrP$^{Sc}$ is mainly confined to the Central Nervous System (CNS), spinal cord, spinal ganglia, retina, bone marrow, distal ileum [93-95], peripheral nerves [96, 97] and skeletal muscle [98];
- Scrapie: PrP$^{Sc}$ was found in CNS, brainstem, palatine tonsils, ileum Peyer's patches, spleen, adrenal gland, pancreas, heart, skin, urinary bladder, mammary glands, salivary gland [99], lung, liver, kidney, skeletal muscle [100], blood [101], milk [102], saliva [103] and oral cavity [104];

- CWD: PrP$^{Sc}$ was found in CNS, brainstem, retina, peripheral nerves, spleen, lymph nodes, tonsils, esophagus, rectum, skin, pancreas [105-107], nasal mucosa, saliva [108, 109], urine [109], feces [110] and blood [108];

- TME: PrP$^{Sc}$ was found in CNS, spleen, mesenteric and retropharyngeal lymph nodes, thymus, kidney, liver, intestine and salivary gland [111, 112];

- FSE: PrP$^{Sc}$ was found in CNS, spinal cord, spinal ganglia, nerve of the tongue, sciatic nerve, optic nerve, enteric nervous system and adrenal gland [113].

## 1.6.2 Human TSEs PrP$^{Sc}$ distribution

As for animal TSEs, also in human TSEs the distribution of PrP$^{Sc}$ depends on the type prion disease. In the most common human prion disease, the sporadic CJD (sCJD), the PrP$^{Sc}$ was found in CNS, retina [114], optic nerve [115], spinal cord [116], peripheral nerves [117], blood [118], urine [119], CSF [120, 121], olfactory mucosa [122] and, in some cases, in spleen and muscle after concentration by sodium phosphotungstic acid (PTA) precipitation [123, 124]. In the variant CJD prion pathology (vCJD) the PrP$^{Sc}$ is more diffuse in peripheral tissues than sCJD and was found in spleens, tonsils, lymph nodes, retina, pituitary gland, thymus, proximal optic nerve [125], appendix, skeletal muscle [124], ileum, adrenal gland, pancreas, blood [126, 127] and urine [128].

## 1.7 Transmissibility of prions

### 1.7.1. Natural transmission of prions

Despite the fact that prion diseases are not contagious by contact they are transmissible (i) per-orally and (ii) parenterally. A classical report of natural transmission of prions is the

BSE epidemic outbreak in the mid-eighties that lead to about 180,000 cases of animals infected caused by the feeding of scrapie-contaminated meal to cattle [129]. Scrapie spreading in sheep appears to propagate by oral route by infected goat milk consumption [130], through ingestion of prion-infected birth-related tissue (placenta) [131] or by contaminated environment with secretion (urine, feces, saliva) of infected animals [132]. Recently, CWD horizontal animal transmission was reported and appears to readily occur via may models like oral and nasal route by direct contact with infected urine, feces or saliva from animals in both clinical and pre-clinical stage of CWD infection [133]. Another evidence of prion transmissibility is the Kuru epidemic in the first half of 20th century in Papua New Guinea. The transmission of Kuru prions was caused by cannibalism associated with funeral rituals [134]. The zoonotic transmission of BSE to humans caused by the ingestion of BSE-contaminated foodstuff was responsible for the emergence of variant CJD (vCJD) [135]. Notably, horizontal transmission of vCJD by blood transfusion have been reported in 5 cases [136].

*1.7.2. Iatrogenic transmission of natural prions*

Almost 300 cases of iatrogenic prion transmission in humans were caused by medical interventions [137]. Most of them were due to (i) administration of cadaveric human growth hormone [138], (ii) transplantation of dura mater [139], (iii) corneal transplants [140], (iv) stereotactic EEG recording [141] and (v) use of contaminated surgical instruments [142].

*1.7.3 Experimental transmission of prions*

By taking advantage of their infectious properties, different PrP$^{Sc}$ conformations were used to perform experimental infection of wild-type and transgenic animal models of the disease with the aim of (i) studying their molecular, biochemical, and infectious features and (ii) assessing the susceptibility to prion infection. The experimental transmission can be achieved by different routes including: intracerebral, intraocular, instraspinal, intraperitoneal [143], intravenous [144], subcutaneous, dental [145], oral [146], intranasal [147] or by aerosol [148]. However, the efficiency of all these transmissions depends on multiple variables including: (i) the route of infection (intracerebral infection is the most efficient) and (ii) the susceptibility of the host where the prion material was transmitted. One of the principal features of PrP$^{Sc}$ is its ability to be transmissible to some host species and not others. Indeed, the transmission of prions occurred in more successful way within the same species and is much less efficient between different species. This phenomenon is known as "species barrier" and produces an extension of the incubation time or total resistance to the disease in inter-species infections [149].

## 1.8 The concept of PrP$^{Sc}$ strains and the species barrier

*1.8.1. Prion strains*

One of the most intriguing aspect of prion pathologies is the fact that the physiological PrP$^{C}$ can misfold in different conformations of PrP$^{Sc}$ [150]. These conformations, referred to as "prion strains", are able to induce unique clinical, neuropathological and biochemical alterations in animal and human hosts [151]. Indeed, in humans there were described at least six different strains of PrP$^{Sc}$ responsible of distinct pathological phenotypes [152]. A

prion strain can be identified on the basis of: (i) the time between the inoculation and the manifestation of the pathological symptoms (incubation time) and the time between the inoculation and the terminal stage of the disease (survival time) [153], (ii) clinical signs, (iii) pattern of PrP$^{Sc}$ deposition in the brain [154] and (iv) degree of spongiform alterations in specific brain areas [155] (Fig. 1.14). Biochemically, there are four main characteristics enabling prion strain classification (after PK digestion): (i) the electrophoretical mobility of the unglycosylated band (21kDa or 19kDa referred as Type1 or Type 2 respectively, Fig 1.13B), (ii) the glycosylsation profile of PrP (glycoform ratio) [156] (Fig. 1.13A), (iii) the extent of protease digestion [157] and (iv) the resistance to denaturation using chaotropic agents (e.g. guanidine-hydrochloride) [158] (Fig. 1.14). After Peptide-N-glycosidase F (PNGase F) digestion which is able to cleave the asparagine-bound N-glycans, the glycosylation of PrP protein were completely removed and only one isoform was observed after Western blot analysis. This treatment permits the precise identification of the molecular weight of the un-glycosylated band corresponding to Type 1 (21kDa) or Type 2 (19kDa) (Fig. 1.13B).
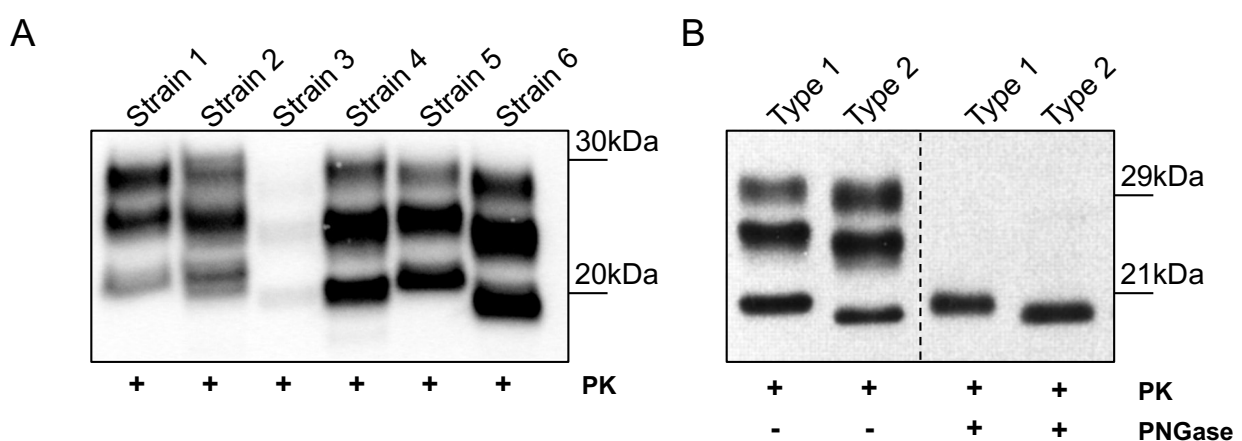


**Fig 1.13. Example of different PrP$^{Sc}$ strains and PNGase experiment.** PK digestion and Western blot analysis of different human prion strains. These PrP$^{Sc}$ showed different electrophoretical mobility of the unglycosylated band (e.g. Strain 5: 19kDa (T1) or Strain 6: 21kDa (T2)) and distinctive glycosylation profile with predominance of one isoform over the others (e.g. Strain 1: di-glycosylated, Strain 6: mono-glycosylated) (A). PNGase digestion which removes the glycosylation of PrP$^{Sc}$ permit the precise identification of the molecular weight of the un-glycosylated isoform of PrP (B).

Different analytical approaches, including Fourier Transform Infrared Spectroscopy (FTIR), Atomic Force Microscopy (AFM) and Circular Dichroism (CD) demonstrated that the differences in prion strains are likely associated to specific conformations of PrP$^{Sc}$ [159, 160]. From the structural point of view, slight differences in the arrangement of β-strands and loops of PrP$^{Sc}$ molecule were suggested as possible sources of structural variability giving rise to different strains of PrP$^{Sc}$ [161]. Particularly, differences in the topography of the upper- or lower-most rung of the proposed β-solenoid structure of the PrP$^{Sc}$ monomer might change the templating surface and permit the generation of specific conformational variants of PrP$^{Sc}$. These considerations were supported by two common behavior observed for prion strains: (i) the ability to transmit the disease *in vivo* and maintain the same characteristics among susceptible host [162] and (ii) the existence of a species barrier that partially hamper the infection between hosts with different PrP$^{C}$ amino acidic sequences [163].
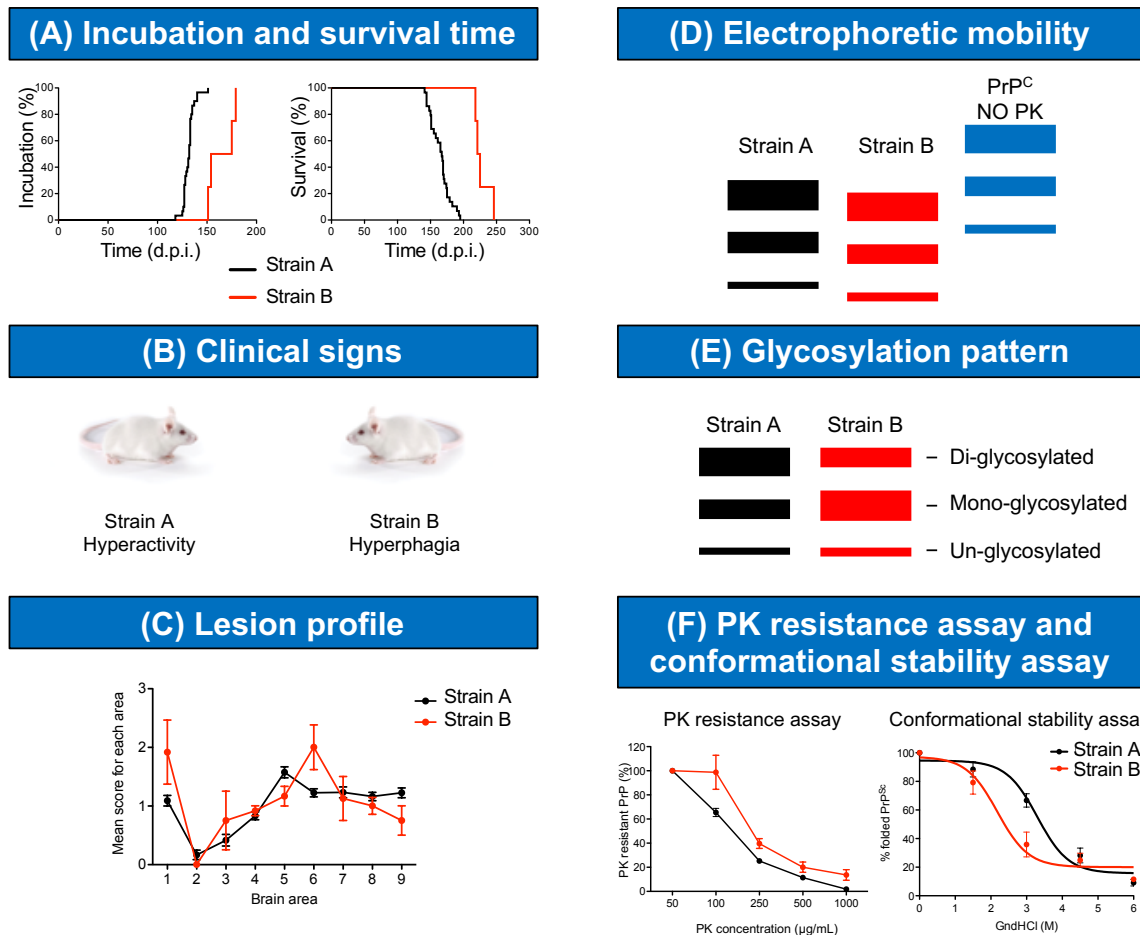
**Fig 1.14. Main biological and biochemical features used to distinguish different prion strains.** Differences between prion strains can be identified on the basis of biological and biochemical features that include: (A) the incubation periods, (B) the clinical signs and (C) the distribution of spongiform lesion and PrP$^{Sc}$ deposition (D) the electrophoretic mobility of PrP$^{Sc}$ after PK treatment, (E) the glycosylation pattern of PrP$^{Sc}$ and (F) its resistance to PK digestion and stability to chaotropic agent (GdnHCl) treatment.

### 1.8.2. The species barrier

A key characteristic of prions is their ability to infect a limited number of other species. This phenomenon, known as species barrier, is likely imposed by the amino acid sequence of host PrP$^{C}$ that may drive the PrP$^{C}$-PrP$^{Sc}$ interactions and permit or prevents prion propagation. In the structurally-based propagation model previously proposed in Fig. 1.9, the entire sequence of PrP seems involved in this mechanism and contributes with its own steric and amino acidic charge constraints. For these reasons, the sequence homology

between PrP$^{Sc}$ and the host PrP$^{C}$ appear significantly involved in inter-species transmission of prion diseases [164-166] and has also been referred to as 'sequence barrier' [167]. Nevertheless, rare cases of natural transmission between different hosts were reported. It's widely accepted that the consumption of BSE infected meat induce in humans a prion pathology named variant Creutzfeldt-Jakob disease (vCJD) [135, 168]. Biochemical studies demonstrated that the vCJD in humans and the BSE in cow arise from the same prion strain confirming the direct relationship between these two pathologies. [135, 169]. Intriguingly, BSE prion strain was able to cross the species barrier not only with humans but also with other animal hosts including exotic felines such as tiger and cheetah [170], non-human primates [171] and domestic cats [172]. In some cases, the same BSE prion strain was able to induce the generation of different host-specific prion strains with differences in clinical changes, neuropathological alterations and biochemical features of PrP$^{Sc}$ [169]. Experimentally, the species barrier can be overcome by repetitive animal passages. If the species barrier is partially permissive to the transmission, the prion strain used as inoculum gradually adapts to the new host and acquires stable infectious properties after a number of passages depending on the characteristics of strain and animals. An example of this "crossing" experiment is the TME transmission to hamsters. The origin of TME was attributed to scrapie-infected foodstuff used to feed minks in UK farms, but studies of the etiology of this prion disorder are not conclusive [173]. The inoculation of TME in the Syrian Hamster gave rise to two different prion strains: the first one induced severe and rapid pathological alterations and hyperactivity in animals (Hyper, HY) while the second one induced slow disease progression and lethargy (Drowsy, DY) [174, 175]. Biochemical and histological analysis of CNS confirmed the presence of different neuropathological alteration likely associated with two different PrP$^{Sc}$ conformations. Such PrP$^{Sc}$ showed unique electrophoretical mobility, resistance to PK

digestion and stability against Guanidine Hydrochloride [160, 176, 177]. A proposed explanation for this phenomenon might be the fact that TME is not a pure strain but is instead composed by at least two pathological PrP$^{Sc}$ conformations and only one prevails in mink [178]. When TME is injected in hamsters, two distinct PrP$^{Sc}$ conformations arises highlighting the possibility that prions undergo to process of adaptation or selection according to changes in the environment of replication although lacking DNA or RNA [179].

## 1.9 Darwinian evolution of prions

When prions are successfully transmitted between different species the characteristics of the original PrP$^{Sc}$ may adapt to the new host environment and result in the generation of a new prion strain or a multitude of them [180]. Particularly, after the inter-species transmission the new prion strain undergoes to a process of "selection/adaptation" accompanied with the reduction of the incubation time, increasing of attack rate, changes in neurotropism and PrP$^{Sc}$ deposition pattern and changes in PrP$^{Sc}$ biophysical properties [181]. With this observation it's possible to speculate that the (i) sequence of host PrP$^{C}$, (ii) species-specific cellular cofactors or (iii) species-specific PrP$^{C}$ glycosyl composition can play a pivotal role in prion transmission and adaptation [182]. However, these considerations suggest that the mechanism behind the species barrier and the phenomenon of prion adaptation might be influenced by different variables.

Two main hypotheses were proposed as possible mechanism for the prion adaptation observed in animals: (i) the "cloud" hypothesis and the (ii) deformed templating model schematically represented in Fig. 1.15.

The cloud hypothesis, originally proposed by Charles Weissmann in 2010 [183], infers that prion strains are composed by a population of isolates with different abnormal conformations (conformational variants) due to spontaneous changing in PrP$^{Sc}$ structure [183, 184]. Modifications of the replication environment allows the most efficient variant to become the predominant component of the population by replicating over the others [185]. This model is in agreement with the natural selection postulated by Charles Darwin in the "The Origin of Species" that described the evolution process of a population over the course of the generations that results in the survival of individuals whose features are most suitable for such environment leading to their perpetuation.

The other mechanism proposed, the deformed templating [186], postulates that the templating process is imperfect and will sometimes result in generation of altered PrP conformations. This process can be enhanced by changes of the replication environment that actively contribute to the generation of PrP$^{Sc}$ variants and impose an "evolutionary pressure" able to select the conformations that better fit in the new context of replication. Particularly, according to this model, when a PrP$^{Sc}$ template is not compatible with (i) the new environment or (ii) the amino acidic sequence of host PrP$^{C}$ a range of new conformational variants of PrP$^{Sc}$ are produced via deformed templating. In other words, this model postulate that one misfolded pattern can seed an alternative self-replicating state with a different folding pattern [187] and the variant that best fits with the new environment can emerge. The deformed templating does not exclude the "cloud" hypothesis but suggests a mechanism by which conformational variants of a "cloud" undergo structural modification in a new environment and gives rise to a new "cloud" of conformations.
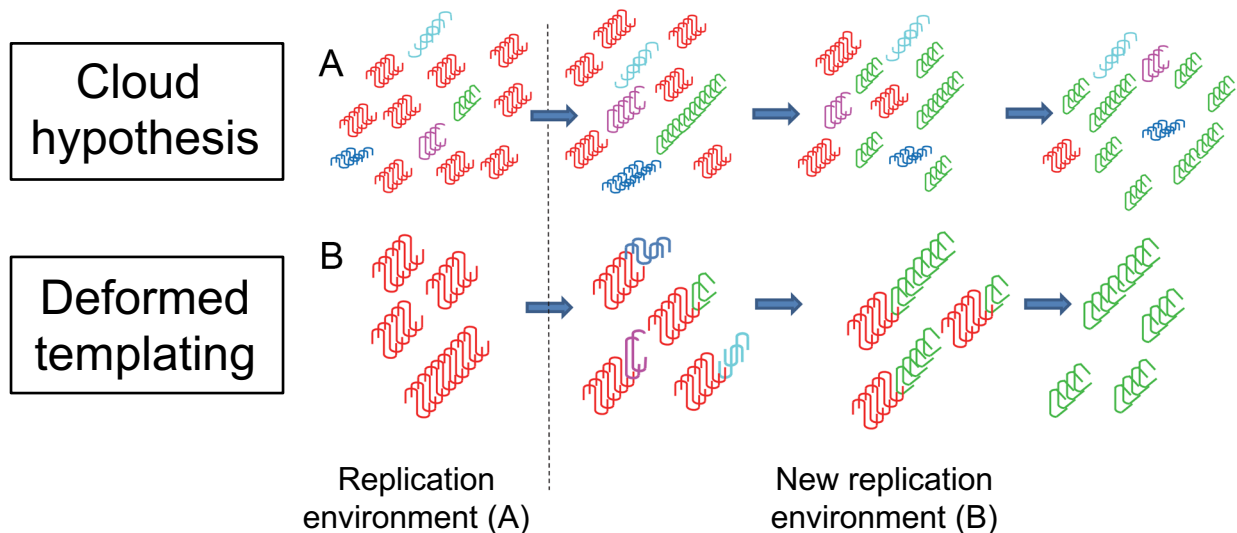
**Fig. 1.15 Schematic representation of proposed mechanism behind prion strain adaptation.** The "cloud" hypothesis (A) infers that a prion isolate is composed by different conformational variants, more (red) or less (other colors) represented. The modification of the environment (from A to B) provides selective advantages to a specific conformation (green) that is able to efficiently replicate and lead to an adaptation of the prion population. The deformed templating mechanism (B) postulates that the PrP$^{Sc}$ variants arises via numerous PrP$^{Sc}$-dependent trial-and-error events that *de novo* generates a conformation that fit better in the new environment and replace the original PrP$^{Sc}$. (modified from Makarava N. and Baskakov I.V., PloS Path 2013)

These models are sustained by experimental evidence that highlight the ability of prions to evolve and adapt to different environment of replication. According to the cloud hypothesis, the classical example of prions heterogeneity is the generation of a multitude of prion strains after the injection of a pool of scrapie-infected sheep brains in mouse models [180]. The biological cloning of prions provides some information regarding the composition of a prion strain. In this experimental procedure, similar to principles used in classical virology, the mice are inoculated with a limiting dilution of prion isolates which consist of 100-10000 PrP$^{Sc}$ particles (referred to uncloned prion strain). The transmission *in vivo* was repeated 2-3 times to the point in which a single prion strain appears to be present. The major limitation of this procedure is represented by the number of PrP$^{Sc}$ particles necessary for the animal infections. Indeed, a limiting dilution of a prion isolate likely contains multiple prion variants that might generate, after biological cloning, prion

strains composed by different PrP$^{Sc}$ conformations. However, this method might permit the isolation of a "cloned" prion strain that maintains stable pathological and biochemical characteristics after animal passages. For example, when an uncloned mouse-adapted prion strain derived from scrapie-infected sheep brains (22C) was inoculated in other mice with different genotypes the appearance of a new prion strain was observed (22H). Cloned 22C prion strain was able to keep its characteristics through animal passages indicating that the uncloned 22C prion strain was composed of a mixture of different conformational variants [180]. Modifications of the replication environment (e.g. with drugs known to interfere with prion replication like quinacrine [188] or swainsonine [183]) lead to the selection of drug-resistant prion populations. Particularly, in animals treated with quinacrine there was a selection of a conformational variant different from that observed in the brains of untreated controls [189]. Also, the inter-species transmission of a prion strain may generate new prion strains. Transmission of cloned 139A prion strain (derived from scrapie) from mouse to hamster and back to mouse generates a new prion strain, the 139H/M [190].

In direct support of the deformed templating model, fibrillization experiment where mouse recombinant PrP was induced to aggregate with hamster amyloids generated fibrils with different folding state within individual amyloid. The folding pattern of hamster amyloids was not compatible with the amino acidic sequence of mouse PrP and hybrid mouse-hamster fibrils, with two distinct folding patterns, were produced [191].

Experimentally, it's difficult to prove that the multitude of PrP$^{Sc}$ appeared upon environment changes can be caused by *de novo* generation of conformational variants or due to preexisting minor PrP$^{Sc}$ structures in the original prion strain [192, 193]. These two models are not mutually exclusive and might represent different aspects of the prion adaptation/selection phenomenon.

**1.10 *In vitro* amplification and detection of PrP<sup>Sc</sup>**

In recent years, two innovative techniques for prions amplification and detection were developed: (i) the Protein Misfolding Cyclic Amplification (PMCA) that allows the amplification of PrP$^{Sc}$ by mimicking *in vitro* the pathogenic replication of prions observed *in vivo* and (ii) the Real-time Quaking Induced Conversion (RT-QuIC) which consent the detection of trace-amount of PrP$^{Sc}$ in biological samples.

*1.10.1 Protein Misfolding Cyclic Amplification*

Originally developed by Claudio Soto in 2001 [194] the Protein Misfolding Cyclic Amplification is an ultrasensitive technique able to sustain the phenomenon of prion replication *in vitro* but in an accelerated manner. Particularly, PMCA consists in cycles of incubation and sonication of samples that contain trace amount of PrP$^{Sc}$ in presence of an excess of PrP$^{C}$ provided by brain homogenates (BH) of healthy animals (wild-type or transgenic). During the incubation phase, PrP$^{Sc}$ induces the conversion and aggregation of PrP$^{C}$ substrate. The sonication phase is able to fragment the PrP$^{Sc}$ aggregates in small polymers (referred as "seeds") which are able to further convert new molecules of PrP$^{C}$ to PrP$^{Sc}$. These two phases are repeated in a cyclic manner (Fig. 1.16). At the end of the reaction an aliquot of amplified products is diluted in freshly prepared substrate and exposed to additional cycles of sonication and incubation (referred to as rounds of PMCA). Therefore, after several rounds, the amount of PrP$^{Sc}$ increase exponentially to a level easily detectable with common biochemical assays (e.g. PK-digestion and Western blot analysis) (Fig. 1.16) [195, 196].
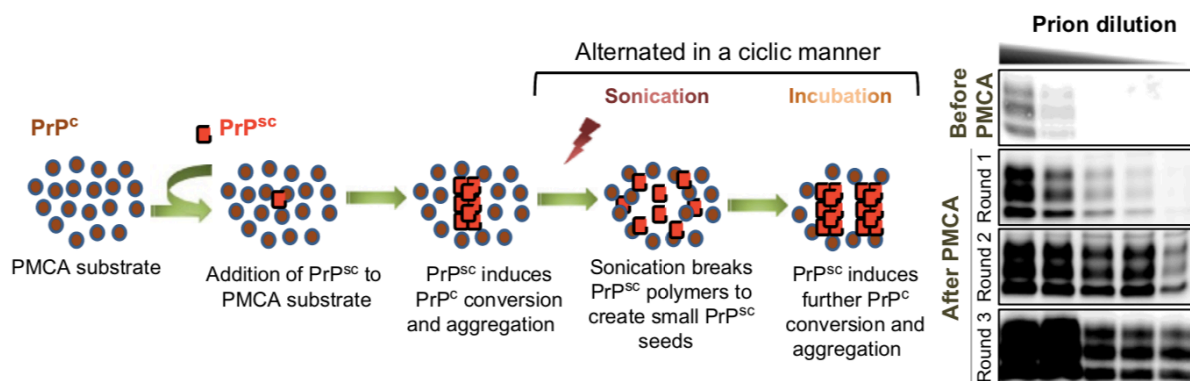
**Fig. 1.16. Schematic representation of PMCA technique.** PrP$^{Sc}$ (red square) are added to the substrate (made of PrP$^{C}$) (purple circles) and then subjected to cycles of sonication and incubation. Western blot analysis (right panel) revealed that after three rounds of PMCA is possible to detect trace amount of prions undetectable before PMCA. (from Moda F., Prog Mol Biol Transl Sci 2017)

One of the most important features of PMCA lies in the fact that the amplified products seem to retain the biochemical and infectious features of the original PrP$^{Sc}$ [197] and for this reason it represents a great tool for studying (i) the prion biology [198], (ii) the mechanism of prion transmission [199], (iii) the species barrier [200], (iv) the strain adaptation phenomena [201] and has been recently optimized for (v) diagnostic purposes [126, 128].

*1.10.2 Application of PMCA to study in vitro the species barrier and prion adaptation*

PMCA has been successfully used for amplifying a large variety of prion strains and the products maintained both infectivity [197, 202] and strain specificity [203]. For this reason PMCA can be applied to study the species barrier and the mechanism of prion adaptation. An example of PMCA application for these studies was reported by Green and coworkers in 2008 [203]. Using as substrate transgenic mice expressing cervid prion protein Tg(CerPrP), PMCA was able to replicate with high fidelity CWD prion strain. Using the

same method to amplify RML, PMCA demonstrate the ability to overcome the species barrier and produced a novel prion strain similarly to that observed in animal transmission experiments using Tg(CerPrP) mice. Notably, the abrogation of the transmission barrier in PMCA required much shorter period of time respect to classical animal transmission and enable the characterization of new prion strains that arose from inter-species transmission. Nevertheless, with PMCA it is possible to generate artificial new prion strains of species resistant to prion infection [204]. The ability of this technique to cross *in vitro* some transmission barriers by forcing the process of amplification and generating prion disorders in species assumed to be resistant to prion infection [204] might turn a disadvantage for studying this phenomenon and correlate the *in vitro* results with the natural mechanism of prion transmission. Another important aspect of prion biology that can be studied with PMCA technique is the adaptation of prions in response to changes of the replication context. Inter-species animal transmission of prions generated new strains with specific biochemical and neuropathological features that were able to change and adapt during animal passages and the same mechanism of adaptation can be studied also *in vitro* by PMCA. Indeed, as reported by Castilla and colleagues in 2008 [200], PMCA was successfully applied to overcome the large *in vivo* species barrier between hamsters and mice [190] and generate new prion strains. Particularly, RML mouse prion strain was added to normal hamster brain homogenate and subjected to PMCA. The amplified product composed by misfolded hamster PrP$^C$ was able to induce prion pathology in wild type hamsters. Similarly, 263K hamster prion strain was subjected to serial rounds of PMCA amplification using mouse brain homogenates and generated a PrP$^{Sc}$ which was infectious when challenged in wild type mice. Notably, these two new prion strains possess different neuropathological and biochemical characteristics from RML mouse and 263K hamster prion strains. Serial rounds of PMCA amplifications revealed a progressive

adaptation of the newly *in vitro* generated prion strains with a progressive change of the biochemical characteristics. These findings suggest that PMCA might mimic the mechanism of prion stabilization following inter-species transmission observed in *in vivo* but in an accelerated manner. In the same year, Meyerett and colleagues [201] described the amplification of D10 strain of CWD prions using serial PMCA (sPMCA) with transgenic mouse expressing cervid PrP (Tg(cerPrP)1536) brain homogenate as substrate. The resultant amplified products induced prion disease in CWD-susceptible Tg(cerPrP)1536 mice with shorter incubation time respect to the D10 original strain, similarly to that observed *in vivo* with sub-passage of D10 inoculum. Notably, *in vitro*-amplified and animal-passaged D10 produced brain lesion profile in animals, glycoform ratios and conformational stability profiles of PrP$^{Sc}$ significantly different than those produced by the original D10 prion strain in Tg(cerPrP)1536 mice. These results highlighted another important aspect involved in prion adaptation, the effect of the biological environment where prion replicate. *In vitro* studies using PMCA may help in dissecting this aspect. As reported by Gonzales-Montalban N. and colleagues in 2013 [205], PMCA adaptation of 263K and HY hamster prion strains to RNA-depleted substrate and then re-adapted by amplification in normal brain homogenate containing RNA resulted in a stable transformation of the biophysical characteristics, in terms of resistance to PK treatment and stability to chaotropic agents, of the original PrP$^{Sc}$. These results suggested that other than changes in PrP amino acidic sequence also modification of the environment of replication can play an active role in prion adaptation and selection. Another experimental evidence of the fundamental role of the environment in prion adaptation was recently reported by Katorcha E. and colleagues [206]. In their work, hamster 263K prion strain was propagated under normal and RNA-depleted conditions using seral PMCA amplification conduct first in mouse brain homogenate and then re-adapted with PMCA in normal

hamster substrate. The amplification in normal mouse brain homogenate and then in hamster substrate produced an amplified product able to induce a prion phenotype in hamsters comparable to the original 263K. Surprisingly, 263K amplified in RNA-depleted mouse substrate and then re-adapted by PMCA amplification with normal hamster brain homogenate generated a new disease phenotype when serially passaged in animals. Notably, 263K amplification in RNA-depleted mouse substrate and then in RNA-depleted hamster homogenate completely abolished its infectivity suggesting that RNAs might be important for assuring a high fidelity of prion replication. Taken together, these lines of experimental evidence suggest that PMCA technique offer a great tool for studying phenomenon of species barrier but also for mimicking the adaptation process after inter-species transmission of prions in a faster manner and in well defined experimental conditions.

*1.10.3 Real-time Quaking Induced Conversion*

The RT-QuIC technique originally developed by Atarashi and colleagues in 2008 [207], is based on cycles of vigorous shaking and incubation in 96-well plates. Soluble recombinant prion protein (recPrP) is used as substrate for detecting trace amount of PrP$^{Sc}$ (referred as seeds), resulting in formation of aggregates and amyloid structures. During incubation, PrP$^{Sc}$ induce the conformational change of recPrP that aggregate and form large amyloid fibrils. These recPrP aggregates can be detected with fluorescence plate readers, using thioflavin-T (ThT) which binds amyloid structures. Thus, the increasing in fluorescence is proportional to the formation of the amyloids and was recorded in a real-time manner. The shaking phase promotes the fragmentation of the amyloid fibrils, forming more reactive seeds able to recruit more recPrP substrates and resulting in an exponential increase in

amyloid formation (Fig. 1.17). The parameters that affect the sensibility and specificity of the technique include: (i) truncation of recPrP substrates, (ii) temperature, (iii) shaking speed, (iv) shaking interval, (v) pH, and (vi) concentrations of detergent.
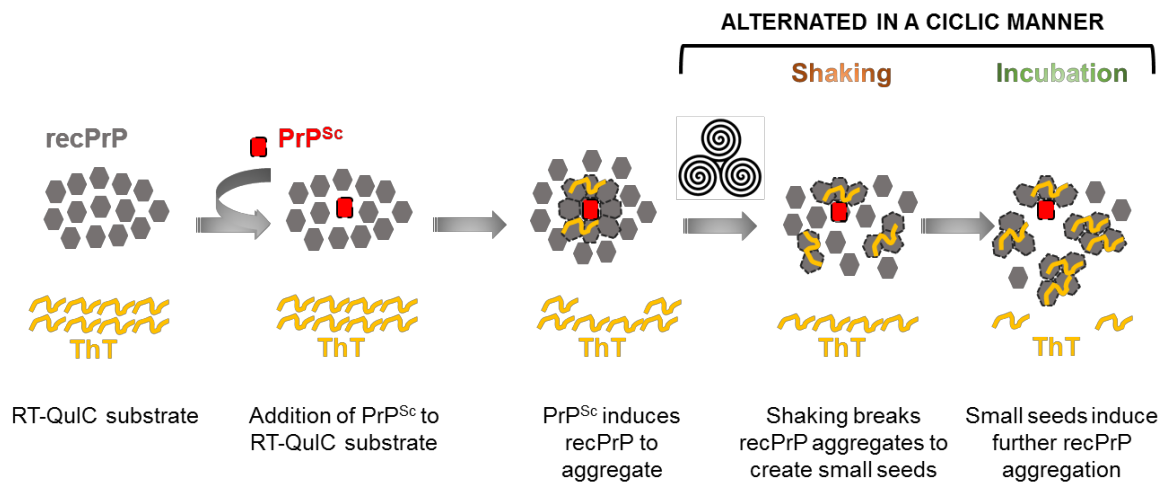


**Fig 1.17. Schematic representation of RT-QuIC technique.** Trace amount of PrP$^{Sc}$ (red square) are added to the substrate of recombinant PrP (recPrP, gray hexagons) with the addition of thioflavin-T amyloid fluorescent dye (ThT). PrP$^{Sc}$ induce recPrP aggregation in amyloid structures that bind ThT. The shaking phase is able to brake the amyloid aggregates and create small seeds that are able to recruit other recPrP molecules during the incubation phase. The signal of ThT is recorded in real-time and proportionally correlate with the amount of amyloid structures. (from Moda F., Prog Mol Biol Transl Sci 2017)

One of the most important aspects of RT-QuIC is the high sensitivity and specificity achieved for prion detection from different sources. This technique was optimized for the detection of different animal and human prion strains including sporadic and genetic human prion strains, classical and atypical scrapie in sheep, BSE in bovine, CWD in elk and deer and different hamster and mouse prion strains [208]. In this case, the "species barrier" appear overcome by the biochemical conditions for amyloid formation and the sequence homology between recombinant substrate and seed is not strictly required. Indeed, hamster recombinant PrP display high sensitivity and specificity to detect PrP$^{Sc}$ derived from human infected samples and enable the detection of PrP$^{Sc}$ in cerebrospinal fluid (CSF) or olfactory mucosa from patients with sCJD [121, 209, 210]. Recently,

recombinant PrP with Bank vole amino acidic sequence were described as "universal acceptor" of a multitude of prion strains from human and animal sources [208].

*1.10.4 Application of RT-QuIC to study in vitro the species barrier and prion adaptation*

RT-QuIC assay can be used for studies the species barrier in highly pure system without the interference of cellular cofactors. However, using RT-QuIC the study of inter-species transmission is limited to the protein-protein interactions without the contribution of other environmental components that might significantly influence the species barrier. Recently, RT-QuIC was used to assess the impact of transmission to a new species of feline CWD (fCWD) and FSE prion strains [211]. This work suggested that, at the level of protein-protein interaction, CWD is able to adapt to a new species more readily than does BSE and the barrier preventing transmission of CWD to humans may be less robust than estimated. However, all these studies are strongly influenced by the experimental settings (e.g. buffer composition, time of shaking and incubation) used for the RT-QuIC reactions. Indeed, similar study on the species barrier between humans and deer, but using different RT-QuIC experimental conditions, conducted to the opposite conclusion suggesting that CWD is not transmissible to humans [212].

## 1.11 Synthetic prions can be generated *in vitro*

One of the most fascinating aspects of prion research is the fact that, under specific biochemical conditions, bacterially-expressed recombinant prion protein (recPrP) can be misfolded *in vitro* thus acquiring infectious properties resembling those of natural prions [213, 214]. Synthetic prions can be used for studying different features of prions, including

the basis of their propagation properties and their capability to modify their conformation in different environments. The use of synthetic prions permits the study of different prion features in a highly pure system without the interference of other components which are instead present in the brain when studying natural prion transmission.

*1.11.1 Historical background on synthetic prions*

The first demonstration that *in vitro* generated synthetic prions could acquire infectious properties came from an important study published in 2000 by Kiotoshi Kaneko and collaborators [215]. Kaneko used in his work a transgenic mouse model expressing low levels of the mutant P101L PrP (Tg196), which spontaneously developed mild alterations in the CNS after more than 600 days [216]. These models were intracerebrally inoculated with a peptide (55 residues) of recombinant mouse PrP carrying the P101L mutation refolded into a β-sheet structure (that was named MoPrP(89-143,P101L)) or folded in different a conformation (without β-structures). Two hundred days post-injection, all mice injected with MoPrP(89-143,P101L) developed severe neuropathological changes typical of prion diseases, while the injection of the other conformation failed to induce any pathological alteration. Neuropathological and biochemical analysis revealed different characteristics with respect to these of typical RML mouse prion strain. Surprisingly, PrP$^{Sc}$ accumulated in the brain was not PK resistant [217]. This uncommon PrP$^{Sc}$ retained its infectious properties when transmitted to the same transgenic mice but the infectivity was lost when injected in wild-type animals [218]. After this first attempt to generate infectivity *in vitro*, several approaches to generate β-sheet rich conformation of misfolded recombinant PrP were explored. All these studies were aimed to address the question

whether PrP<sup>C</sup> alone is the necessary and sufficient molecule for the spontaneous formation of prions without the presence of any exogenous agent [219].

*1.11.2 Generation of synthetic infectious prions starting from recPrP*

In 2002, Ilia V. Baskakov and collaborators started to characterize the kinetic pathways of *in vitro* amyloid formation using bacterially-expressed recombinant mouse PrP corresponding to the PrP27-30 peptide (residues 89-231). In details, under specific biochemical conditions PrP27-30 acquired two different conformations: β-oligomers (in the presence of acidic pH and urea) and fibrillar structures (neutral pH and low concentration of urea), which possessed typical tinctorial properties of amyloid structures. The kinetic of the protein aggregation was measured in real-time manner with Thioflavin-T (ThT) [220]. An important discovery achieved in this work was the fact that the kinetic of amyloid formation could be considerably anticipated by the addition of pre-formed amyloid assemblies (seeds) with respect to the self-aggregation of the protein alone. This evidence showed for the first time that the formation of recombinant PrP fibrils can be promoted by seeding. This observation led to the development of the Amyloid Seeding Assay (ASA) [221] and, most recently, the RT-QuIC [207]. Then the infectivity of these fibrils was assessed with animal bioassays [213]. Particularly, transgenic mice (Tg9949) overexpressing (16-32 X) N-terminally truncated PrP (residues 89-231), were intracerebrally inoculated with (i) *in vitro* generated PrP amyloid fibrils (unseeded amyloids) and (ii) amyloids generated from recombinant PrP with the addition of pre-formed amyloid aggregates (seeded amyloids). All mice injected developed prion disease. Notably, the first group exhibited longer incubation time (474 days post infection) than the second one (382 days post infection). Nevertheless, both groups were characterized by neuropathological changes (vacuolation profile and the presence of PK-resistant PrP) that

differ from known mouse prion strains. Biochemically, the brains of animals injected with seeded amyloid fibrils were characterized by more PK-resistant PrP than the other mice. The prion generated in the brains of Tg9949 mice inoculated with seeded amyloid fibrils was designated as MoSP1 and this new prion isolate was successfully passaged into wild-type mice and acquired protease resistance. After the first synthetic prion experiment [213] different recombinant mouse PrP amyloid fibrils were produced by the same laboratory and challenged *in vivo*. Particularly, David Colby and coworkers were able to produce a subset of 11 PrP amyloids with different conformations. These different preparations were obtained by changing the biochemical and physical conditions used for their formation, including pH, chaotropic agent concentration (urea) and temperature [214]. The infectivity of these preparations was assessed in transgenic mice overexpressing (4-8 X) the wild-type mouse prion protein (Tg4053). Ten out of eleven preparations caused disease with distinguishable patterns of neuropathological alterations and PrP$^{Sc}$ deposition in the brain, suggesting that each preparation was able to induce a specific prion disease in these animals. This work indicates that recombinant amyloids generated with different conformations can induce diverse pathologies in susceptible hosts then linking the structures of the infectious amyloids with the phenotype of the disease (resembling the strain phenomenon observed with natural prions).

The majority of the studies on synthetic prion infectivity were carried on transgenic mouse models overexpressing wild-type or mutated PrP$^{C}$ for increasing the susceptibility to the infection. However, another study [222] based on the generation of synthetic hamster prions demonstrated that wild-type hamsters are susceptible to synthetic prion infections and the use of genetically modified animals is not always required. Particularly, the β-sheet rich conformation produced with full-length hamster PrP under chaotropic conditions were subjected to "annealing" prior to inoculation. Basically, this procedure

consists of an incubation of the amyloids with hamster normal brain homogenate (NBH) and subjected to cycles of heating at 80°C followed by and incubation at 37°C for 5 times. The resulting homogenate was analyzed by Western blotting and a 16kDa PK-resistant band was detected. Amyloids annealed in bovine serum albumin (BSA) instead of brain homogenate failed to produce PK-resistant band. The same samples (NBH and BSA annealed fibrils) were intracerebrally inoculated in wild-type hamsters. The NBH-annealed preparation induced the accumulation of PrP$^{Sc}$ but failed to induce clinical disease at the first passage. Only after serial transmissions, wild-type animals developed the disease. The lack of clinical symptoms in the first passage was ascribed to different factors: (i) the slow replication of PrP$^{Sc}$ and (ii) the low titer of the infectious species presents in the inoculum (only a small subpopulation of fibrils may be infectious). Moreover, the differences between the structure of the host PrP$^{C}$ and recombinant amyloids may decrease the seeding activity and consequently extend the incubation time of the disease [223]. This newly generated prion isolate named SSLOW (Synthetic Strain Leading to OverWeight) produced a new type of prion disease characterized by (i) a very long incubation time, (ii) peculiar patterns of PrP$^{Sc}$ deposition and (iii) specific neurotropism (lower involvement of the cerebellum). Notably, both NBH and BSA annealed preparation were able to induce prion disorder at second passage in wild-type animals and the PK-resistant PrP showed identical band shift suggesting the possibility that the same prion isolate might emerge in serial passages from two different inocula. While the conformational stability of SSLOW appeared similar to that of 263K the differences in the incubation time of these two strains indicate that other factors than PrP$^{Sc}$ stability can play an important role in prion replication mechanism.

*1.11.3 Contribution of PMCA to generate and study synthetic prions*

Another strategy exploited to generate synthetic infectious prion is the PMCA, a technique developed by Claudio Soto's group [194]. Using different sources of PrP$^C$ (recombinant, purified from animal brains or from total bran homogenates) PMCA demonstrates the ability to generate *de novo* infectious PrP$^{Sc}$ in well defined *in vitro* conditions. In 2007, the group of Surachai Supattapone [224] showed that using a purified PrP$^C$ preparation from hamster brain homogenate, efficient PMCA propagation of infectious prions required the presence of polyanion molecules, such as nucleic acids, glycosaminoglycans, phospholipid-rich membranes and chaperone proteins suggesting their involvement in prion replication. Although polyanions may not be absolutely required to form an infectious prion, they may increase the efficiency of prion conversion or modify some biochemical properties of PrP$^{Sc}$ [205]. Most notably, this work demonstrated that PrP$^{Sc}$ could be spontaneously generated *de novo* in PMCA from these components in a stochastic manner. Remarkably, this preparation was able to produce prion pathology in wild-type hamsters. Different negatively charged macromolecules, in particular RNA [225], synthetic lipid in combination with purified RNA [226] or only synthetic lipids [227, 228] were reported to enhance PrP$^C$ conversion and promote the *de novo* generation of prion. In 2013, Zhihong Zhang et al. [229] reported that after several rounds of PMCA amplification using recombinant mouse PrP two types of PK-resistant and self-perpetuating structures (recPrP$^{res}$) were generated *de novo*. In particular, these structures were produced using recombinant prion protein, synthetic phospholipid 1-palmitoyl-2-oleoylphosphati-dylglycerol (POPG) and total RNA isolated from normal mouse liver. After several rounds of PMCA two recPrP$^{res}$ characterized by a PK-resistant core of 17KDa and 14KDa were generated (11 rounds for the 17kDa form and 5 rounds for 14kDa recPrP$^{res}$). Only the 17kDa recPrP$^{res}$ was able to induce prion disease when injected in wild-type mice (CD1), with an

average survival time of about 172 days. In contrast, 14kDa recPrP$^{res}$ totally failed to induce any disease. Notably, second-round transmission *in vivo* confirmed the infectivity of 17kDa recPrP$^{res}$ with an average survival time of about 161 days. The same group in 2012 [230] demonstrated that infectious prions can be generated *de novo* by replacing the total liver RNA with a synthetic polyriboadenylic acid [poly(rA)]. The use of [poly(rA)] instead of mouse-derived RNA for the generation of infectious recPrP$^{res}$ exclude the possibility that RNA-like molecules or information contained in RNA sequence were necessary for *in vitro* conversion of PrP$^{C}$ in its infectious isoform.

PMCA technique can be also used for generating *de novo* infectious PrP$^{Sc}$ from normal brain homogenates. As reported by Barria and colleagues in 2009 [231], PMCA were able to generate *de novo* PrP$^{Sc}$ using hamster and mouse brain homogenates. Precisely, in standard PMCA amplification (rounds of 144 cycles of incubation and sonication) the spontaneous formation of hamster and mouse PrP$^{Sc}$ does not occur. The extension of the number of cycles per round (from 144 to 240 cycles) of PMCA induces the generation of PrP$^{Sc}$ in both hamster and mouse brain homogenates (used as PMCA substrates) after 9 and 10 rounds, respectively. Notably, *de novo* hamster PrP$^{Sc}$ was infectious in wild-type animals and produced a new disease phenotype. Taken together these findings demonstrate that this technique is an useful tool for studying the role of different cofactors to influence the generation of infectious synthetic prions.


*1.11.4 Autocatalytic propagation versus infectivity*

The protein-only hypothesis proposed that every PrP capable to replicate in an autocatalytic manner is infectious. However, not all synthetic prions able to self-replicate are infectious or the infectivity level is undetectable with common bioassays. In 2015, the group of Surachai Supattappone observed structural and functional differences between

infectious and non-infectious autocatalytic *in vitro* generated PrP conformers from recPrP [232]. Particularly, two distinct conformers were produced with or without the addition of cofactors. Amyloids produced with cofactor were infectious in wild type animals while the preparation without cofactors was not able to efficiently induce prion pathology. [227]. Both conformers are able to efficiently replicate in PMCA using recPrP as substrate but only the high infectious conformer (generated with cofactors) is able to convert *in vitro* the native PrP$^C$ from brain homogenate. Structural hydrogen/deuterium exchange mass spectrometry (DXMS) studies revealed similar solvent accessibility between these two conformers except for two domains (including AA 91-115 and 144-167) of the PK-resistant C-terminal core. Raman spectroscopy and immunoprecipitation experiments confirmed that these domains adopt distinct conformations between the high infectious and low infectious structures suggesting specific structural constrains required for the infectivity. Wang and colleagues in 2017 [233], generated different recPrP conformations using PMCA in presence of different concentration of mouse liver RNA as cofactor. Conformers generated with low concentrations of RNA were not infectious while structures generate with high concentrations of RNA were infectious in wild-type mice. The overall architecture of these conformation was similar but, despite their ability to efficiently replicate *in vitro*, slightly structural differences might govern the *in vivo* infectivity. These reports highlighted that the *in vitro* ability to self-replicate of recombinant prions does not necessary result in pathogenicity that is instead enciphered in fine structural arrangement of the infectious conformers.

### 1.11.5 From recombinant amyloids to bona fide PrP$^{Sc}$

The generation of synthetic prions from recombinant source of PrP$^C$ *in vitro* have provided the strongest proof for the protein-only hypothesis. However, these preparations generally

fail to induce prion pathology with high efficiency as expected, especially in wild-type

animals. In fact, synthetic preparation display infectivity in transgenic animals with high

expression of PrP$^C$ or wild type after relatively long incubation time, long silent clinical

stage and with low efficiency. Two models might explain this behavior: the first (i) assumes

that the amyloid fibrils preparation contains minute amount of PrP$^{Sc}$ that needs long time

and repetitive *in vivo* passages for replicating at a level sufficient to induce pathological

alteration, the second (ii) infers that recombinant amyloid preparations does not contain

PrP$^{Sc}$ but are able to convert PrP$^C$ in atypical form of PrP that, after long silent stage,

evolve in authentic PrP$^{Sc}$. These two models are schematically represented in Fig 1.18.
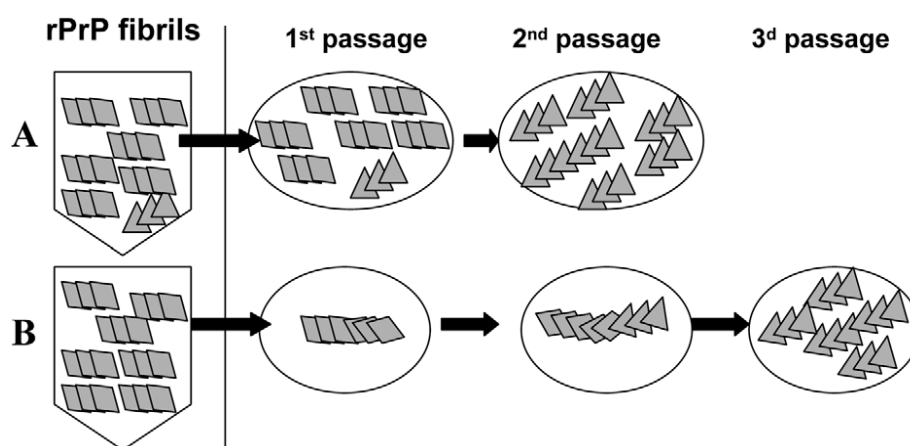


**Fig. 1.18 Schematic representation of two mechanisms responsible for generating transmissible prion diseases from recombinant amyloids.**
Two mechanisms were proposed for the generation of PrP$^{Sc}$ from recombinant amyloids. According to the first mechanism (A) the amyloid fibrils preparation contains very small amounts of PrP$^{Sc}$ (triangles). The silent stage of the disease among *in vivo* passages is attributed to the long time required for amplification of PrP$^{Sc}$ at sufficient levels to induce the pathology. A second mechanism (B) referred to as deformed templating postulates that there are no PrP$^{Sc}$ particles in the preparations of amyloid fibrils. When inoculated into animals, amyloid fibrils can convert PrP$^C$ into an atypical form of PrP named atypical PrP$^{res}$. Atypical PrP$^{res}$ undergoes slow transformation, a process that might require long silent stage, before authentic PrP$^{Sc}$ emerges after repetitive passages. (from Makarava *et al.*, PlosPath 2011)

The classical templating mechanism postulates that PrP$^{Sc}$ induce the conformational

conversion of PrP$^C$ and transmit its misfolding with high fidelity. However, experimental

evidence highlights that the structure of recombinant amyloids used for inoculation and the infectious PrP$^{Sc}$ detected in animals appear very different [76, 234] suggesting that the transition between these two structures might involve several steps. A mechanism involving two steps was proposed for explaining this phenomenon [235]. As a first step, synthetic prion fibrils induced PrP$^{C}$ misfolding in alternative self-replicating state, referred as atypical PrP$^{res}$. This mechanism is supported by the fact that atypical PrP$^{res}$ characterized by short C-terminal PK resistant core was detected in hamsters injected with synthetic amyloid [236]. At this stage, atypical PrP$^{res}$ is able to replicate without causing disease. Particularly, atypical PrP$^{res}$ preferred mono-glycosylated PrP$^{C}$ as substrate and its amplification is RNA-independent. During the second step the authentic PrP$^{Sc}$ were formed via rare and stochastic deformed templating events (See section Darwinian evolution of prions) as reported in the schematic representation in Fig. 1.19.
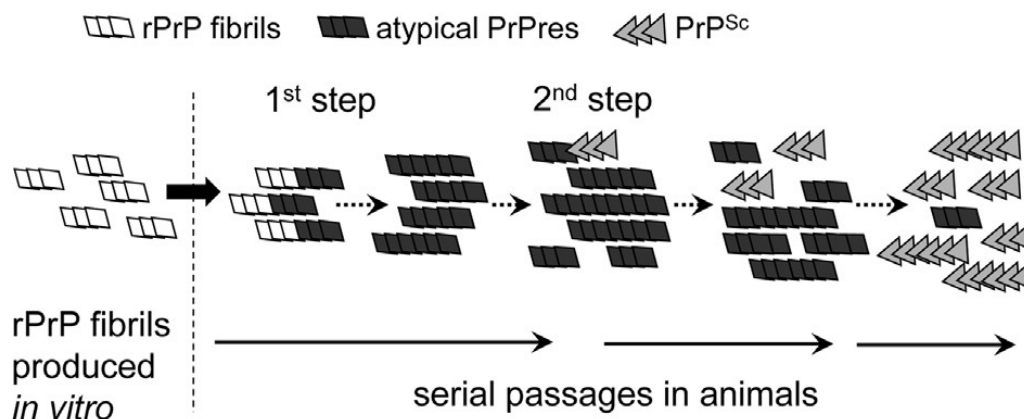


**Fig. 1.19 Schematic representation of the PrP$^{Sc}$ genesis from rPrP synthetic fibrils.**
This model is composed by two steps: in the first rPrP trigger the formation of an atypical PrP$^{res}$ that replicates silently without causing clinical disease. The replication of atypical PrP$^{res}$ occasionally produces PrP$^{Sc}$ (second step) that replicates faster than the atypical isoform. For synthetic hamster prion strains, both forms of PrP can be detectable after PK treatment with antibodies that recognize C-terminal fragment (both atypical PrP$^{res}$ and PrP$^{Sc}$) or N-terminal fragment (only PrP$^{Sc}$). (from Makarava N *et al.*, Am J Pathol 2016)

After the formation of the first PrP$^{Sc}$, this latter can replicate independently of atypical PrP$^{res}$. Supporting this model, *in vitro* generated amyloid fibrils from recombinant Syrian hamster PrP lacked any detectable PrP$^{Sc}$ particles but were able to induce transmissible

prion disease in animals on serial passaging [234]. This mechanism proposed two main barriers between the injection of synthetic amyloids to the generation of authentic PrP$^{Sc}$. The first is attributed to a change in substrate from recombinant PrP to PrP$^{C}$ that possess GPI-anchor and N-linked glycans. These post-translational modifications may affect the ability of synthetic prions to transmit their misfolding to the PrP$^{C}$. The second barrier is constituted by the low rate of deformed templating events that lead, in this model, to authentic PrP$^{Sc}$. High concentration of PrP$^{C}$ helped to cross the first barrier while the second barrier step seems to be independent from PrP$^{C}$ expression [235]. However, although the deformed templating events are not affected by PrP$^{C}$ expression, this mechanism is likely controlled by (i) the nature of the template, (ii) intrinsic rate of conformational errors in templating and (iii) the environment of prion replication. Particularly, cofactors present in the replication context not only shape the strain-specific structures [227] but may participate to the evolution process.

However, atypical PrP$^{res}$ were described in synthetic hamster prion strains transmission but no mouse atypical PK-resistant PrP were detected suggesting that this mechanism might be not assumed as general model.


## 1.12 Synthetic prions adaptation and selection

Several studies conducted with the aim of assessing the stability of synthetic prion strains after serial passages in animals highlighted the ability of these preparations to change their pathological features similarly to that observed in inter-species transmission of prions. Accordingly, experimental findings suggest the possibility that different conformation of PrP$^{Sc}$ might be originated by the same amyloid preparation. This heterogeneity can arise from: (i) the presence of a mixture of PrP$^{Sc}$ conformations in the original amyloid preparations, (ii) stochastic events of conformational changes of PrP$^{Sc}$ or (iii) infrequent

lack of fidelity during the prion replication process (deformed templating). Moreover, these hypotheses are in agreement with experimental observations that synthetic prions are able to: (i) change their pathological features trough *in vivo* passages and (ii) generate in animals two or more PrP$^{Sc}$ conformations.

Indeed, during serial animal passages within the same host, these preparations can undergo to a period of adaptation were their biochemical and neuropathological characteristics gradually change to reach stable pathological phenotype. An example of this adaptation was described for synthetic hamster prions [237]. Particularly, at least four serial passages in hamsters were required to stabilize SSLOW hamster prion strain characteristics including: incubation period, neuropathological features and tissue tropism. These changes in strain properties are frequently observed upon cross-species transmission and were attributed in large part to the sequence differences between PrP$^{Sc}$ and host PrP$^{C}$ [174, 238]. The adaptation observed within the same host might involve a selection process of a PrP$^{Sc}$ subpopulation that was best suited to replicate in a particular cellular environment (different tissues or different brain regions). Similarly to hamster synthetic strain evolution, changes in biochemical and physical properties of synthetic mouse prions were reported after serial passages in animals [214, 239, 240]. Particularly, a set of synthetic amyloids (generated under different chaotropic conditions) were inoculated in transgenic animal model overexpressing PrP$^{C}$ (Tg4053). On initial infection, the synthetic prion amyloids were able to induce different prion pathologies [214]. However, after serial passages, the neuropathological and biochemical features of each preparation gradually adapt and converge to a similar prion isolate characterized by analogous conformational stability and glycoform ratio [240]. This report demonstrated the ability of different amyloid preparation to change their physical and biochemical properties

on repeated passage within the same host and converge to one conformation by mechanism of selection and adaptation.

Supporting the fact that synthetic prions might generate different prion isolates the transmission of MoSP1 [213] in transgenic mice expressing truncated PrP$^C$ (89-230) (Tg9949) and FVB mice revealed the presence of, at least, two distinct prion isolates named MoSP1(1) and MoSP1(2) [241, 242]. Additional studies on MoSP1(1) and MoSP1(2) revealed that these two strains were characterized by two different molecular mass of the unglycosylated PK-resistant PrP, 21kDa and 19kDa, respectively [239]. Particularly, when inoculated in cell cultures, MoSP1(1) and MoSP1(2) propagate with high fidelity. When both prion isolates were incubated together in the same cells, MoSP1(1) prevail on MoSP1(2) which slowly disappear. Most notably, the subsequent inoculation of cloned MoSP1(2) in animals overexpressing PrP$^C$ (Tg4053) resulted in the reappearance of small amounts of MoSP1(1). The model proposed for this phenomenon was based on the competitive selection. Thus, MoSP1(1) replicates faster than MoSP1(2), and this isolate might be more effective at interacting with PrP$^C$ (or other factors) competing with MoSP1(2) for the substrates required for its propagation [243, 244]. In that scenario, the faster replicating prion causes disease with shorter incubation time and induces the host death before the accumulation of the slower prion strain.

These reports highlighted the ability of synthetic preparation to undergo to a process of selection and adaptation similar to that observed in cross-species transmission of prion strains. As shown for natural prions, the context of replication might play a role in selecting specific PrP$^{Sc}$ conformations and actively participate to the adaptation process.

*1.12.1 In vitro studies of synthetic prion selection and adaptation*

As for natural prions, *in vitro* amplification techniques like PMCA might be a fundamental tool for studying synthetic prion selection and adaptation mechanisms. The advantage of this technique is the possibility to alter in a precise manner the replication environment by adding or removing single components from the substrate of amplification such as RNA, lipids and other molecules in order to evaluate their effect on PrP$^{Sc}$ replication. In 2012, Makarava and colleagues reported that modifications of PMCA conditions can lead to the amplification of different PrP$^{Sc}$ using as source of infectious prions the brain of hamster injected with synthetic isolate [179]. Precisely, brain homogenates of hamster infected with LOTSS (LOw Toxicity Synthetic Strain) containing a mixture of atypical PrP$^{res}$ and PrP$^{Sc}$ were used as seed for PMCA amplification with (i) normal hamster brain homogenate and (ii) partially de-glycosylated substrate (treated with PNGase F under non-denaturing conditions). This substrate treatment partially removes N-linked glycans leading to a shifting of the ratio of PrP$^{C}$ glycoforms from predominantly di-glycosylated to predominantly mono-glycosylated. After PMCA, the analysis of the amplified products revealed that standard PMCA was able to selectively amplify PrP$^{Sc}$ while PMCA with partially de-glycosylated substrate (dgPMCA) preferentially amplified atypical PrP$^{res}$. Notably, after only 4 rounds of standard PMCA, no signal from atypical PrP$^{res}$ were detected while dgPMCA amplify both PrP$^{Sc}$ and atypical PrP$^{res}$, but this latter preferentially. To test the infectious properties of standard PMCA amplified LOTSS, animal bioassays were performed. Surprisingly, in contrast to the animals inoculated with the original seed, hamsters injected with the PMCA amplified LOTSS developed clinical symptoms with 100% attack rate. Notably, clinical manifestation of the disease was identical from that observed in animals after conventional *in vivo* passages of LOTSS suggesting that PMCA is able to mimic *in vitro* the process of *in vivo* strain evolution of prions. Another report

sustaining the role of the environment on prion selection and adaptation was published recently by Natalia Fernàndez-Borges and colleagues [245]. Particularly, they demonstrated that a synthetic prion conformation can be selected in PMCA from a mixed population using recombinant substrates in presence or absence of different cofactors like deaxtran, RNA and DNA. Notably, these selected synthetic prions were able to either replicate in PMCA (with brain homogenate of transgenic mice expressing bank vole PrP (TgVole) and bank vole 109I brain homogenates) or induce different prion pathologies when injected in animals.

Taken together, these reports highlighted the fact that the alteration of the *in vitro* context of synthetic prion replication is able to modify their characteristics in a very similar manner to that of natural prions adaptation and selection.

# AIM

Aim of my PhD work was to evaluate the infectious, clinical neuropathological, biochemical and biophysical properties of a new synthetic prion isolate previously generated by our group and assess its ability to undergo to process of selection/adaptation in response to changes in the replication environment. For this purpose, we have performed serial transmission passages in wild-type mice and *in vitro* analysis with two innovative techniques named Protein Misfolding Cyclic Amplification (PMCA) and Real Time Quaking Induced Conversion (RT-QuIC) for deepening these phenomena.

# Materials and methods

*2.1 Intracerebral inoculation*

Six weeks-old Crl:CD1(ICR) (CD-1) mice (35–40 g) were anesthetized with Tribromoethanol (100µL/10g) i.p.-administered and 20µL of amyloid preparation or 2µl of each brain homogenate collected from terminally sick animals [246] and prepared in sterile phosphate buffer (10%, weight/volume) was stereotactically injected in the striatum (raw amyloids) or in the hippocampus (brain homogenate). All surgical procedures were performed under sterile conditions. Incubation time (I.T.) was calculated considering the days between inoculation and symptoms onset including: ataxia (uncoordinated movement), tail rigidity and kyphosis (hunched back). Survival time (S.T.) was calculated considering the days between the inoculation and the sacrifice of the animals at terminal stages of the disease. Brains were then harvested and half of them were collected for biochemical analysis and the other half was processed for histological evaluations.

*2.2 Neuropathological analysis*

Brains were fixed in Alcolin (Diapath), dehydrated and embedded in paraplast. Seven-micrometer thick serial sections were stained with hematoxylin-eosin (H&E), thioflavin S, or immunostained with monoclonal antibodies to PrP (6H4, Prionics), and polyclonal

antibodies to glial fibrillary acidic protein (GFAP, Dako). Before PrP immunostaining the sections were pre-treated with Proteinase K (10 µg/mL, 5 min, room temperature, Invitrogen) and guanidine isothiocyanate (3M, 20 min, room temperature). Non-specific binding of the antibody was prevented using ARK kit (Dako). Immunoreactions were visualized using 3–3'-diaminobenzidine (DAB, Dako) as chromogen. Lesion profile was performed on H&E stained sections according to Fraser H. et al 1968 [155]. The areas evaluated were: **1.** Dorsal medulla; **2.** Cerebellar cortex; **3.** Superior culliculus; **4.** Hypothalamus; **5.** Thalamus; **6.** Hippocampus; **7.** Septum; **8.** Retrosplenial and adjacent motor cortex; **9.** Cingulated and adjacent motor cortex. For each area, the severity of vacuolar lesions was graded 0 (no lesions) to 3 (extensive vacuolization) and the mean scores were calculated and then plotted with ±S.E.M. IHC images were acquired at 10X magnification with Nikon Eclipse E800 microscope equipped with Nikon digital camera DXM 1200 and Nikon ACT-1 (v2.63) acquisition software.

*2.3 Biochemical analysis*

Ten percent (weight/volume) brain homogenates were prepared in lysis buffer (NaCl 100mM, EDTA 10mM, NP40 0,5%, Na-deoxycholate 0,5%, Tris-HCl pH 7.4 10mM). After a brief centrifugation (800 x g, 1 minute) 20µL of cleared lysate was digested with 50 µg/mL of Proteinase K (1h, 37°C, 550rpm, Invitrogen). PK digestion was stopped by adding Loading buffer (Sample buffer 4X and DTT 10X, Thermo Scientific) and the samples were boiled (100°C, 10 minutes). The proteins were separated using 12% Bis-Tris plus gels (Thermo Scientific) and transferred into polyvinylidene difluoride membranes (PVDF, Millipore). After non-fat dry milk blocking (1h, room temperature) the membrane was probed using anti-PrP antibodies (see List of antibodies) diluted in TBST and 0.05%-

Tween-20 (Sigma). After incubation with Fab fragment anti-mouse IgG conjugated with horseradish peroxidase (HRP) (GE), blots were developed using the ECL Prime detection system (Amersham) and chemiluminescence was visualized using a G:BOX Chemi Syngene system.

List of antibodies

| Antibody | Epitope (AA) |
|----------|--------------|
| 6D11     | 93-109       |
| SAF-61   | 144-152      |
| SAF-84   | 160-170      |

*2.4 PNGase experiment*

Fifty µl of brain homogenates was digested with PK (100 µg/mL) for 1 hour at 37°C with shaking. PNGase digestion was performed following the instructions provided with the kit (PNGase F, P0704S, 15.000 units, New England Biolabs). Briefly, 4 µL of 10X glycoprotein denaturing buffer (provided with the kit) was added to the homogenate and the samples were boiled for 10 minutes at 100°C. Subsequently, 4 µL of G7 buffer (provided with kit), 4 µL of NP-40 (provided with kit), 4 µL of PNGase F and 4 µL of PBS were added to reach the final volume of 40 µL. Each sample was incubated 2 hours at 37°C with shaking. The reaction was stopped by adding NuPAGE LDS sample buffer and Western blotting was performed.

*2.5 PMCA procedures*

PMCA was performed as previously described [194]. Briefly, as a substrate, were used brain homogenate from outbred CD-1 mice prepared in conversion buffer (PBS 1X containing 150 mM sodium chloride and 1% Triton X-100) with the addition of Complete

protease inhibitor cocktail (Roche). Ten µL of brain homogenate from infected mice was added to the substrate and transferred in 0.2mL PCR tubes, positioned on an adaptor placed on the plate holder of a micro-sonicator (Misonix, Model S3000) and subjected to 96 cycles of PMCA. Each cycle (referred as PMCA round) consisted of 29' and 40" sec of incubation at 37/40°C and 20" pulse of sonication set at potency of 260–270 Watt. After one round of PMCA, 10µl of the amplified material was diluted 10-folds into fresh substrate and a further PMCA rounds were performed. In order to increase the efficiency of amplification, 3 teflon beads were added to the reaction tube. To prevent samples cross-contamination all the instruments and equipment were decontaminated using 2N sodium hydroxide (NaOH, Sigma) or 4M guanidine hydrochloride (GdnHCl, Sigma) and all the experiments were conducted with appropriate negative control.

## 2.6 Blood processing

Blood from symptomatic animals (140 days post inoculation) was collected from the tail in a 1.5 mL tube containing EDTA as anticoagulant. Four hundred µL of blood was treated with Ficol reagent to separate plasma from white cells and red cells. Plasma and white cells were collected and centrifuged at high speed (100.000 x g) for 1h at 4°C. Resulting pellets were washed with PBS, suspended in 100 µL of CD1 brain homogenate and subjected to PMCA.

## 2.7 PK resistance assay

Twenty µl of brain homogenate or PMCA products was digested with five increasing concentrations of PK enzyme (50, 100, 250, 500, 1000 µg/mL) for 1 hour at 37°C with

shaking. Samples were then immunoblotted with 6D11 antibody and densitometric analysis of resulting PK-resistant PrP band were performed.

*2.8 Conformational stability assay*

Fifty μl of brain homogenate or PMCA products was incubated with 450μL of guanidine hydrochloride (GdnHCl) solutions (Sigma) at different molar concentrations (0, 1.5, 3, 4.5 and 6M) for 2h at 25°C with agitation (550rpm). Subsequently, an equal volume of Sarkosyl 20% was added to the samples and incubated for 10 minutes with gentle shaking. Samples were then centrifuged at 100 000 x g for 1h at 4°C. Pellets were washed with equal volume of PBS 1X (Gibco) and then centrifuged at 100 000 x g, 30' at 4°C. The pellets were finally suspended in 50μL of Loading buffer and then processed for Western blot analysis (see *Biochemical analysis* for details). The membrane was incubated with anti-PrP 6D11 primary antibody (0.2 μg/mL, Covance). Densitometric analysis were performed. The concentration of GdnHCl required to unfold half of $PrP^{Sc}$ ($[GdnHCl]_{1/2}$) was then calculated with GrapPad software (v5.0) after non-linear regression curve fit (Boltzmann sigmoidal) of densitometric data.

*2.9 Recombinant full-length mouse PrP production and purification*

The pET-11a plasmid (Novagen) encoding for the full-length MoPrP(23–231) was kindly provided by Dr. J.R. Requena (University of Santiago de Compostela, Santiago de Compostela, Spain). The mouse construct was expressed in competent BL21 Rosetta2 (DE3) cells *Escherichia coli* (Stratagene). Freshly transformed overnight culture was inoculated into Luria Bertani (LB) medium and 100 μg/mL ampicillin and 30 μg/mL

chloramphenicol. At 0.8 $OD_{600}$ expression was induced with isopropyl b-D galactopyranoside (IPTG) to a final concentration of 1 mM. Cells were grown in a BioStat-B plus fermentor (Sartorius). The cells were lysed by a homogenizer (PandaPLUS 2000) and the inclusion bodies were suspended in buffer containing 25 mM Tris-HCl, 5 mM EDTA, 0.8% TritonX100, pH 8, and then in bi-distilled water several times. Inclusion bodies containing MoPrP(23-231) were dissolved in 5 volumes of 8 M guanidine hydrochloride (GdnHCl), loaded onto pre-equilibrated HiLoad 26/60 Superdex 200-pg column, and eluted in 25 mM Tris–HCl (pH 8.0), 5 mM ethylenediaminetetraacetic acid, and 5 M GdnHCl at a flow/rate of 1.5 mL/min. Proteins refolding was performed by dialysis against refolding buffer [20 mM sodium acetate and 0.005% $NaN_3$ (pH 5.5)] using a Spectrapor membrane (molecular weight, 10000Da). Purified protein was analyzed by SDS-polyacrylamide gel electrophoresis under reducing conditions and Western blot.

*2.10 RT-QuIC analysis*

RT-QuIC was performed as previously described with few modifications [247]. Briefly, recombinant full length mouse PrP (23-231) were filtered through a 100 kDa Nanosep centrifugal device (Pall Corporation) and mixed with the reaction buffer composed as follow: 0.2mg/mL recMoPrP(23-231), 10mM PBS, 130mM NaCl, 1mM EDTA, 0.002% SDS and 10µM ThT (all reagents from Sigma). 98 µL of the final reaction volume were dispensed in black 96-well optical flat bottom plate (Thermoscientific). To avoid contaminations, reaction mix was prepared in a prion-free laboratory and all the sample were analyzed in triplicate. After the addition of 2µL of brain homogenate or PMCA amplified products, the plate was sealed with a sealing film (Thermoscientific) and inserted into a FLUOstar OPTIMA microplate reader (BMG Labtech). The plate was shaken for 1

minute at 600 rpm (double orbital) and incubated for 1 minute at 42°C. A sample was considered positive if two out of three replicates crossed the threshold of 30% of the maximum ThT signal. Brain homogenate from terminally sick mice infected with RML prion strain (either subjected to PMCA or not) were used as control.

*2.11 Statistical analysis*

Means values are presented with their standard errors of the mean (S.E.M.). Log-rank test was used for the survival and incubation time analysis. Unpaired t-test, two tailed was used for *p* calculation. Statistical analysis and graphic representations were performed with Prism software (5.0v GraphPad). Densitometric analysis were performed using ImageJ software (1.48v).

# Results

We previously generated different synthetic prion amyloid preparations using only recombinant full-length mouse PrP (recMoPrP) and common chemicals but systematically altering the conditions for their formation, including denaturant concentrations, pH and buffer composition. These results were published in 2015 in Plos Pathogens [246] and showed the ability of one of these amyloids (named amyloid #4) to induce the accumulation of PK resistant PrP in cells or to replicate *in vitro* by means of PMCA. For this reason, we decided to analyze the infectious properties of this amyloid in wild type mice.

*3.1 PMCA analysis of raw amyloid #4 and lysates from infected GT-1 and N2a cell lines*

First, we assessed the ability of amyloid #4 to propagate *in vitro* by means of PMCA using CD1 mouse brain homogenate as substrate for amplification. This preparation showed a PK resistant PrP signal after three rounds of PMCA (Fig. 3.1A). Subsequently, cell lysates collected from both N2a and GT1 cells infected with amyloid #4 were used as seed for PMCA reaction. The lysates of both cell lines were able to amplify in PMCA harboring a PK resistant signal after 3 rounds of amplification (Fig. 3.1B). Remarkably, the glycoform ratio of PK-resistant amplified product derived from amyloid #4 (either from raw amyloid or cell lysates) was characterized by a prevalence of the di-glycosylated band while the un-glycosylated form migrated at around 20 kDa after PK digestion.
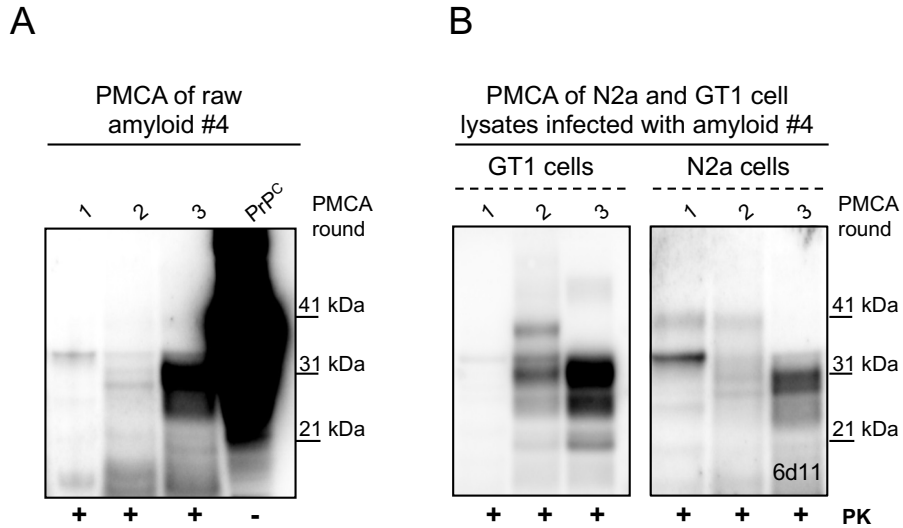
**Fig. 3.1 PMCA analysis of amyloid #4 raw fibrils and cell lysates from infected cell lines.** (A) Seeding ability of amyloid #4 by means of PMCA using CD1 brain homogenate as substrates. (B) PMCA amplification of GT1 and N2a cell lysates infected with amyloid #4.

## 3.2 First in vivo transmission (FP) of amyloid #4

Amyloid #4 preparation was intracerebrally inoculated in Crl:CD1(ICR) (CD-1) mice (n=7) (Fig. 3.2A) and a group of animals were injected with normal PBS as control. None of the animals of first passage (referred to as FP) injected with raw amyloids showed clinical signs of prion pathology and were culled at the end of their lifespan. Neuropathological and biochemical analysis confirmed the lack of PK-resistant PrP, absence of spongiform alteration, PrP$^{Sc}$ deposition and astroglial activation (Fig. 3.2B and 3.2C). Immunoblots with different C-terminal anti PrP antibodies (SAF-84, residues 160–170; SAF-61 which recognize residues 144–152) was performed for checking the presence of atypical PrP$^{res}$ but no signals were detected.
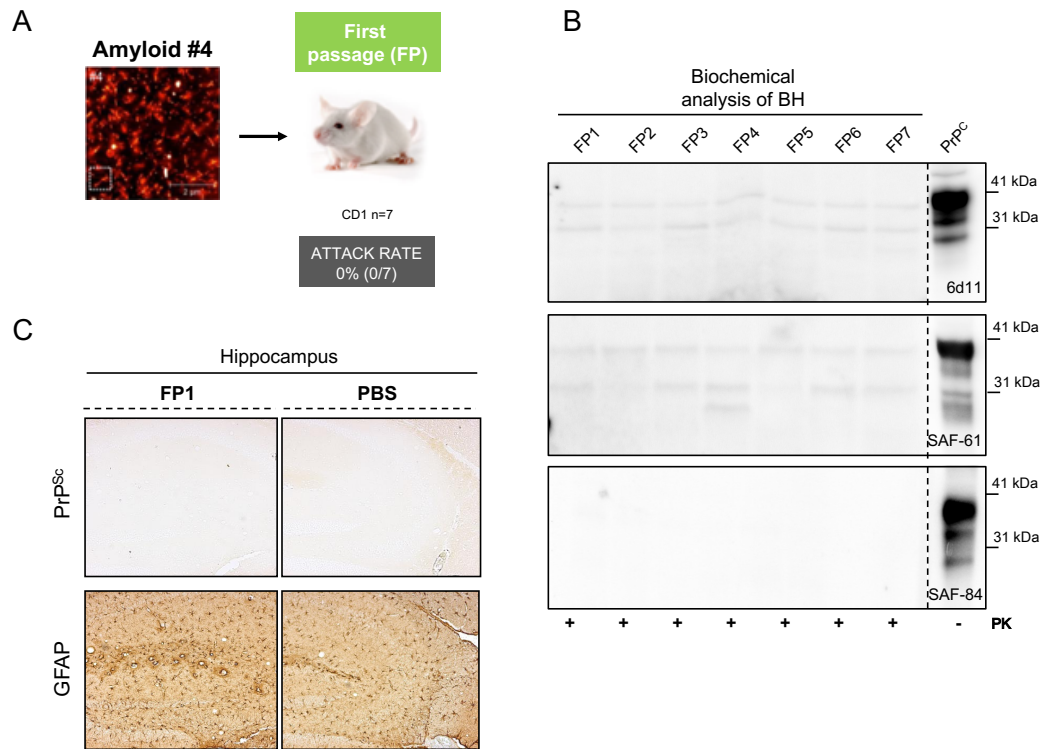
**Fig. 3.2 Neuropathological analysis of first passage (FP) mouse brains.** (A) Schematic diagram of first transmission passage (FP). (B) Western blot analysis of brains collected from FP animals with three monoclonal antibodies for PrP. PrP$^C$ indicates the cellular prion protein (C) Immunostaining for PK-resistant PrP (after PK treatment, 10µg/mL) and Glial Fibrillary Acidic Protein (GFAP) of hippocampus of FP1 and PBS injected mice. Images were acquired at 10X magnification.

## 3.3 PMCA analysis of amyloid #4 injected animals and characterization of a new prion isolate

Brain homogenates of animals injected with amyloid #4 (referred to as FP) were subjected to PMCA amplification and showed the presence in one mouse of a PrP$^{Sc}$ signal after three rounds of PMCA (Fig. 3.3A). Notably, the amplified PrP$^{Sc}$ (named PMCA-FP2) was characterized by the prevalence of the di-glycosylated isoform of PrP while no PrP$^{Sc}$ was observed after the amplification of the other brain homogenates. PMCA-FP2 was biochemically analyzed and compared with known prion strains: (i) mouse adapted-vCJD (mo-vCJD), (ii) RML and (iii) ME7. With this experiment, we noticed that the un-glycosylated band of PMCA-FP2 migrated at around 20 kDa, in an intermediate position

compared with the same band of RML or ME7 (migrating at 21kDa) and the one of mo-vCJD (migrating at 19kDa) (Fig. 3.3B). Peptide N-glycosidase F (PNGase) digestion experiment, that remove all N-linked oligosaccharides from PrP, confirmed the molecular mass of the un-glycosylated band of PrP migrating at 20kDa. This observation also rules out the possible contamination of PMCA reactions with vCJD or BSE prion strains that are also characterized by the prevalence of the di-glycosylated form of PrP$^{Sc}$ (Fig. 3.3C).
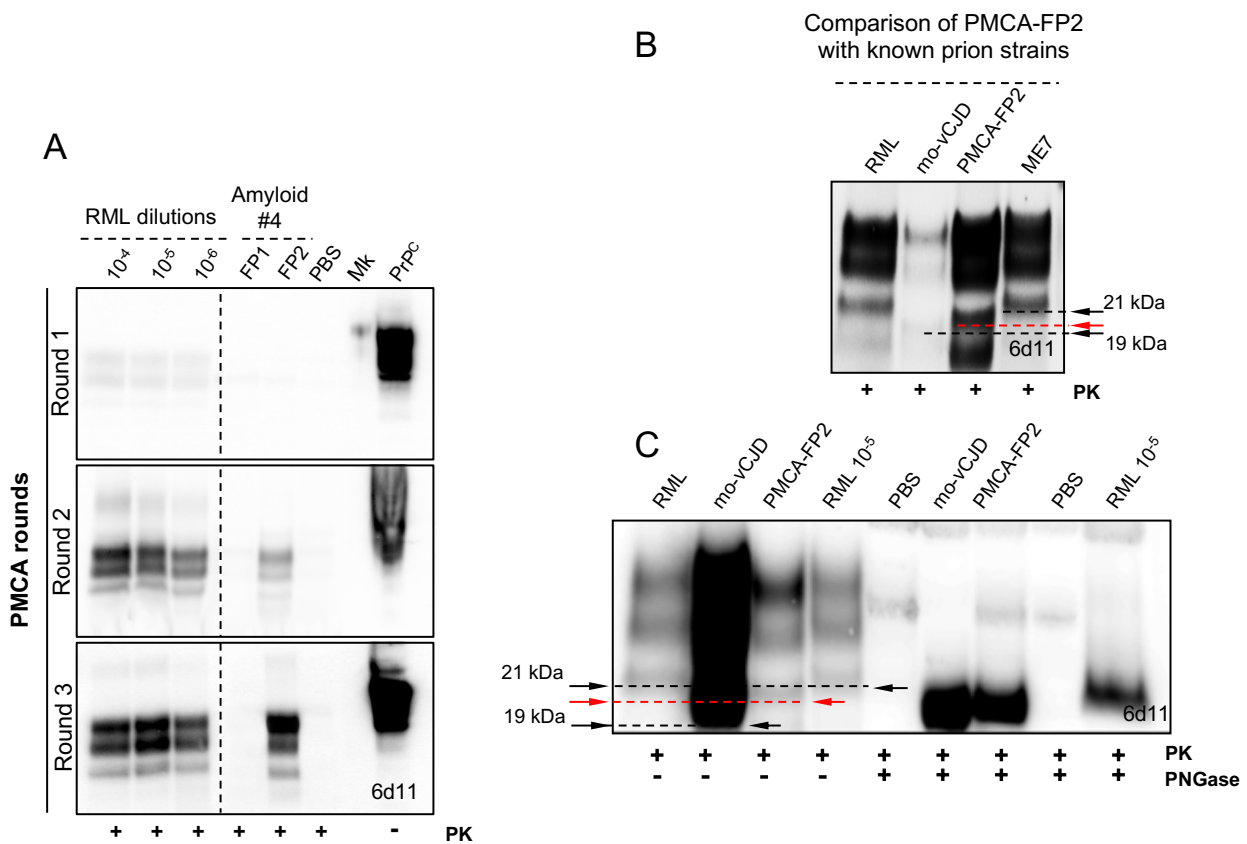


**Fig. 3.3 PMCA amplification and characterization of PMCA-FP2 prion isolate.** (A) PMCA analysis of brain homogenates from FP animals using CD1 homogenate as substrate. Serial dilutions of RML prion strain were used as control. (B) Western blot comparison of PMCA-FP2 with RML, mo-vCJD and ME7 prions strains. (C) PNGase comparison of PMCA-FP2 with known prion strains. (Red arrow indicates the un-glycosylated band of PMCA-FP2).

## 3.4 Second in vivo transmission (SP) of amyloid #4

A second passage transmission (SP) was performed as schematically reported in Fig. 3.4A. Particularly, two groups of CD1 mice (n=10) were intracerebrally injected with brain homogenate obtained either from the animal injected with amyloid #4 or PBS. No animals of the second passage developed prion disorders after 700 days post injection. Biochemical and neuropathological analysis confirmed the lack of PrP$^{Sc}$ accumulation either in Western blot and immunohistochemical evaluation (Fig 3.4B and 3.4C). These brains were subjected to PMCA analysis and five rounds of amplification (R5) were performed. No PK-resistant PrP signal was detected suggesting (i) the absence of PrP$^{Sc}$ in the brains of injected animals or (ii) the presence of a PrP conformation that was not able to replicate *in vitro* (Fig. 3.5).
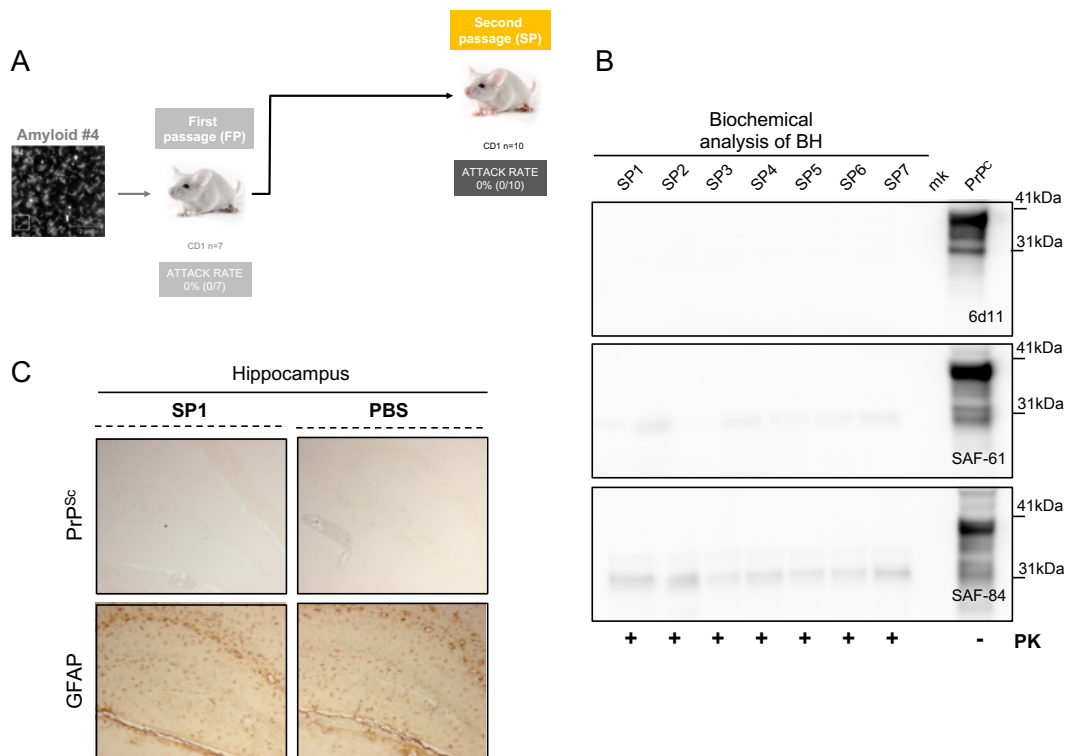


**Fig. 3.4 Biochemical and immunohistochemical analysis of Second passage transmission (SP).** (A) Schematic diagram of second passage transmission (SP). (B) Biochemical analysis of brain homogenates collected from SP animals. (C) Immunostaining for PK-resistant PrP (after PK treatment, 10µg/mL) and Glial Fibrillary Acidic Protein (GFAP) of hippocampus of SP1 animal and PBS injected mice. Images were acquired at 10X magnification.
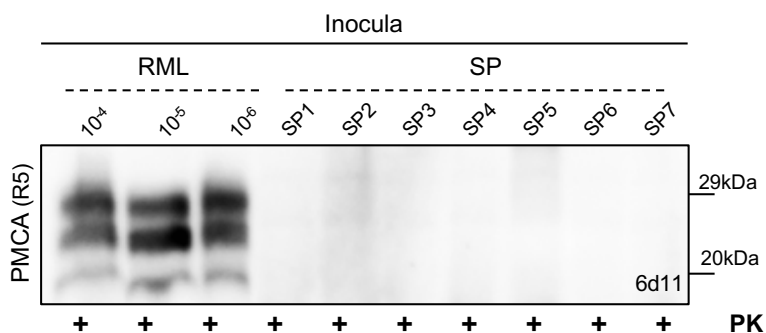
**Fig. 3.5 PMCA analysis of brain homogenates from SP.** PMCA amplification (five rounds, R5) of brains collected from mice of the SP. RML serial dilutions were used as control of PMCA efficiency.

*3.5 First in vivo transmission (PP1) of PMCA amplified new prion isolate (PMCA-FP2)*

For verifying the infectivity of PMCA-FP2 amplified products we injected two groups of 10 animals with either PMCA-FP2 or PMCA-PBS (Fig. 3.6A). All the animals injected with PMCA-FP2 developed prion disease with 100% attack rate. These animals (coded PP1) showed an incubation and survival time of 130 ± 4 and 160 ± 3.85 days (mean ± S.E.M.) respectively (Fig 3.6B).
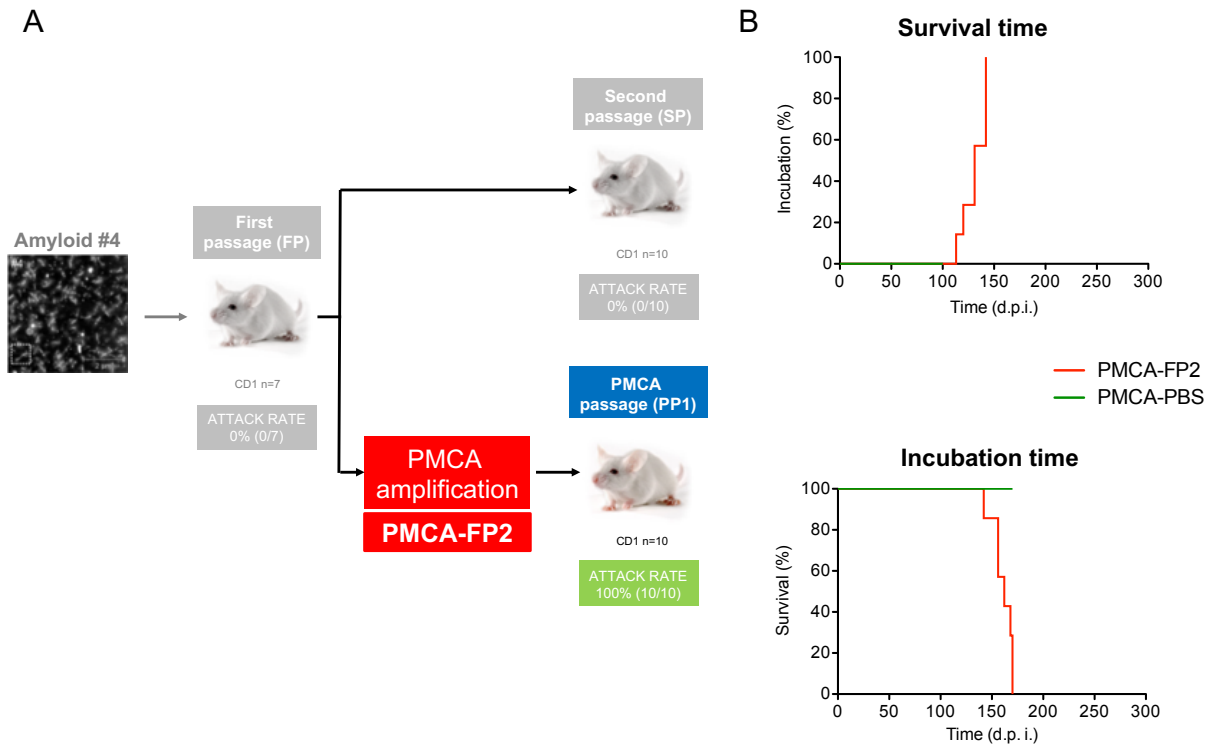
**Fig. 3.6 First transmission passage of PMCA-FP2 isolate.** (A) Schematic diagram of the first transmission of PMCA-FP2 referred as PMCA Passage 1 (PP1). (B) Incubation and survival time analysis of PP1 mice injected with PMCA-FP2 and PMCA-PBS as control.

*3.6 Biochemical and PMCA analysis of mice injected with PMCA-FP2 prion isolate*

Brains and different tissues of terminally sick animals were collected and used for biochemical and immunohistochemical studies. PK-resistant PrP was detected in brains and spinal cord while in other tissues (spleen, eyes, kidney, muscle and liver) PrP$^{Sc}$ were not detectable (Fig. 3.7A). Biochemical analysis showed the presence of a PK resistant PrP with di-glycosylated profile similar to that of the inoculum (PMCA-FP2) (Fig. 3.7A). PMCA analysis was carried out on eyes, spleens and blood samples. We detected resistant PrP amplification after one round in eyes and spleen tissues and after two rounds in blood (Fig. 3.7B) Particularly, blood samples from symptomatic animals were collected after 140 days post injection. Using the RML as positive control for PMCA, we could

estimate that the concentration of infectious prion circulating in blood is similar to that of a $10^{-10}$ dilution of brain homogenate. Notably, all the PMCA amplified products maintained the predominance of the di-glycosylated isoform of PrP as observed in brains of the animals (Fig. 3.7B).
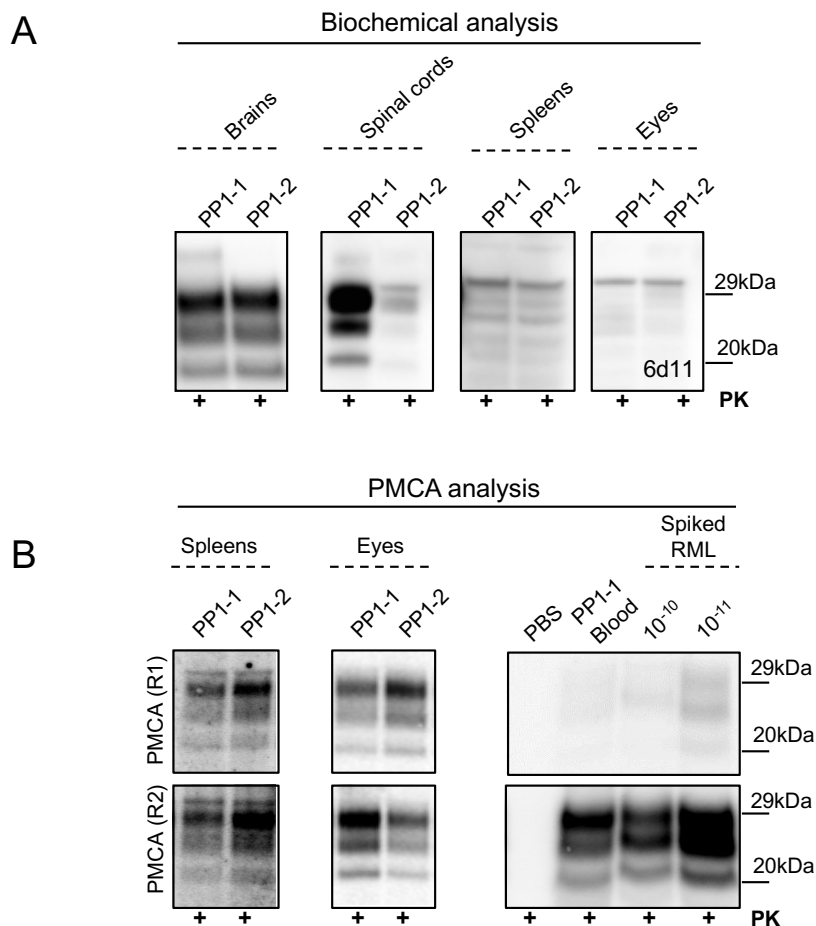


**Fig. 3.7 Biochemical and PMCA analysis of tissues collected from PP1 animals.** (A) PK-digestion and Western blot analysis of brains, spinal cords, spleens and eyes of PP1 mice. (B) PMCA amplification of spleens, eyes and blood of PP1 animals. Dilutions of RML prion strain were used as internal control.

Brains of PP1 were analyzed by means of PMCA to assess their ability to retain the biochemical features of the original inoculum. The phenotype of PrP$^{Sc}$, with the predominance of the di-glycosylated isoform, was maintained after 2 rounds of amplification (Fig. 3.8A). PK-resistant assay was performed on non-amplified and

amplified products (after 2 rounds) that showed similar resistance to proteolytic treatment with PK indicating that the biochemical characteristics of the prion isolate after PMCA were faithfully retained (Fig. 3.8B).
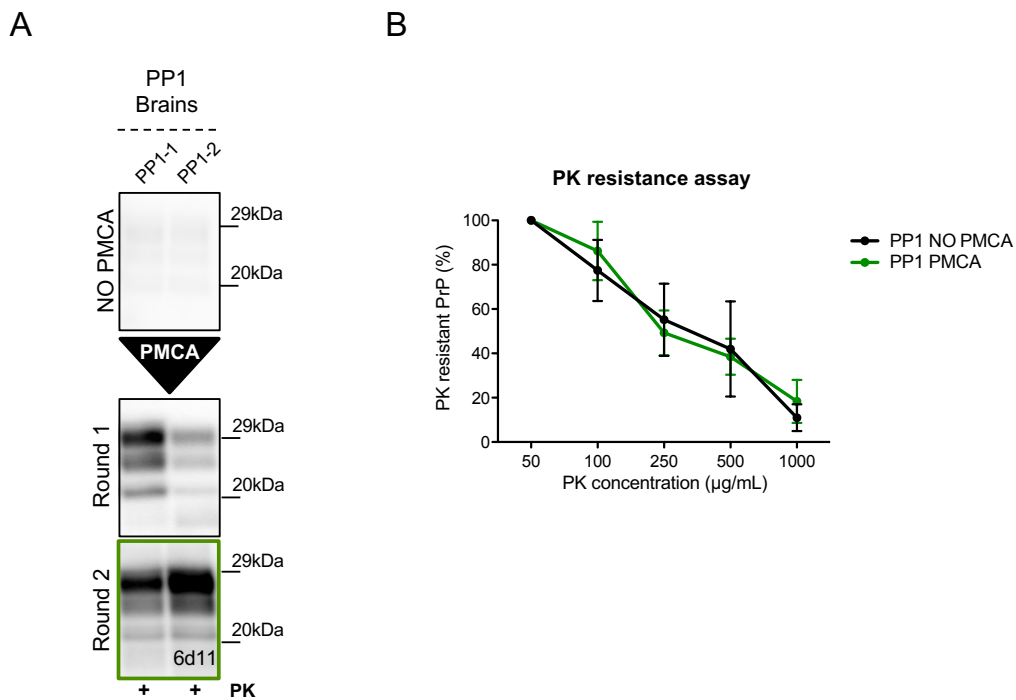


**Fig. 3.8 PMCA analysis and PK-resistance assay of PP1 animals.** (A) *In vitro* amplification of PP1 brains by means of PMCA using CD1 brain homogenate as substrate. (B) PK resistance assay and western blot analysis before and after PP1 PMCA amplification. Errors bars represent the standard error of the mean (S.E.M).

*3.7 Neuropathological analysis of mice injected with PMCA-FP2 prion isolate.*

Neuropathological examination of brains was performed in order to characterize the spongiform alterations and PrP$^{Sc}$ deposition pattern induced by PMCA-FP2 prion isolate. The animals showed widespread PrP$^{Sc}$ deposition, prevalently affecting the hippocampus, thalamus and striatum with focal deposits mainly observed in the submeningeal region of the cerebral cortex and occasionally found in the striatum (Fig. 3.9A). Thioflavin-S staining revealed that these deposits did not possess the amyloid tintorial properties and for this reason were defined as plaque-like (Fig. 3.9B). GFAP immunostaining confirmed

prominent gliosis in PMCA-FP2 injected animals. The lesion profile analysis revealed severe spongiosis in the hippocampus and dorsa medulla while less vacuolization was found in the rest of the brain, including cerebral cortex and thalamus (Fig. 3.9C).
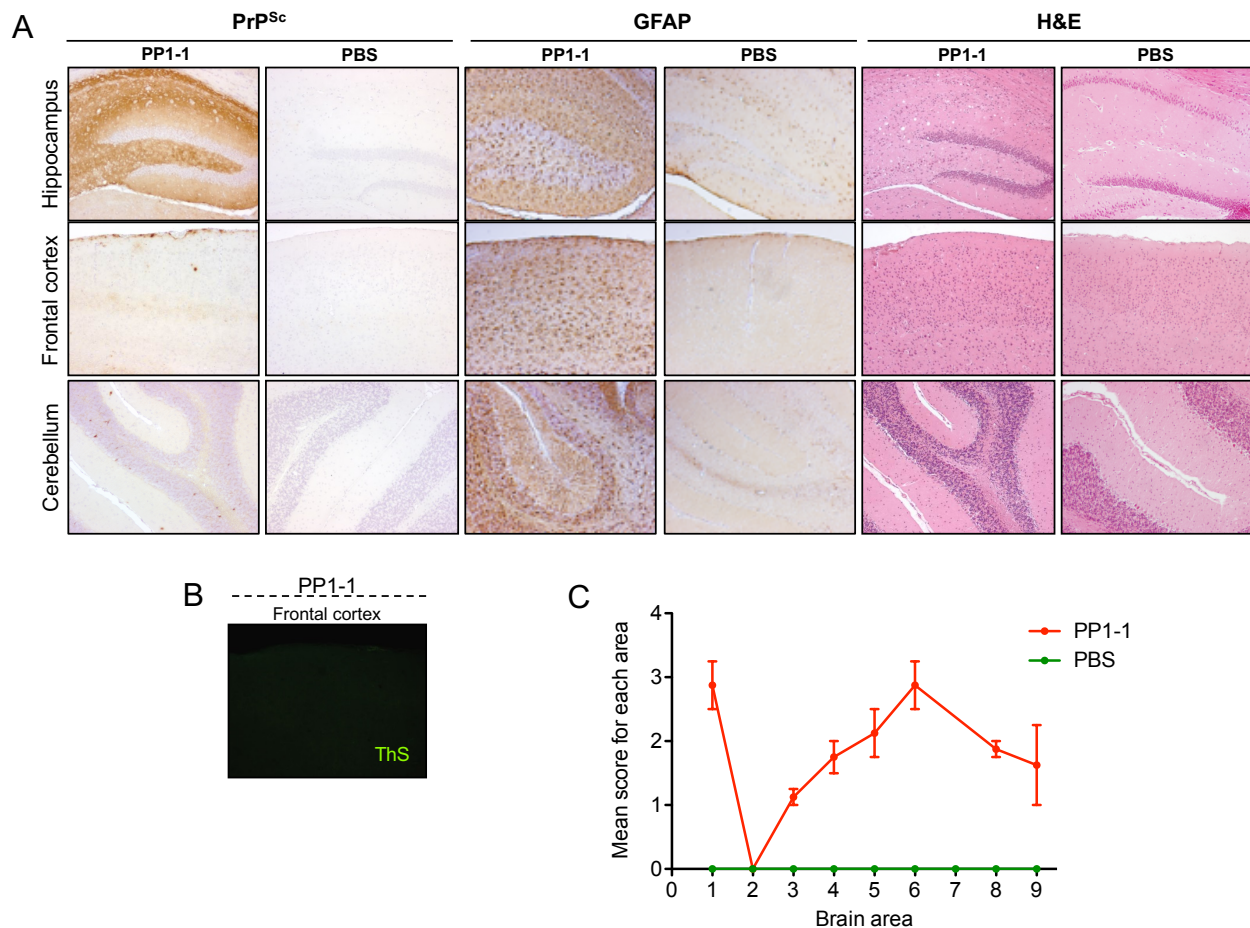


**Fig. 3.9 Neuropathological and immunohistochemical characterization of PP1 animals.** (A) Immunostaining for PK-resistant PrP, GFAP and hematoxylin and eosin staining of hippocampus, frontal cortex and cerebellum of PP1-1 animal and PBS injected mice. (B) Thioflavin-S (ThS) staining of PP1-1 frontal cortex. Images were acquired at 10X magnification. (C) Lesion profile of PP1 and PBS injected animals. The mean score for each area were reported in the graph. 1. Dorsal medulla; 2. Cerebellar cortex; 3. Superior culliculus; 4. Hypothalamus; 5. Thalamus; 6. Hippocampus; 7. Septum; 8. Retrosplenial and adjacent motor cortex; 9. Cingulated and adjacent motor cortex. Errors bars represent the standard error of the mean (S.E.M).

## 3.8 Second in vivo transmission (PP2) of PMCA amplified prion isolate PMCA-FP2.

With the aim of assessing if PMCA-FP2 was able to maintain its biochemical characteristics also through *in vivo* passages, a second transmission experiment (PP2)

was then performed (schematically represented in Fig. 3.10A). All injected mice succumbed to prion pathology with 100% attack rate but two different phenotypes of the disease were observed. The first was characterized by fast incubation and short survival time, respectively of 130.90 ± 0.86 and 164.66 ± 2.81 days post injection (mean±S.E.M.) (Profile 1, black lines) (Fig. 3.10B). These animals showed constant decreasing of body weight during the course of the disease (Fig. 3.10C). By contrast, the other group of PP2 animals (Profile 2, red lines) was characterized by statistically significant longer disease duration with respect to that of Profile 1 (incubation time of 162 ± 6.18 and survival time of 227.50 ± 6.33 days post injection, (mean±S.E.M.)) (Fig. 3.10B). A constant increasing of the body weight during the symptomatic phases that decreased only in the final stages of the disease was observed in this animal group (Fig. 3.10C).
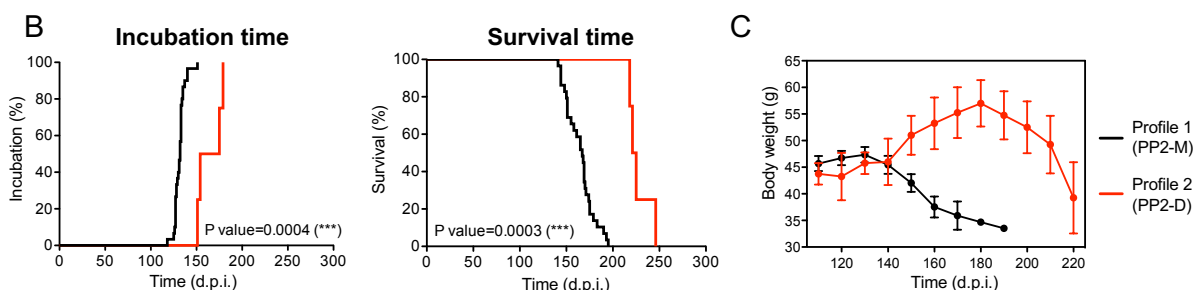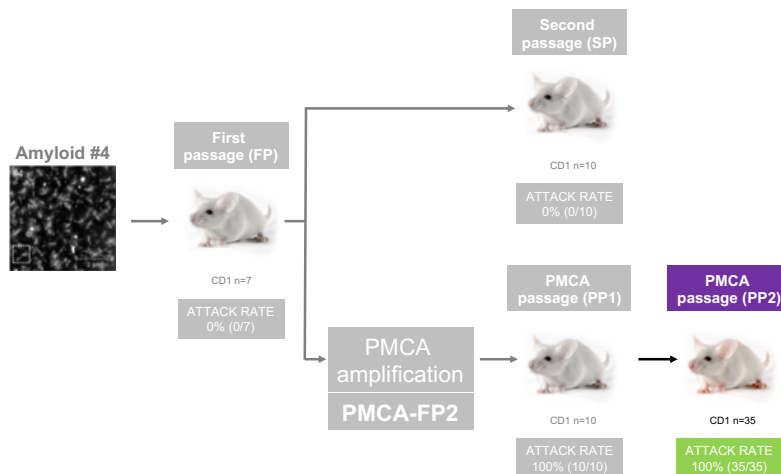
**Fig. 3.10 Second transmission passage (PMCA passage 2, PP2) of PMCA-FP2 isolate.** (A) Schematic diagram of PMCA-FP2 second *in vivo* transmission. (B) Incubation and survival analysis of PP2 animals (Profile-1 (PP2-M) black lines, Profile-2 (PP2-D) red lines) (Log-rank test, * p<0.05, ** p<0.01, *** p<0.001) (C) Body weight assessment of PP2 animals during the symptomatic stage of the disease. Errors bars represent the standard error of the mean (S.E.M).

## 3.9 Biochemical analysis of mice from second in vivo transmission of PMCA-FP2

Biochemical analysis of PP2 brains revealed that the 80% of the animals contained a PrP$^{Sc}$ characterized by the prevalence of the mono-glycosilated band (PP2-M), while the remaining 20% accumulated PrP$^{Sc}$ with a prevalence of the di-glycosylated band (PP2-D) (Fig 3.11). Spleens and eyes of these animals were also analyzed to assess the tropism of both isolates for peripheral tissues. We have found PrP$^{Sc}$ in the eyes of all the animals, which maintained the biochemical properties of those present in the brain. On the contrary, mice with PP2-D in the brain did not have resistant PrP in the spleen, while mice with PP2-

M had a strong PrP$^{Sc}$ signal but surprisingly the biochemical profile of this protein was different from that present in the brain. It was indeed characterized by a prevalence of the di-glycosylated band (Fig. 3.11). These observations indicate that PrP present in our inoculum was able to adopt two alternative conformations, named PP2-M and PP2-D, associated with different disease phenotypes.
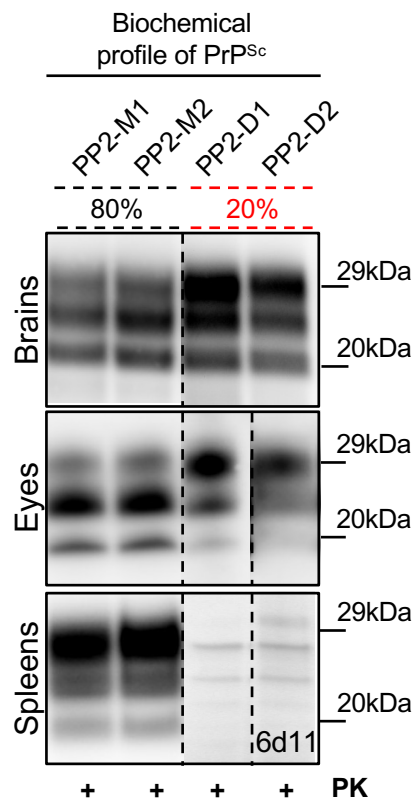


**Fig. 3.11 Biochemical analysis of different tissues collected from PP2 mice.** PK-digestion and Western blot analysis of brains, eyes and spleens of PP2 animals.

*3.10 Neuropathological analysis of mice from second in vivo transmission of PMCA-FP2.*

Immunohistochemical analysis confirmed that PP2-M and PP2-D produced different neuropathological alterations in the brain of injected animals. In particular, after treatment with PK, samples were immunostained with anti-PrP antibody (6H4) and revealed that mice with PP2-M had a synaptic and widespread deposition of prion throughout the brain.

On the contrary, mice with PP2-D showed prion deposition mainly confined to the *stratum lacunosum moleculare* of the hippocampus and to the deep layers of the cortex with the presence of few plaque-like deposits, which did not possess the tintorial properties of amyloid (Fig. 3.12A and 3.12B). Few depositions of PrP$^{Sc}$ was observed in the cerebellar cortex of both group of animals. Glial activation was found to correlate with PrP$^{Sc}$ deposition in frontal cortex and hippocampus (either in terms of localization or intensity of the signal), which was different between both groups of animals (Fig 3.12A).
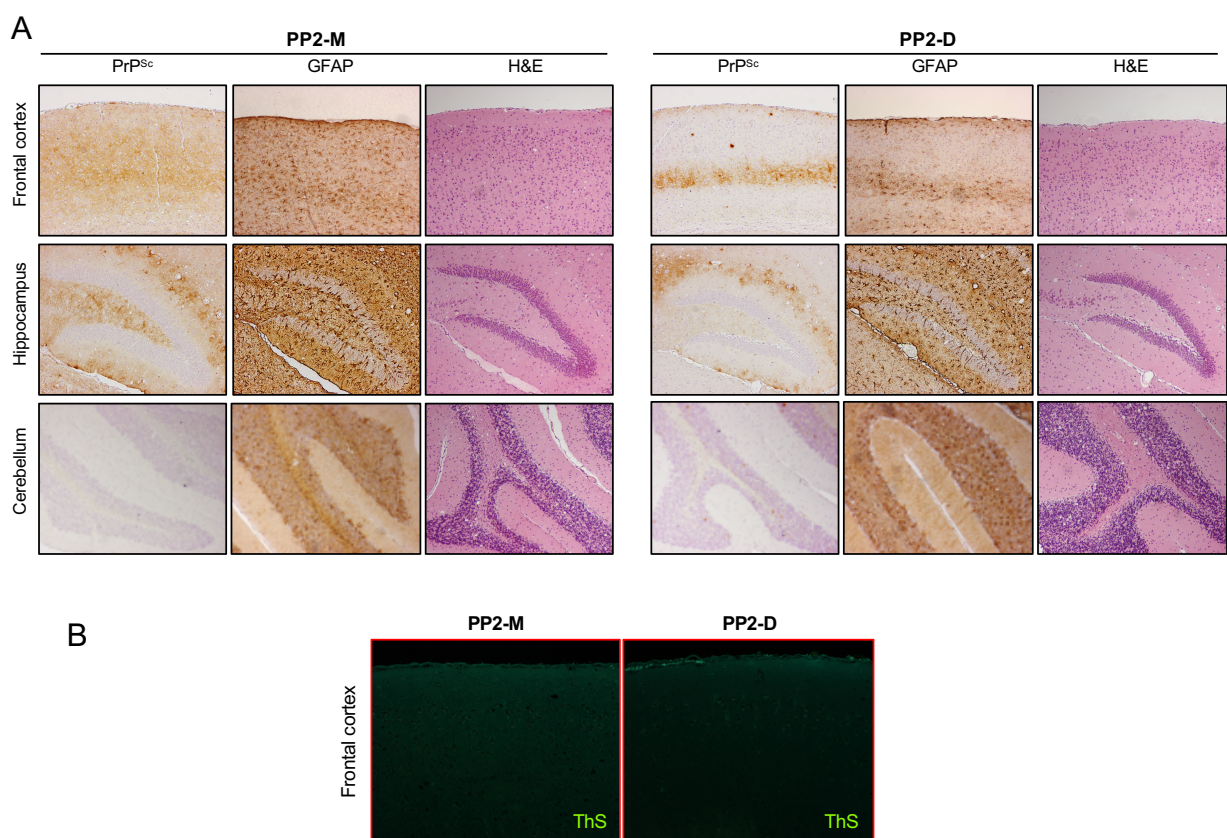


**Fig. 3.12 Neuropathological and immunohistochemical analysis of animals with PP2-M and PP2-D.** (A) Immunostaining for PK-resistant PrP, Glial fibrillary acidic protein (GFAP) and hematoxylin and eosin staining of frontal cortex, hippocampus, and cerebellum of mice with PP2-M and PP2-D. (B) Thioflavin-S (ThS) staining of frontal cortex of mice with PP2-M and PP2-D. Images were acquired at 10X magnification.

Lesion profile analysis clearly showed that PP2-M and PP2-D animals possess different topographic distribution of spongiform alterations (Fig. 3.13A). In particular, medulla and

hippocampus are mostly affected in PP2-D animals, while thalamus and cingulated cortex are mostly involved in PP2-M animals (Fig 3.13B).
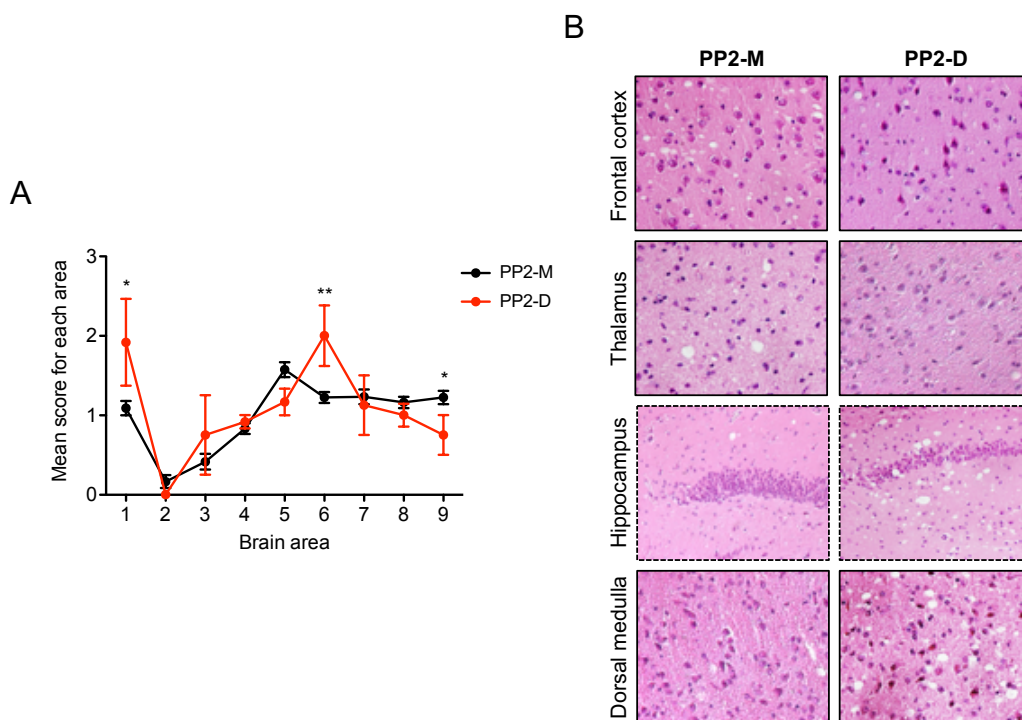


**Fig. 3.13 Lesion profile of PP2 animals.** (A) Lesion profile of animals with PP2-M and PP2-D. Brain areas correspond to: 1. Dorsal medulla; 2. Cerebellar cortex; 3. Superior culliculus; 4. Hypothalamus; 5. Thalamus; 6. Hippocampus; 7. Septum; 8. Retrosplenial and adjacent motor cortex; 9. Cingulated and adjacent motor cortex (* p<0.05, ** p<0.01, *** p<0.001). Errors bars represent the standard error of the mean (S.E.M). (B) Hematoxylin and eosin stained sections of most representative brain areas of PP2. Images with solid box were acquired at 40X magnification while image with dotted box were acquire at 20X magnification.

*3.11 Biochemical and biophysical analysis of PP2-M and PP2-D in vivo generated prion isolates.*

To better characterize the biochemical and biophysical properties of PP2-M and PP2-D we performed (i) PK-resistance and (ii) conformational stability assays. The samples were then analyzed by means of Western blotting and densitometric analysis. The results were plotted in a graph and revealed that PP2-D appeared to be more resistant to PK digestion than PP2-M (Fig. 3.14A). Statistically significant differences were observed at 100, 250

and 1000 µg/mL concentration of PK. Conformational stability assay revealed that PP2-M is more stable against to GdnHCl treatment with respect to PP2-D. Especially, significant differences were observed at 3M concentration of chaotropic agent (Fig. 3.14B). Thus, PP2-M is less resistant to PK digestion but more stable against guanidine treatment than PP2-D which is instead more resistant to PK but less stable in GdnHCl. We have finally determined the concentration of GdnHCl required to unfold half of PrP$^{Sc}$ ([GdnHCl$_{1/2}$]). As reported in the graph (Fig. 3.14C) we found statistically significant differences between the [GdnHCl$_{1/2}$] of PP2-M (3.344±0.1663) and PP2-D (1.904±0.2695) (mean(M)±S.E.M.).
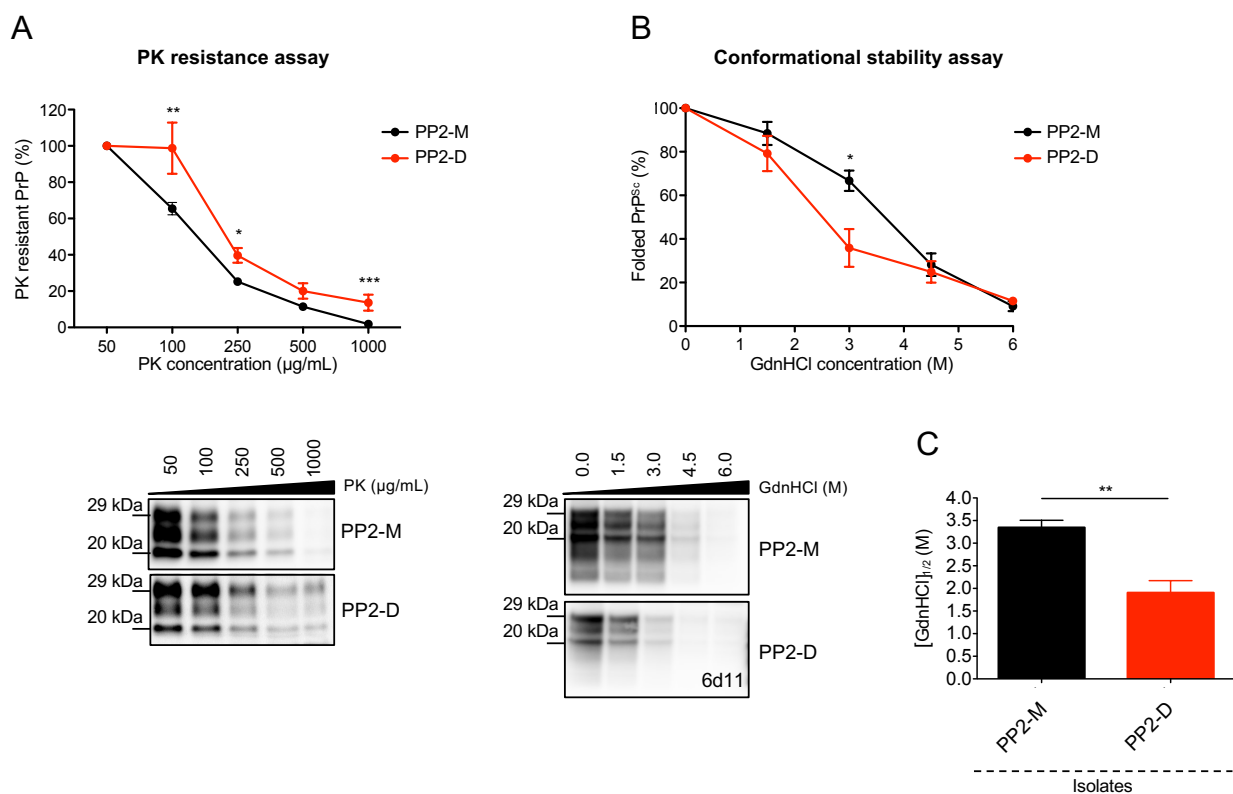


**Fig. 3.14 Biochemical and biophysical assessment of PP2-M and PP2-D prion isolates.** (A) PK-resistance assay and (B) Conformational stability assay of animals with PP2-M (black lines) and PP2-D (red lines). (C) [Gdn-HCl]$_{1/2}$ of PP2-M and PP2-D isolates. (* $p<0.05$, ** $p<0.01$, *** $p<0.001$). Errors bars represent the standard error of the mean (S.E.M).

*3.12 PMCA analysis of in vivo generated prion isolates.*

PP2-M and PP2-D tissues (brains, eyes and spleens) were analyzed by means of PMCA to assess their amplification's efficiency and their ability to retain the biochemical features of the original inoculum. Results confirmed that both isolates were able to efficiently amplify from all the tissues analyzed but, regardless of the inoculum (PP2-M or PP2-D) the final products of amplification were characterized by a $PrP^{Sc}$ with a prevalence of the diglycosylated band (Fig 3.15A). Notably, despite $PrP^{Sc}$ was not detectable in PP2-D spleens, after 1 round of PMCA a PK-resistant signal was detected. These results indicates that the biochemical profile of PP2-D was maintained while that of PP2-M was lost during the amplification process and new biochemical features were acquired. To exclude any technical bias, we tested the fidelity of PMCA amplification by subjecting mouse adapted-vCJD (mo-vCJD) and RML prion strains to several rounds of PMCA. mo-vCJD is indeed characterized by the prevalence of di-glycosylated PrP isoform, while RML by the mono-glycosylated one. After amplification, the biochemical characteristics of both prion strains were retained, thus suggesting that PMCA is able to amplify different prion strains with high fidelity (Fig. 3.15B). For this reason, the amplification products of PP2-M suggest that a process of adaptation or selection might have occurred and gave rise to the formation of an isolate with different biochemical features.
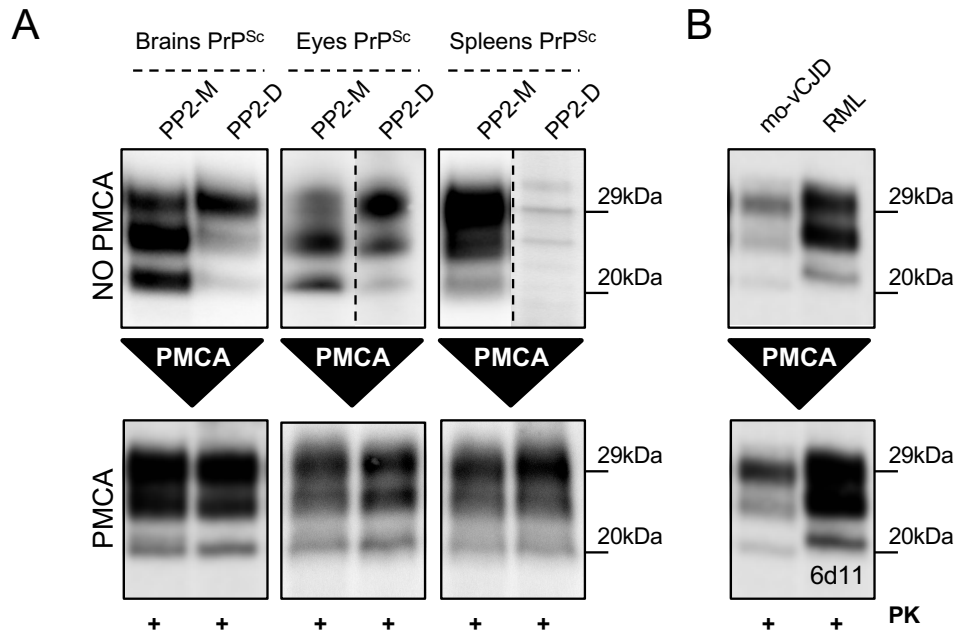
**Fig. 3.15 PMCA analysis of PP2-M and PP2-D isolates.** (A) PMCA amplification of PP2-M and PP2-D isolates from brains, eyes and spleens of PP2 animals. (B) Internal control of PMCA amplification fidelity with mo-vCJD and RML prion strains.

We then performed PMCA analysis of PP2-M and PP2-D with the aim of evaluating if PP2-M and PP2-D are "pure" isolates or a mixture of different PrP$^{Sc}$. For these reasons, we performed serial dilutions (from $10^{-3}$ to $10^{-12}$ dilution of brain homogenate) of both PP2-M and PP2-D isolates in PMCA substrate and subjected these samples to amplification. With this experiment, we give the opportunity to under-represented conformation of PrP$^{Sc}$ eventually present in our isolates to replicate *in vitro*. Both PP2-M and PP2-D, independently from the dilution performed showed di-glycosylated amplified product after one and two rounds of amplification (Fig. 3.16). These data suggest that the PMCA context of replication might be able to selectively amplify a PrP isoform characterized by di-glycosylated profile.

**Fig 3.16 PMCA amplification of serial dilution of PP2-M and PP2-D isolates.** PMCA amplification of serially diluted PP2-M and PP2-D (from $10^{-3}$ to $10^{-12}$ dilution of brain homogenates) using CD1 brain homogenate as substrate.

## 3.13 Biochemical, biophysical and RT-QuIC analysis of the final PMCA products and comparison with the original isolates.

Since this biochemical profile is similar to that of PP2-D we wondered whether PMCA might have indeed preferentially amplified PP2-D, thus demonstrating that it might coexist with PP2-M, or was able to sustain the replication of a different PrP$^{Sc}$ isoform. For these reasons, PMCA products (either from PP2-M or PP2-D) were subjected to biochemical and biophysical analysis, including (i) PK resistance assay (Fig. 3.17A) and (ii) conformational stability assay with GdnHCl (Fig. 3.17B). All the PMCA amplified samples showed similar resistance to PK digestion and stability in the presence of GdnHCl, supporting the fact that, regardless of the inoculum (PP2-M or PP2-D), PMCA was able to

generate a unique isolate, termed PP2-PMCA. This isolate was characterized by the presence of a PrP$^{Sc}$ with a predominance of the di-glycosylated band. Surprisingly, PK resistance and GdnHCl assays showed that PP2-PMCA (Fig. 3.17 solid lines) possessed biophysical features quite different from those of either PP2-M or PP2-D (Fig. 3.17 dotted lines). In particular, PP2-PMCA was much more resistant to PK and more stable in GdnHCl than PP2-M and PP2-D (Fig. 3.17A and B).
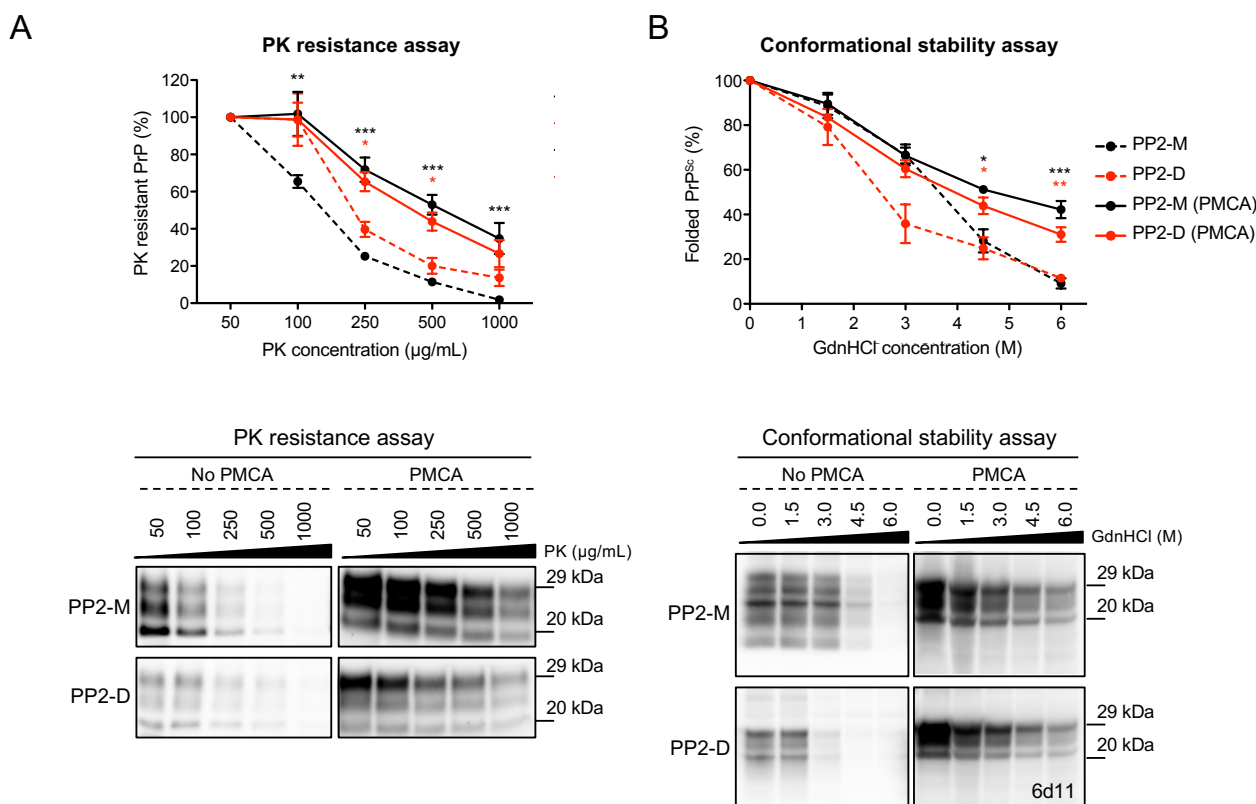


**Fig. 3.17 Biophysical characterization of PP2-PMCA isolate.** (A) PK-resistance assay and (B) Conformational stability assays of PMCA-PP2 amplified isolates (PP2-M (PMCA) and PP2-D (PMCA)) (* $p<0.05$, ** $p<0.01$, *** $p<0.001$). Errors bars represent the standard error of the mean (S.E.M).

PP2-M, PP2-D and PP2-PMCA were finally analyzed by means of RT-QuIC to assess whether these isolates were characterized by different seeding activity. All the isolates possessed seeding activity of mouse recombinant PrP (23-231), which was efficiently triggered by all of them, without significant differences in terms of kinetic of aggregation

and fluorescence intensity (Fig. 3.18A). By further analyzing the slope, that numerically describe the steepness of the kinetic curves, we have found that the slope of PP2-M was smaller than that of PP2-D (Fig. 3.18B) thus further sustaining the fact that both isolates are different from each other. The slope of PP2-PMCA acquired an intermediate value between PP2-M and PP2-D but still statistically different from either of them. These findings suggested that also PP2-PMCA seems to be a different isolate characterized by its own seeding activity. As control, we analyzed the seeding activity of RML brain homogenate either before or after PMCA amplification. In this case, the slopes of the curves were similar and not statistically significant differences were found thus confirming that, likely, PMCA amplified this strain with high fidelity (Fig.3.18C).
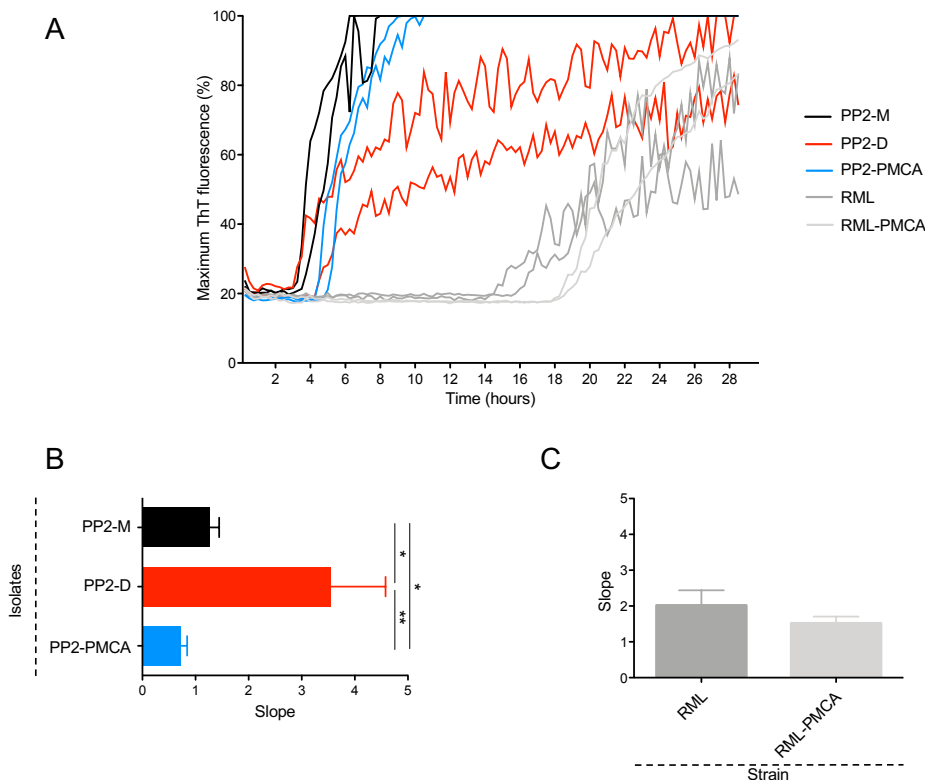


**Fig. 3.18 RT-QuIC assay of PP2-M and PP2-D isolates.** (A) Representative kinetic curves of recombinant mouse PrP (23-231) seeded with PP2-M, PP2-D, PP2-PMCA, RML and RML-PMCA. (B) Analysis of the slope of PP2-M and PP2-D and PP2-PMCA aggregation kinetic curves. (* $p<0.05$, ** $p<0.01$) (C) Analysis of the slope of RML and RML-PMCA aggregation kinetic curves. Errors bars represent the standard error of the mean (S.E.M).

# Discussion

In recent years, a body of evidence demonstrated that under specific biochemical conditions, recombinant PrP$^C$ can be misfolded *in vitro* into amyloid structures which were able to cause illness and produced pathological features in animals similar to that observed in natural occurring prion diseases. The advent of synthetic prions permitted the study of different aspects of prion biology including the basis of prion replication and the phenomenon of prion adaptation and selection with highly pure preparations instead of natural derived prion strains. We have previously shown the ability of a synthetic amyloid (amyloid #4) to induce accumulation of PrP$^{Sc}$ in both N2a and GT-1 cell lines [246]. The synthetic amyloid and the lysates from infected cell lines were analyzed by means of PMCA for assessing the ability of the synthetic prion to propagate *in vitro*. In both cases, we were able to detect a PrP$^{Sc}$ signal after three rounds of PMCA characterized by the predominance of the di-glycosylated band of PrP. When injected in wild-type animals, the synthetic prion did not produce any evident prion pathology in the (i) first (FP) and (ii) second passage (SP). This phenomenon could have several explanations. For example, Makarava et al. [234] reported that there is a period of time where the amyloid structure is converted to an intermediate and atypical form of PrP$^{res}$ (deformed templating) before producing the classical PrP$^{Sc}$ which is able to trigger evident pathological changes in mice. Since the atypical PrP$^{res}$ is characterized by a short PK-resistant core, we have digested the brain of amyloid #4 injected mice with different concentrations of PK and used antibodies which recognize more C-terminal fragments of PrP (SAF-84, residues 160–170;

SAF-61 antibody which recognize residues 144–152). Even with these modifications we could never detect any typical or atypical PK resistant PrP. Another explanation for the lack of pathological changes in mice injected with amyloid #4 could be attributable to the small amount of infectious material used to challenge the animals. In this case, the amount of amyloids could not have been sufficient to misfold enough PrP$^C$ and induce disease.

We have subjected the CNS of the FP animals to PMCA analysis and we detected the presence of a PK-resistant PrP in 1 out of 7 CNS analyzed after 3 rounds of amplification. Notably, the amplified product maintained the predominance of di-glycosylated PrP isoform previously observed from the amplification of the raw synthetic prion and was characterized by the presence of an un-glycosylated band migrating at around 20kDa.

This product (referred as PMCA-FP2), was challenged in mice for assessing its infectious properties. PMCA-FP2 isolate was able to induce highly aggressive prion pathology in animals with 100% attack rate. Biochemical analysis confirmed the ability of the amplified product to induce the formation of PrP$^{Sc}$ characterized by the same biochemical features of the inoculum (predominance of the di-glycosylated form of the protein). PrP$^{Sc}$ were detected also in blood of symptomatic animals confirming the aggressiveness of the new prion isolate. Neuropathologically, PMCA-FP2 was able to induce spongiform lesions with distinct distribution with respect to standard mouse prion strains.

Brain homogenate of these animals where used to perform a second transmission experiment (PP2). All the animals succumbed to prion disease but in their brains we could detect the presence of two different prion isolates. In the 80% of the cases the PrP$^{Sc}$ was characterized by a predominance of the mono-glycosylated band (PP2-M), while in the other 20% it was characterized by a predominance of the di-glycosylated isoform (PP2-D).

These differences in the biochemical profiles were associated to different (i) clinical manifestations of the disease (including incubation time, survival time and body weight changes) (ii) neuropathological changes (deposition of PrP$^{Sc}$ and spongiform alterations) (iii) biochemical and biophysical features of both PrP$^{Sc}$ (PK-resistance assay and GdnHCl conformational stability assays) and different seeding activity when assessed by means of RT-QuIC. In particular, PP2-M induced a faster disease progression, was less resistant to PK digestion and showed higher stability to GdnHCl denaturation compared to PP2-D.

Considering data from the literature, the conformational stability of prion strains appear closely related to the clinical course of the disease [248]. For instance, as reported for hyper (HY) and drowsy (DY) in hamsters, PrP$^{Sc}$ associated to HY is characterized by high conformational stability and induce faster disease progression while that associated to DY possesses low conformational stability and is responsible for longer disease duration. This correlation was also found in our synthetic prion isolates, where PP2-M is more stable and it induced shorter disease duration than PP2-D, which in turn is less stable and leads to longer disease duration. As reported by previous studies [241, 248, 249] the inverse relationship between PrP$^{Sc}$ stability and disease duration cannot be assumed as general model, particularly in the case of synthetically derived prion strains. Recent data [250] suggest that this characteristic might be influenced by (i) recPrP primary sequence of synthetic prions and (ii) the animal model used for bioassays. Altogether these data support the hypothesis that the serial *in vivo* passages were able to generate two different isolates that spontaneously arose from our original inoculum due to mechanisms of selection or adaptation that are not understood yet. It seems that the context of prion replication plays an important role in guiding these phenomena.

These insights suggest the intrinsically heterogeneous composition of prion strains and their ability to adapt in response to environment pressure in agreement to the

Darwinian evolution theory [185]. Two main hypotheses were proposed as possible mechanism: the "cloud" hypothesis and the adaptation mechanism. The cloud hypothesis infers that the prion population is composed of a multitude of conformational variants. Changing the replication environment allows the most efficiently replicating variant to becomes the predominant component of the population which then constitutes a distinct sub-strain [185]. On the contrary, the adaptation mechanism consists of a long clinically silent stage which is accompanied by a slow modification of the biophysical and neuropathological properties of $PrP^{Sc}$. The long adaptation period of synthetic prion when injected in animals is attributed to structural changes of PrP conformation that, in a mechanism named "deformed templating", lead to a generation of an authentic $PrP^{Sc}$. The deformed templating mechanism proposed that the first product of $PrP^{C}$ misfolding triggered by recombinant amyloids generate a self-replicating state of PrP named atypical $PrP^{Sc}$. After several serials passages the atypical $PrP^{Sc}$ gave rise to a $PrP^{Sc}$ with specific biochemical and neuropathological characteristics [187, 236].

We are not able to determine whether the generation of two isolates is mainly due to either a process of selection or adaptation. Indeed, the original inoculum, although produced using highly pure source of recombinant PrP and strictly controlled biochemical conditions, might have produced different isolates of misfolded PrP. When passaged in mice, only two of these isolates seemed to replicate with higher efficiency compared to others, which induced different pathologies. It is reasonable to argue that, although not detectable, the other isolates might still be present and able to replicate with lower efficiency. The amplification of the two isolates might have also been favored by the characteristics of the outbred animals utilized in the *in vivo* experiments. Recent evidence shows that minimal variations in the genetic background of the host animals can significantly influence the biochemical features of $PrP^{Sc}$ [251]. Therefore, differences in the

genetic background of CD-1 animals might have favored the replication of PP2-M or PP2-D while interfering with the replication of other isolates. However, differences in the level of PrP$^C$ expression were shown to play a role in driving the glycosylation pattern of PrP$^{Sc}$ [252]. Considering that PP2-M and PP2-D differentially accumulated in distinct brain regions, we might speculate that (i) such areas might be characterized by the presence of slightly different levels of PrP$^C$ that can significantly influence the glycosylation of our isolates or (ii) PP2-M and PP2-D might preferentially replicate in different cell types such as neurons or astrocytes. Furthermore, the ubiquitin-proteasome system (UPS) and lysosomal systems may contribute to the prevalent selection of some prion isolates more resistant to proteolytic degradation [253, 254]. Compelling evidence indicates that prions can change their abnormal conformation in response to events unrelated to changes of the environment of replication by spontaneous structural modifications of the PrP$^{Sc}$ [167]. These phenomena might also explain the appearance of new prion strains after inter-species prion transmission. In this scenario, the pressure exerted either by the new environment or by differences in PrP$^C$ sequence might force the protein to misfold with different conformation.

Through PMCA analysis of PP2-M and PP2-D we observed the generation of an amplified product (PP2-PMCA), which was not found *in vivo* and showed different biophysical properties from those of PP2-M and PP2-D. We do not know the precise mechanisms which led to the preferential replication of PP2-PMCA but a fundamental aspect that we need to consider is that PMCA provides solely the permissive environment for prion replication, without the presence of any cellular interactions or compartments (Endosomes with acidic pH). Acidic pH of endosomal compartments have been suggested as relevant for PrP$^C$/PrP$^{Sc}$ conversion [255] while the pH of the PMCA reaction is neutral, homogenous and stable. Thus, these conditions might have favored the replication of a

third isolate different from PP2-M and PP2-D. Indeed, PMCA exposes the samples to high power of cyclical sonication and might contribute in changing the biochemical and biophysical features of the final amplified product.

Likely, the context of PMCA amplification can impose an *evolutionary* pressure that may select the isolate able to better replicate in this environment. Therefore, we can infer that the PrP$^{Sc}$ conformation amplified by PMCA might have been present in all the animal brains but was not able to replicate *in vivo*.

In conclusion, our data indicate that putative infectious materials can be generated *in vitro*, under controlled and well-defined biophysical and biochemical conditions using solely recombinant PrP and some simple chemicals, without employing prion infected brain homogenate or purified PrP$^{Sc}$. We observed that the amyloid #4 maintained the same biochemical profile when amplified from (i) the synthetic preparation or (ii) the infected cell lysates and finally (iii) from the brain of infected mouse. Nevertheless, after PMCA amplification, this newly generated synthetic prion was found to induce a severe prion pathology when injected in mice.

Notably, that synthetic prion amyloids are able to change their biochemical and infectious properties in response to (i) repetitive animal passages and (ii) changes in the context of replication through phenomena of prion adaptation and selection. As observed for natural-derived prion strains, also synthetic prion strains may undergo a process of adaptation after animal passages. These data show that either the environment or other factors contribute to (i) altering the conformation of PrP giving rise to new ones whose replication is more efficient in the modified environment or (ii) favoring the replication of few prion isolates over others that might coexist in the same strain.

The two main mechanisms proposed for prion "evolution", the cloud hypothesis and the deformed templating (detailed in Introduction) might explain the behavior of our synthetic prion but we are not able to determine whether the generation of different PrP$^{Sc}$ conformations is mainly due to either a process of selection of pre-existing PrP$^{Sc}$ or an adaptation of PrP$^{Sc}$ isolate through animal passages. These insights suggest the intrinsically heterogeneous composition of prion strains and their ability to adapt in response to environment pressure.

Events of prions selection were already observed after pharmacological treatment of cell cultures [185] or infected animals [188, 189] where the generation of drug-resistant variants of the original PrP strain were described. This because the pharmacological treatments were able to modify the environment thus inhibiting the replication of specific strains while selecting drug-resistant conformations that can replicate in the new environment and sustain the pathological process. This might explain why there are still no effective therapies for these devastating disorders.

The possibility to modulate the replication environment by exploiting innovative techniques such as PMCA and RT-QuIC would help to an understanding of the mechanism of prion selection and adaptation in response to cellular environmental changes and identify novel pharmacological target for anti-prion compound.

# References

1.  Wood, J.L., L.J. Lund, and S.H. Done, *The natural occurrence of scrapie in moufflon.* Vet Rec, 1992. **130**(2): p. 25-7.
2.  Barlow, R.M., *Transmissible mink encephalopathy: pathogenesis and nature of the aetiological agent.* J Clin Pathol Suppl (R Coll Pathol), 1972. **6**: p. 102-9.
3.  Williams, E.S. and S. Young, *Spongiform encephalopathy of Rocky Mountain elk.* J Wildl Dis, 1982. **18**(4): p. 465-71.
4.  Wells, G.A., et al., *A novel progressive spongiform encephalopathy in cattle.* Vet Rec, 1987. **121**(18): p. 419-20.
5.  Wyatt, J.M., et al., *Naturally occurring scrapie-like spongiform encephalopathy in five domestic cats.* Vet Rec, 1991. **129**(11): p. 233-6.
6.  Sigurdson, C.J. and M.W. Miller, *Other animal prion diseases.* Br Med Bull, 2003. **66**: p. 199-212.
7.  Babelhadj, B., et al., *Prion Disease in Dromedary Camels, Algeria.* Emerg Infect Dis, 2018. **24**(6): p. 1029-1036.
8.  Gambetti, P., G. Puoti, and W.Q. Zou, *Variably protease-sensitive prionopathy: a novel disease of the prion protein.* J Mol Neurosci, 2011. **45**(3): p. 422-4.
9.  Masters, C.L., D.C. Gajdusek, and C.J. Gibbs, Jr., *Creutzfeldt-Jakob disease virus isolations from the Gerstmann-Straussler syndrome with an analysis of the various forms of amyloid plaque deposition in the virus-induced spongiform encephalopathies.* Brain, 1981. **104**(3): p. 559-88.
10. Medori, R., et al., *Fatal familial insomnia, a prion disease with a mutation at codon 178 of the prion protein gene.* N Engl J Med, 1992. **326**(7): p. 444-9.
11. Gambetti, P., et al., *Sporadic and familial CJD: classification and characterisation.* Br Med Bull, 2003. **66**: p. 213-39.
12. Mastrianni, J.A., *The genetics of prion diseases.* Genet Med, 2010. **12**(4): p. 187-95.
13. Gajdusek, D.C., C.J. Gibbs, and M. Alpers, *Experimental transmission of a Kuru-like syndrome to chimpanzees.* Nature, 1966. **209**(5025): p. 794-6.
14. Chen, C. and X.P. Dong, *Epidemiological characteristics of human prion diseases.* Infect Dis Poverty, 2016. **5**(1): p. 47.
15. Liberski, P.P., *Historical overview of prion diseases: a view from afar.* Folia Neuropathol, 2012. **50**(1): p. 1-12.
16. Gordon W.S., *Louping ill, tickbome fever and scrapie.* Vet Rec, 1946. **47**: p. 516-20.
17. Millson G.C., et al., *The physico-chemical nature of the scrapie agent. In: Kimberlin R.H. (ed.). Slow virus diseases of animals and man.* North-Holland Publ Comp, Amsterdam, 1976. p. 243-66.
18. Chandler, R.L., *Encephalopathy in mice produced by inoculation with scrapie brain material.* Lancet, 1961. **1**(7191): p. 1378-9.
19. Gibbons, R.A. and G.D. Hunter, *Nature of the scrapie agent.* Nature, 1967. **215**(5105): p. 1041-3.
20. Adams, D.H., *The nature of the scrapie agent. A review of recent progress.* Pathol Biol (Paris), 1970. **18**(9): p. 559-77.
21. Bastian, F.O., *Spiroplasma as a candidate agent for the transmissible spongiform encephalopathies.* J Neuropathol Exp Neurol, 2005. **64**(10): p. 833-8.
22. Liberski, P.P., *Kuru and D. Carleton Gajdusek: a close encounter.* Folia Neuropathol, 2009. **47**(2): p. 114-37.
23. Cho, H.J., *Is the scrapie agent a virus?* Nature, 1976. **262**(5567): p. 411-2.
24. Alper, T., et al., *Does the agent of scrapie replicate without nucleic acid?* Nature, 1967. **214**(5090): p. 764-6.
25. Kimberlin, R.H., *Scrapie agent: prions or virinos?* Nature, 1982. **297**(5862): p. 107-8.
26. Griffith, J.S., *Self-replication and scrapie.* Nature, 1967. **215**(5105): p. 1043-4.

27. Prusiner, S.B., *Novel proteinaceous infectious particles cause scrapie.* Science, 1982. **216**(4542): p. 136-44.

28. Bolton, D.C., M.P. McKinley, and S.B. Prusiner, *Identification of a protein that purifies with the scrapie prion.* Science, 1982. **218**(4579): p. 1309-11.

29. Gabizon, R., et al., *Immunoaffinity purification and neutralization of scrapie prion infectivity.* Proc Natl Acad Sci U S A, 1988. **85**(18): p. 6617-21.

30. Chesebro, B., et al., *Identification of scrapie prion protein-specific mRNA in scrapie-infected and uninfected brain.* Nature, 1985. **315**(6017): p. 331-3.

31. Stahl, N., et al., *Structural studies of the scrapie prion protein using mass spectrometry and amino acid sequencing.* Biochemistry, 1993. **32**(8): p. 1991-2002.

32. Hsiao, K., et al., *Linkage of a prion protein missense variant to Gerstmann-Straussler syndrome.* Nature, 1989. **338**(6213): p. 342-5.

33. Collinge, J., *Prion diseases of humans and animals: their causes and molecular basis.* Annu Rev Neurosci, 2001. **24**: p. 519-50.

34. Bueler, H., et al., *Mice devoid of PrP are resistant to scrapie.* Cell, 1993. **73**(7): p. 1339-47.

35. Stahl, N., et al., *Scrapie prion protein contains a phosphatidylinositol glycolipid.* Cell, 1987. **51**(2): p. 229-40.

36. Colby, D.W. and S.B. Prusiner, *Prions.* Cold Spring Harb Perspect Biol, 2011. **3**(1): p. a006833.

37. Millhauser, G.L., *Copper and the prion protein: methods, structures, function, and disease.* Annu Rev Phys Chem, 2007. **58**: p. 299-320.

38. Abskharon, R.N., et al., *Probing the N-terminal beta-sheet conversion in the crystal structure of the human prion protein bound to a nanobody.* J Am Chem Soc, 2014. **136**(3): p. 937-44.

39. Turk, E., et al., *Purification and properties of the cellular and scrapie hamster prion proteins.* Eur J Biochem, 1988. **176**(1): p. 21-30.

40. Maiti, N.R. and W.K. Surewicz, *The role of disulfide bridge in the folding and stability of the recombinant human prion protein.* J Biol Chem, 2001. **276**(4): p. 2427-31.

41. Rudd, P.M., et al., *Glycosylation differences between the normal and pathogenic prion protein isoforms.* Proc Natl Acad Sci U S A, 1999. **96**(23): p. 13044-9.

42. Locht, C., et al., *Molecular cloning and complete sequence of prion protein cDNA from mouse brain infected with the scrapie agent.* Proc Natl Acad Sci U S A, 1986. **83**(17): p. 6372-6.

43. Caughey, B., et al., *Prion protein biosynthesis in scrapie-infected and uninfected neuroblastoma cells.* J Virol, 1989. **63**(1): p. 175-81.

44. Monari, L., et al., *Fatal familial insomnia and familial Creutzfeldt-Jakob disease: different prion proteins determined by a DNA polymorphism.* Proc Natl Acad Sci U S A, 1994. **91**(7): p. 2839-42.

45. Petersen, R.B., et al., *Effect of the D178N mutation and the codon 129 polymorphism on the metabolism of the prion protein.* J Biol Chem, 1996. **271**(21): p. 12661-8.

46. Liang, J. and Q. Kong, *alpha-Cleavage of cellular prion protein.* Prion, 2012. **6**(5): p. 453-60.

47. Brown, D.R., *Prion and prejudice: normal protein and the synapse.* Trends Neurosci, 2001. **24**(2): p. 85-90.

48. Amin, L., et al., *Characterization of prion protein function by focal neurite stimulation.* J Cell Sci, 2016. **129**(20): p. 3878-3891.

49. Chen, S., et al., *Prion protein as trans-interacting partner for neurons is involved in neurite outgrowth and neuronal survival.* Mol Cell Neurosci, 2003. **22**(2): p. 227-33.

50. Gasperini, L., et al., *In Absence of the Cellular Prion Protein, Alterations in Copper Metabolism and Copper-Dependent Oxidase Activity Affect Iron Distribution.* Front Neurosci, 2016. **10**: p. 437.

51. Viles, J.H., M. Klewpatinond, and R.C. Nadal, *Copper and the structural biology of the prion protein.* Biochem Soc Trans, 2008. **36**(Pt 6): p. 1288-92.

52. Roucou, X., M. Gains, and A.C. LeBlanc, *Neuroprotective functions of prion protein.* J Neurosci Res, 2004. **75**(2): p. 153-61.

53. Milhavet, O. and S. Lehmann, *Oxidative stress and the prion protein in transmissible spongiform encephalopathies.* Brain Res Brain Res Rev, 2002. **38**(3): p. 328-39.

54. Brown, D.R., et al., *Normal prion protein has an activity like that of superoxide dismutase.* Biochem J, 1999. **344 Pt 1**: p. 1-5.

55. Papassotiropoulos, A., et al., *The prion gene is associated with human long-term memory.* Hum Mol Genet, 2005. **14**(15): p. 2241-6.

56. Konopka, G., et al., *Human-specific transcriptional regulation of CNS development genes by FOXP2.* Nature, 2009. **462**(7270): p. 213-7.

57. Ben-Moshe, Z., et al., *The light-induced transcriptome of the zebrafish pineal gland reveals complex regulation of the circadian clockwork by light.* Nucleic Acids Res, 2014. **42**(6): p. 3750-67.

58. Sales, N., et al., *Cellular prion protein localization in rodent and primate brain.* Eur J Neurosci, 1998. **10**(7): p. 2464-71.

59. Mouillet-Richard, S., et al., *Signal transduction through prion protein.* Science, 2000. **289**(5486): p. 1925-8.

60. Schmitt-Ulms, G., et al., *Binding of neural cell adhesion molecules (N-CAMs) to the cellular prion protein.* J Mol Biol, 2001. **314**(5): p. 1209-25.

61. Rieger, R., et al., *The human 37-kDa laminin receptor precursor interacts with the prion protein in eukaryotic cells.* Nat Med, 1997. **3**(12): p. 1383-8.

62. Khosravani, H., et al., *Prion protein attenuates excitotoxicity by inhibiting NMDA receptors.* J Gen Physiol, 2008. **131**(6): p. i5.

63. Gasperini, L., et al., *Prion protein and copper cooperatively protect neurons by modulating NMDA receptor through S-nitrosylation.* Antioxid Redox Signal, 2015. **22**(9): p. 772-84.

64. Black, S.A., et al., *Cellular prion protein and NMDA receptor modulation: protecting against excitotoxicity.* Front Cell Dev Biol, 2014. **2**: p. 45.

65. Beraldo, F.H., et al., *Role of alpha7 nicotinic acetylcholine receptor in calcium signaling induced by prion protein interaction with stress-inducible protein 1.* J Biol Chem, 2010. **285**(47): p. 36542-50.

66. Beraldo, F.H., et al., *Metabotropic glutamate receptors transduce signals for neurite outgrowth after binding of the prion protein to laminin gamma1 chain.* FASEB J, 2011. **25**(1): p. 265-79.

67. Kretzschmar, H.A., *Neuropathology of human prion diseases (spongiform encephalopathies).* Dev Biol Stand, 1993. **80**: p. 71-90.

68. Merz, P.A., et al., *Scrapie-associated fibrils in Creutzfeldt-Jakob disease.* Nature, 1983. **306**(5942): p. 474-6.

69. Silveira, J.R., et al., *The most infectious prion protein particles.* Nature, 2005. **437**(7056): p. 257-61.

70. Wille, H., et al., *Structural studies of the scrapie prion protein by electron crystallography.* Proc Natl Acad Sci U S A, 2002. **99**(6): p. 3563-8.

71. Govaerts, C., et al., *Evidence for assembly of prions with left-handed beta-helices into trimers.* Proc Natl Acad Sci U S A, 2004. **101**(22): p. 8342-7.

72. Vazquez-Fernandez, E., et al., *The Structural Architecture of an Infectious Mammalian Prion Using Electron Cryomicroscopy.* PLoS Pathog, 2016. **12**(9): p. e1005835.

73. Telling, G.C., et al., *Evidence for the conformation of the pathologic isoform of the prion protein enciphering and propagating prion diversity.* Science, 1996. **274**(5295): p. 2079-82.

74. Safar, J.G., et al., *Structural determinants of phenotypic diversity and replication rate of human prions.* PLoS Pathog, 2015. **11**(4): p. e1004832.

75. Kajava, A.V. and A.C. Steven, *Beta-rolls, beta-helices, and other beta-solenoid proteins.* Adv Protein Chem, 2006. **73**: p. 55-96.

76. Wille, H., et al., *Natural and synthetic prion structure from X-ray fiber diffraction.* Proc Natl Acad Sci U S A, 2009. **106**(40): p. 16990-5.

77. Zou, W.Q., et al., *Identification of novel proteinase K-resistant C-terminal fragments of PrP in Creutzfeldt-Jakob disease.* J Biol Chem, 2003. **278**(42): p. 40429-36.

78. Zanusso, G., et al., *Identification of distinct N-terminal truncated forms of prion protein in different Creutzfeldt-Jakob disease subtypes.* J Biol Chem, 2004. **279**(37): p. 38936-42.

79. Pirisinu, L., et al., *Small ruminant nor98 prions share biochemical features with human gerstmann-straussler-scheinker disease and variably protease-sensitive prionopathy.* PLoS One, 2013. **8**(6): p. e66405.

80. Gambetti, P., et al., *A novel human disease with abnormal prion protein sensitive to protease.* Ann Neurol, 2008. **63**(6): p. 697-708.

81. Gotte, D.R., et al., *Atypical scrapie isolates involve a uniform prion species with a complex molecular signature.* PLoS One, 2011. **6**(11): p. e27510.

82. Vazquez-Fernandez, E., et al., *The Structure of Mammalian Prions and Their Aggregates.* Int Rev Cell Mol Biol, 2017. **329**: p. 277-301.

83. Richardson, J.S. and D.C. Richardson, *Natural beta-sheet proteins use negative design to avoid edge-to-edge aggregation.* Proc Natl Acad Sci U S A, 2002. **99**(5): p. 2754-9.

84. Bryan, A.W., Jr., et al., *Structure-based prediction reveals capping motifs that inhibit beta-helix aggregation.* Proc Natl Acad Sci U S A, 2011. **108**(27): p. 11099-104.

85. Wille, H. and J.R. Requena, *The Structure of PrP(Sc) Prions.* Pathogens, 2018. **7**(1).

86. Ironside, J.W., D.L. Ritchie, and M.W. Head, *Prion diseases.* Handb Clin Neurol, 2017. **145**: p. 393-403.

87. Budka, H., et al., *Neuropathological diagnostic criteria for Creutzfeldt-Jakob disease (CJD) and other human spongiform encephalopathies (prion diseases).* Brain Pathol, 1995. **5**(4): p. 459-66.

88. Almer, G., et al., *Fatal familial insomnia: a new Austrian family.* Brain, 1999. **122 ( Pt 1)**: p. 5-16.

89. Hu, P.P., et al., *Role of Prion Replication in the Strain-dependent Brain Regional Distribution of Prions.* J Biol Chem, 2016. **291**(24): p. 12880-7.

90. DeArmond, S.J. and E. Bouzamondo, *Fundamentals of prion biology and diseases.* Toxicology, 2002. **181-182**: p. 9-16.

91. Betmouni, S., V.H. Perry, and J.L. Gordon, *Evidence for an early inflammatory response in the central nervous system of mice with scrapie.* Neuroscience, 1996. **74**(1): p. 1-5.

92. Aguzzi, A. and C. Zhu, *Microglia in prion diseases.* J Clin Invest, 2017. **127**(9): p. 3230-3239.

93. Wells, G.A., et al., *Infectivity in the ileum of cattle challenged orally with bovine spongiform encephalopathy.* Vet Rec, 1994. **135**(2): p. 40-1.

94. Wells, G.A., et al., *Preliminary observations on the pathogenesis of experimental bovine spongiform encephalopathy (BSE): an update.* Vet Rec, 1998. **142**(5): p. 103-6.

95. Wells, G.A., et al., *Limited detection of sternal bone marrow infectivity in the clinical phase of experimental bovine spongiform encephalopathy (BSE).* Vet Rec, 1999. **144**(11): p. 292-4.

96. Terry, L.A., et al., *Detection of disease-specific PrP in the distal ileum of cattle exposed orally to the agent of bovine spongiform encephalopathy.* Vet Rec, 2003. **152**(13): p. 387-92.

97. Buschmann, A. and M.H. Groschup, *Highly bovine spongiform encephalopathy-sensitive transgenic mice confirm the essential restriction of infectivity to the nervous system in clinically diseased cattle.* J Infect Dis, 2005. **192**(5): p. 934-42.

98. Okada, H., et al., *The presence of disease-associated prion protein in skeletal muscle of cattle infected with classical bovine spongiform encephalopathy.* J Vet Med Sci, 2014. **76**(1): p. 103-7.

99. Vascellari, M., et al., *PrPSc in salivary glands of scrapie-affected sheep.* J Virol, 2007. **81**(9): p. 4872-6.

100. Garza, M.C., et al., *Distribution of peripheral PrP(Sc) in sheep with naturally acquired scrapie.* PLoS One, 2014. **9**(5): p. e97768.

101. Terry, L.A., et al., *Detection of PrPsc in blood from sheep infected with the scrapie and bovine spongiform encephalopathy agents.* J Virol, 2009. **83**(23): p. 12552-8.

102. Maddison, B.C., et al., *Prions are secreted in milk from clinically normal scrapie-exposed sheep.* J Virol, 2009. **83**(16): p. 8293-6.

103. Tamguney, G., et al., *Salivary prions in sheep and deer.* Prion, 2012. **6**(1): p. 52-61.

104. Maddison, B.C., et al., *Prions are secreted into the oral cavity in sheep with preclinical scrapie.* J Infect Dis, 2010. **201**(11): p. 1672-6.

105. Sigurdson, C.J. and A. Aguzzi, *Chronic wasting disease.* Biochim Biophys Acta, 2007. **1772**(6): p. 610-8.

106. Selariu, A., et al., *In utero transmission and tissue distribution of chronic wasting disease-associated prions in free-ranging Rocky Mountain elk.* J Gen Virol, 2015. **96**(11): p. 3444-55.

107. Haley, N.J. and E.A. Hoover, *Chronic wasting disease of cervids: current knowledge and future perspectives.* Annu Rev Anim Biosci, 2015. **3**: p. 305-25.

108. Mathiason, C.K., et al., *Infectious prions in the saliva and blood of deer with chronic wasting disease.* Science, 2006. **314**(5796): p. 133-6.

109. Haley, N.J., et al., *Detection of CWD prions in urine and saliva of deer by transgenic mouse bioassay.* PLoS One, 2009. **4**(3): p. e4848.

110. Tamguney, G., et al., *Asymptomatic deer excrete infectious prions in faeces.* Nature, 2009. **461**(7263): p. 529-32.

111. Schneider, D.A., et al., *Disease-associated prion protein in neural and lymphoid tissues of mink (Mustela vison) inoculated with transmissible mink encephalopathy.* J Comp Pathol, 2012. **147**(4): p. 508-21.

112. Hadlow, W.J., R.E. Race, and R.C. Kennedy, *Temporal distribution of transmissible mink encephalopathy virus in mink inoculated subcutaneously.* J Virol, 1987. **61**(10): p. 3235-40.

113. Eiden, M., et al., *Biochemical and immunohistochemical characterization of feline spongiform encephalopathy in a German captive cheetah.* J Gen Virol, 2010. **91**(Pt 11): p. 2874-83.

114. Head, M.W., et al., *Prion protein accumulation in eyes of patients with sporadic and variant Creutzfeldt-Jakob disease.* Invest Ophthalmol Vis Sci, 2003. **44**(1): p. 342-6.

115. Head, M.W., et al., *Abnormal prion protein in the retina of the most commonly occurring subtype of sporadic Creutzfeldt-Jakob disease.* Br J Ophthalmol, 2005. **89**(9): p. 1131-3.

116. Goodbrand, I.A., et al., *Prion protein accumulation in the spinal cords of patients with sporadic and growth hormone associated Creutzfeldt-Jakob disease.* Neurosci Lett, 1995. **183**(1-2): p. 127-30.

117. Ishida, C., et al., *Involvement of the peripheral nervous system in human prion diseases including dural graft associated Creutzfeldt-Jakob disease.* J Neurol Neurosurg Psychiatry, 2005. **76**(3): p. 325-9.

118. Douet, J.Y., et al., *Detection of infectivity in blood of persons with variant and sporadic Creutzfeldt-Jakob disease.* Emerg Infect Dis, 2014. **20**(1): p. 114-7.

119. Luk, C., et al., *Diagnosing Sporadic Creutzfeldt-Jakob Disease by the Detection of Abnormal Prion Protein in Patient Urine.* JAMA Neurol, 2016. **73**(12): p. 1454-1460.

120. Atarashi, R., et al., *Ultrasensitive human prion detection in cerebrospinal fluid by real-time quaking-induced conversion.* Nat Med, 2011. **17**(2): p. 175-8.

121. McGuire, L.I., et al., *Real time quaking-induced conversion analysis of cerebrospinal fluid in sporadic Creutzfeldt-Jakob disease.* Ann Neurol, 2012. **72**(2): p. 278-85.

122. Bongianni, M., et al., *Diagnosis of Human Prion Disease Using Real-Time Quaking-Induced Conversion Testing of Olfactory Mucosa and Cerebrospinal Fluid Samples.* JAMA Neurol, 2016.

123. Glatzel, M., et al., *Extraneural pathologic prion protein in sporadic Creutzfeldt-Jakob disease.* N Engl J Med, 2003. **349**(19): p. 1812-20.

124. Peden, A.H., et al., *Detection and localization of PrPSc in the skeletal muscle of patients with variant, iatrogenic, and sporadic forms of Creutzfeldt-Jakob disease.* Am J Pathol, 2006. **168**(3): p. 927-35.

125. Ramasamy, I., et al., *Organ distribution of prion proteins in variant Creutzfeldt-Jakob disease.* Lancet Infect Dis, 2003. **3**(4): p. 214-22.

126. Concha-Marambio, L., et al., *Detection of prions in blood from patients with variant Creutzfeldt-Jakob disease.* Sci Transl Med, 2016. **8**(370): p. 370ra183.

127. Bougard, D., et al., *Detection of prions in the plasma of presymptomatic and symptomatic patients with variant Creutzfeldt-Jakob disease.* Sci Transl Med, 2016. **8**(370): p. 370ra182.

128. Moda, F., et al., *Prions in the urine of patients with variant Creutzfeldt-Jakob disease.* N Engl J Med, 2014. **371**(6): p. 530-9.

129. Kimberlin, R.H. and J.W. Wilesmith, *Bovine spongiform encephalopathy. Epidemiology, low dose exposure and risks.* Ann N Y Acad Sci, 1994. **724**: p. 210-20.

130. Konold, T., et al., *Evidence of scrapie transmission to sheep via goat milk.* BMC Vet Res, 2016. **12**: p. 208.

131. Ryder, S., et al., *Demonstration of lateral transmission of scrapie between sheep kept under natural conditions using lymphoid tissue biopsy.* Res Vet Sci, 2004. **76**(3): p. 211-7.

132. Seidel, B., et al., *Scrapie Agent (Strain 263K) can transmit disease via the oral route after persistence in soil over years.* PLoS One, 2007. **2**(5): p. e435.

133. Waddell, L., et al., *Current evidence on the transmissibility of chronic wasting disease prions to humans-A systematic review.* Transbound Emerg Dis, 2018. **65**(1): p. 37-49.

134. Gajdusek, D.C., *Unconventional viruses and the origin and disappearance of kuru.* Science, 1977. **197**(4307): p. 943-60.

135. Hill, A.F., et al., *The same prion strain causes vCJD and BSE.* Nature, 1997. **389**(6650): p. 448-50, 526.

136. Diack, A.B., et al., *Variant CJD. 18 years of research and surveillance.* Prion, 2014. **8**(4): p. 286-95.

137. Brown, P., et al., *Iatrogenic Creutzfeldt-Jakob disease at the millennium.* Neurology, 2000. **55**(8): p. 1075-81.

138. Gibbs, C.J., Jr., et al., *Clinical and pathological features and laboratory confirmation of Creutzfeldt-Jakob disease in a recipient of pituitary-derived human growth hormone.* N Engl J Med, 1985. **313**(12): p. 734-8.

139. Centers for Disease, C. and Prevention, *Creutzfeldt-Jakob disease associated with cadaveric dura mater grafts -- Japan, January 1979-May 1996.* MMWR Morb Mortal Wkly Rep, 1997. **46**(45): p. 1066-9.

140. Duffy, P., et al., *Letter: Possible person-to-person transmission of Creutzfeldt-Jakob disease.* N Engl J Med, 1974. **290**(12): p. 692-3.

141. Bernoulli, C., et al., *Danger of accidental person-to-person transmission of Creutzfeldt-Jakob disease by surgery.* Lancet, 1977. **1**(8009): p. 478-9.

142. Williams, D., *New thoughts on CJD, surgical instruments and disease transmission.* Med Device Technol, 2006. **17**(1): p. 7-8.

143. Weissmann, C., et al., *Transmission of prions.* Proc Natl Acad Sci U S A, 2002. **99 Suppl 4**: p. 16378-83.

144. Andreoletti, O., et al., *Highly efficient prion transmission by blood transfusion.* PLoS Pathog, 2012. **8**(6): p. e1002782.

145. Ingrosso, L., F. Pisani, and M. Pocchiari, *Transmission of the 263K scrapie strain by the dental route.* J Gen Virol, 1999. **80 ( Pt 11)**: p. 3043-7.

146. Weissmann, C., et al., *Transmission of prions.* J Infect Dis, 2002. **186 Suppl 2**: p. S157-65.

147. Hamir, A.N., et al., *Experimental transmission of US scrapie agent by nasal, peritoneal, and conjunctival routes to genetically susceptible sheep.* Vet Pathol, 2008. **45**(1): p. 7-11.

148. Haybaeck, J., et al., *Aerosols transmit prions to immunocompetent and immunodeficient mice.* PLoS Pathog, 2011. **7**(1): p. e1001257.

149. Pattison, I.H., *The relative susceptibility of sheep, goats and mice to two types of the goat scrapie agent.* Res Vet Sci, 1966. **7**(2): p. 207-12.

150. Tanaka, M., et al., *Conformational variations in an infectious protein determine prion strain differences.* Nature, 2004. **428**(6980): p. 323-8.

151. Bartz, J.C., *Prion Strain Diversity.* Cold Spring Harb Perspect Med, 2016. **6**(12).

152. Gambetti, P., et al., *Molecular biology and pathology of prion strains in sporadic human prion diseases.* Acta Neuropathol, 2011. **121**(1): p. 79-90.

153. Dickinson, A.G. and V.M. Meikle, *Host-genotype and agent effects in scrapie incubation: change in allelic interaction with different strains of agent.* Mol Gen Genet, 1971. **112**(1): p. 73-9.

154. Fraser, H., *Diversity in the neuropathology of scrapie-like diseases in animals.* Br Med Bull, 1993. **49**(4): p. 792-809.

155. Fraser, H. and A.G. Dickinson, *The sequential development of the brain lesion of scrapie in three strains of mice.* J Comp Pathol, 1968. **78**(3): p. 301-11.
156. Khalili-Shirazi, A., et al., *PrP glycoforms are associated in a strain-specific ratio in native PrPSc.* J Gen Virol, 2005. **86**(Pt 9): p. 2635-44.
157. McKinley, M.P., D.C. Bolton, and S.B. Prusiner, *A protease-resistant protein is a structural component of the scrapie prion.* Cell, 1983. **35**(1): p. 57-62.
158. Peretz, D., et al., *A change in the conformation of prions accompanies the emergence of a new prion strain.* Neuron, 2002. **34**(6): p. 921-32.
159. Safar, J., et al., *Eight prion strains have PrP(Sc) molecules with different conformations.* Nat Med, 1998. **4**(10): p. 1157-65.
160. Caughey, B., G.J. Raymond, and R.A. Bessen, *Strain-dependent differences in beta-sheet conformations of abnormal prion protein.* J Biol Chem, 1998. **273**(48): p. 32230-5.
161. Langedijk, J.P., et al., *Two-rung model of a left-handed beta-helix for prions explains species barrier and strain variation in transmissible spongiform encephalopathies.* J Mol Biol, 2006. **360**(4): p. 907-20.
162. Westaway, D., et al., *Distinct prion proteins in short and long scrapie incubation period mice.* Cell, 1987. **51**(4): p. 651-62.
163. Moore, R.A., I. Vorberg, and S.A. Priola, *Species barriers in prion diseases--brief review.* Arch Virol Suppl, 2005(19): p. 187-202.
164. Prusiner, S.B., et al., *Transgenetic studies implicate interactions between homologous PrP isoforms in scrapie prion replication.* Cell, 1990. **63**(4): p. 673-86.
165. Bartz, J.C., et al., *Transmissible mink encephalopathy species barrier effect between ferret and mink: PrP gene and protein analysis.* J Gen Virol, 1994. **75 ( Pt 11)**: p. 2947-53.
166. Scott, M., et al., *Transgenic mice expressing hamster prion protein produce species-specific scrapie infectivity and amyloid plaques.* Cell, 1989. **59**(5): p. 847-57.
167. Weissmann, C., et al., *Prions on the move.* EMBO Rep, 2011. **12**(11): p. 1109-17.
168. Bruce, M.E., et al., *Transmissions to mice indicate that 'new variant' CJD is caused by the BSE agent.* Nature, 1997. **389**(6650): p. 498-501.
169. Collinge, J., *Variant Creutzfeldt-Jakob disease.* Lancet, 1999. **354**(9175): p. 317-23.
170. Imran, M. and S. Mahmood, *An overview of animal prion diseases.* Virol J, 2011. **8**: p. 493.
171. Bons, N., et al., *Natural and experimental oral infection of nonhuman primates by bovine spongiform encephalopathy agents.* Proc Natl Acad Sci U S A, 1999. **96**(7): p. 4046-51.
172. Pearson, G.R., et al., *Feline spongiform encephalopathy: fibril and PrP studies.* Vet Rec, 1992. **131**(14): p. 307-10.
173. Liberski, P.P., et al., *Transmissible mink encephalopathy - review of the etiology of a rare prion disease.* Folia Neuropathol, 2009. **47**(2): p. 195-204.
174. Bartz, J.C., et al., *Adaptation and selection of prion protein strain conformations following interspecies transmission of transmissible mink encephalopathy.* J Virol, 2000. **74**(12): p. 5542-7.
175. Bessen, R.A. and R.F. Marsh, *Identification of two biologically distinct strains of transmissible mink encephalopathy in hamsters.* J Gen Virol, 1992. **73 ( Pt 2)**: p. 329-34.
176. Bessen, R.A. and R.F. Marsh, *Distinct PrP properties suggest the molecular basis of strain variation in transmissible mink encephalopathy.* J Virol, 1994. **68**(12): p. 7859-68.
177. Bessen, R.A. and R.F. Marsh, *Biochemical and physical properties of the prion protein from two strains of the transmissible mink encephalopathy agent.* J Virol, 1992. **66**(4): p. 2096-101.
178. Morales, R., K. Abid, and C. Soto, *The prion strain phenomenon: molecular basis and unprecedented features.* Biochim Biophys Acta, 2007. **1772**(6): p. 681-91.
179. Makarava, N., R. Savtchenko, and I.V. Baskakov, *Selective amplification of classical and atypical prions using modified protein misfolding cyclic amplification.* J Biol Chem, 2013. **288**(1): p. 33-41.
180. Bruce, M.E., *Scrapie strain variation and mutation.* Br Med Bull, 1993. **49**(4): p. 822-38.
181. Lasmezas, C.I., et al., *Transmission of the BSE agent to mice in the absence of detectable abnormal prion protein.* Science, 1997. **275**(5298): p. 402-5.

182. Baskakov, I.V., *The many shades of prion strain adaptation.* Prion, 2014. **8**(2).

183. Li, J., et al., *Darwinian evolution of prions in cell culture.* Science, 2010. **327**(5967): p. 869-72.

184. Collinge, J., *Medicine. Prion strain mutation and selection.* Science, 2010. **328**(5982): p. 1111-2.

185. Mahal, S.P., et al., *Transfer of a prion strain to different hosts leads to emergence of strain variants.* Proc Natl Acad Sci U S A, 2010. **107**(52): p. 22653-8.

186. Makarava, N. and I.V. Baskakov, *The evolution of transmissible prions: the role of deformed templating.* PLoS Pathog, 2013. **9**(12): p. e1003759.

187. Makarava, N. and I.V. Baskakov, *Genesis of tramsmissible protein states via deformed templating.* Prion, 2012. **6**(3): p. 252-5.

188. Bian, J., H.E. Kang, and G.C. Telling, *Quinacrine promotes replication and conformational mutation of chronic wasting disease prions.* Proc Natl Acad Sci U S A, 2014. **111**(16): p. 6028-33.

189. Ghaemmaghami, S., et al., *Continuous quinacrine treatment results in the formation of drug-resistant prions.* PLoS Pathog, 2009. **5**(11): p. e1000673.

190. Kimberlin, R.H., S. Cole, and C.A. Walker, *Temporary and permanent modifications to a single strain of mouse scrapie on transmission to rats and hamsters.* J Gen Virol, 1987. **68 ( Pt 7)**: p. 1875-81.

191. Makarava, N., et al., *Conformational switching within individual amyloid fibrils.* J Biol Chem, 2009. **284**(21): p. 14386-95.

192. Mahal, S.P., et al., *Propagation of RML prions in mice expressing PrP devoid of GPI anchor leads to formation of a novel, stable prion strain.* PLoS Pathog, 2012. **8**(6): p. e1002746.

193. Cancellotti, E., et al., *Post-translational changes to PrP alter transmissible spongiform encephalopathy strain properties.* EMBO J, 2013. **32**(5): p. 756-69.

194. Saborio, G.P., B. Permanne, and C. Soto, *Sensitive detection of pathological prion protein by cyclic amplification of protein misfolding.* Nature, 2001. **411**(6839): p. 810-3.

195. Saa, P., J. Castilla, and C. Soto, *Ultra-efficient replication of infectious prions by automated protein misfolding cyclic amplification.* J Biol Chem, 2006. **281**(46): p. 35245-52.

196. Bieschke, J., et al., *Autocatalytic self-propagation of misfolded prion protein.* Proc Natl Acad Sci U S A, 2004. **101**(33): p. 12207-11.

197. Castilla, J., et al., *Cell-free propagation of prion strains.* EMBO J, 2008. **27**(19): p. 2557-66.

198. Gonzalez-Montalban, N. and I.V. Baskakov, *Assessment of strain-specific PrP(Sc) elongation rates revealed a transformation of PrP(Sc) properties during protein misfolding cyclic amplification.* PLoS One, 2012. **7**(7): p. e41210.

199. Barria, M.A., et al., *Molecular barriers to zoonotic transmission of prions.* Emerg Infect Dis, 2014. **20**(1): p. 88-97.

200. Castilla, J., et al., *Crossing the species barrier by PrP(Sc) replication in vitro generates unique infectious prions.* Cell, 2008. **134**(5): p. 757-68.

201. Meyerett, C., et al., *In vitro strain adaptation of CWD prions by serial protein misfolding cyclic amplification.* Virology, 2008. **382**(2): p. 267-76.

202. Castilla, J., et al., *In vitro generation of infectious scrapie prions.* Cell, 2005. **121**(2): p. 195-206.

203. Green, K.M., et al., *Accelerated high fidelity prion amplification within and across prion species barriers.* PLoS Pathog, 2008. **4**(8): p. e1000139.

204. Chianini, F., et al., *Rabbits are not resistant to prion infection.* Proc Natl Acad Sci U S A, 2012. **109**(13): p. 5080-5.

205. Gonzalez-Montalban, N., et al., *Changes in prion replication environment cause prion strain mutation.* FASEB J, 2013. **27**(9): p. 3702-10.

206. Katorcha, E., et al., *Prion replication environment defines the fate of prion strain adaptation.* PLoS Pathog, 2018. **14**(6): p. e1007093.

207. Atarashi, R., et al., *Simplified ultrasensitive prion detection by recombinant PrP conversion with shaking.* Nat Methods, 2008. **5**(3): p. 211-2.

208. Orru, C.D., et al., *Bank Vole Prion Protein As an Apparently Universal Substrate for RT-QuIC-Based Detection and Discrimination of Prion Strains.* PLoS Pathog, 2015. **11**(6): p. e1004983.

209. Orru, C.D., et al., *Rapid and sensitive RT-QuIC detection of human Creutzfeldt-Jakob disease using cerebrospinal fluid.* MBio, 2015. **6**(1).

210. Orru, C.D., et al., *A test for Creutzfeldt-Jakob disease using nasal brushings.* N Engl J Med, 2014. **371**(6): p. 519-29.

211. Kristen A. Davenport, D.M.H., Candace K. Mathiason and Edward A. Hoover,

*Insights into CWD and BSE species barriers using real-time conversion.* JVI, 2015.

212. Luers, L., et al., *Seeded fibrillation as molecular basis of the species barrier in human prion diseases.* PLoS One, 2013. **8**(8): p. e72623.

213. Legname, G., et al., *Synthetic mammalian prions.* Science, 2004. **305**(5684): p. 673-6.

214. Colby, D.W., et al., *Design and construction of diverse mammalian prion strains.* Proc Natl Acad Sci U S A, 2009. **106**(48): p. 20417-22.

215. Kaneko, K., et al., *A synthetic peptide initiates Gerstmann-Straussler-Scheinker (GSS) disease in transgenic mice.* J Mol Biol, 2000. **295**(4): p. 997-1007.

216. Hsiao, K.K., et al., *Serial transmission in rodents of neurodegeneration from transgenic mice expressing mutant prion protein.* Proc Natl Acad Sci U S A, 1994. **91**(19): p. 9126-30.

217. Nazor, K.E., et al., *Immunodetection of disease-associated mutant PrP, which accelerates disease in GSS transgenic mice.* EMBO J, 2005. **24**(13): p. 2472-80.

218. Tremblay, P., et al., *Mutant PrPSc conformers induced by a synthetic peptide and several prion strains.* J Virol, 2004. **78**(4): p. 2088-99.

219. Benetti, F. and G. Legname, *De novo mammalian prion synthesis.* Prion, 2009. **3**(4): p. 213-9.

220. Baskakov, I.V., et al., *Pathway complexity of prion protein assembly into amyloid.* J Biol Chem, 2002. **277**(24): p. 21140-8.

221. Colby, D.W., et al., *Prion detection by an amyloid seeding assay.* Proc Natl Acad Sci U S A, 2007. **104**(52): p. 20914-9.

222. Makarava, N., et al., *Recombinant prion protein induces a new transmissible prion disease in wild-type animals.* Acta Neuropathol, 2010. **119**(2): p. 177-87.

223. Baskakov, I.V. and L. Breydo, *Converting the prion protein: what makes the protein infectious.* Biochim Biophys Acta, 2007. **1772**(6): p. 692-703.

224. Deleault, N.R., et al., *Formation of native prions from minimal components in vitro.* Proc Natl Acad Sci U S A, 2007. **104**(23): p. 9741-6.

225. Geoghegan, J.C., et al., *Selective incorporation of polyanionic molecules into hamster prions.* J Biol Chem, 2007. **282**(50): p. 36341-53.

226. Wang, F., et al., *Lipid interaction converts prion protein to a PrPSc-like proteinase K-resistant conformation under physiological conditions.* Biochemistry, 2007. **46**(23): p. 7045-53.

227. Deleault, N.R., et al., *Cofactor molecules maintain infectious conformation and restrict strain properties in purified prions.* Proc Natl Acad Sci U S A, 2012. **109**(28): p. E1938-46.

228. Deleault, N.R., et al., *Isolation of phosphatidylethanolamine as a solitary cofactor for prion formation in the absence of nucleic acids.* Proc Natl Acad Sci U S A, 2012. **109**(22): p. 8546-51.

229. Zhang, Z., et al., *De novo generation of infectious prions with bacterially expressed recombinant prion protein.* FASEB J, 2013. **27**(12): p. 4768-75.

230. Wang, F., et al., *Genetic informational RNA is not required for recombinant prion infectivity.* J Virol, 2012. **86**(3): p. 1874-6.

231. Barria, M.A., et al., *De novo generation of infectious prions in vitro produces a new disease phenotype.* PLoS Pathog, 2009. **5**(5): p. e1000421.

232. Noble, G.P., et al., *A Structural and Functional Comparison Between Infectious and Non-Infectious Autocatalytic Recombinant PrP Conformers.* PLoS Pathog, 2015. **11**(6): p. e1005017.

233. Wang, F., et al., *Self-propagating, protease-resistant, recombinant prion protein conformers with or without in vivo pathogenicity.* PLoS Pathog, 2017. **13**(7): p. e1006491.

234. Makarava, N., et al., *Genesis of mammalian prions: from non-infectious amyloid fibrils to a transmissible prion disease.* PLoS Pathog, 2011. **7**(12): p. e1002419.

235. Makarava, N., et al., *New Molecular Insight into Mechanism of Evolution of Mammalian Synthetic Prions.* Am J Pathol, 2016. **186**(4): p. 1006-14.

236. Makarava, N., et al., *A new mechanism for transmissible prion diseases.* J Neurosci, 2012. **32**(21): p. 7345-55.

237. Makarava, N., et al., *Stabilization of a prion strain of synthetic origin requires multiple serial passages.* J Biol Chem, 2012. **287**(36): p. 30205-14.

238. Pattison, I.H. and K.M. Jones, *Modification of a strain of mouse-adapted scrapie by passage through rats.* Res Vet Sci, 1968. **9**(5): p. 408-10.

239. Ghaemmaghami, S., et al., *Conformational transformation and selection of synthetic prion strains.* J Mol Biol, 2011. **413**(3): p. 527-42.

240. Ghaemmaghami, S., et al., *Convergent replication of mouse synthetic prion strains.* Am J Pathol, 2013. **182**(3): p. 866-74.

241. Legname, G., et al., *Continuum of prion protein structures enciphers a multitude of prion isolate-specified phenotypes.* Proc Natl Acad Sci U S A, 2006. **103**(50): p. 19105-10.

242. Legname, G., et al., *Strain-specified characteristics of mouse synthetic prions.* Proc Natl Acad Sci U S A, 2005. **102**(6): p. 2168-73.

243. Shikiya, R.A., et al., *Coinfecting prion strains compete for a limiting cellular resource.* J Virol, 2010. **84**(11): p. 5706-14.

244. Kimberlin, R.H. and C.A. Walker, *Competition between strains of scrapie depends on the blocking agent being infectious.* Intervirology, 1985. **23**(2): p. 74-81.

245. Fernandez-Borges, N., et al., *Cofactors influence the biological properties of infectious recombinant prions.* Acta Neuropathol, 2018. **135**(2): p. 179-199.

246. Moda, F., et al., *Synthetic prions with novel strain-specified properties.* PLoS Pathog, 2015. **11**(12): p. e1005354.

247. Vascellari, S., et al., *Prion seeding activities of mouse scrapie strains with divergent PrPSc protease sensitivities and amyloid plaque content using RT-QuIC and eQuIC.* PLoS One, 2012. **7**(11): p. e48969.

248. Ayers, J.I., et al., *The strain-encoded relationship between PrP replication, stability and processing in neurons is predictive of the incubation period of disease.* PLoS Pathog, 2011. **7**(3): p. e1001317.

249. Bett, C., et al., *Biochemical properties of highly neuroinvasive prion strains.* PLoS Pathog, 2012. **8**(2): p. e1002522.

250. Hannaoui, S., et al., *Destabilizing polymorphism in cervid prion protein hydrophobic core determines prion conformation and conversion efficiency.* PLoS Pathog, 2017. **13**(8): p. e1006553.

251. Lloyd, S.E., et al., *Characterization of two distinct prion strains derived from bovine spongiform encephalopathy transmissions to inbred mice.* J Gen Virol, 2004. **85**(Pt 8): p. 2471-8.

252. Le Dur, A., et al., *Divergent prion strain evolution driven by PrP(C) expression level in transgenic mice.* Nat Commun, 2017. **8**: p. 14170.

253. Goold, R., C. McKinnon, and S.J. Tabrizi, *Prion degradation pathways: Potential for therapeutic intervention.* Mol Cell Neurosci, 2015. **66**(Pt A): p. 12-20.

254. McKinnon, C., et al., *Prion-mediated neurodegeneration is associated with early impairment of the ubiquitin-proteasome system.* Acta Neuropathol, 2016. **131**(3): p. 411-25.

255. Yim, Y.I., et al., *The multivesicular body is the major internal site of prion conversion.* J Cell Sci, 2015. **128**(7): p. 1434-43.